# 11

# Variational and approximate solutions

## 11.1 Approach

In chapter 1, the fundamental equations of linear elasticity are developed, and fifteen equations fully describe the mechanics of deformable bodies. Unfortunately, these governing equations are partial differential equations in three dimensions, and although of first order only, their solution cannot be completed in closed form for most practical problems. Open form or series solutions have been developed for a limited number of applications, but no general approach exists for solving these equations in closed form. A barrier to the development of closed-form solutions to partial differential equations is the fact the arbitrary integration constants involved in the solution of ordinary differential equations are now replaced by arbitrary integration functions. Consequently, boundary conditions often play a greater role in the solution process for partial differential equations.

A very successful approach for dealing with complex problems is to reduce their geometric dimensionality from three to one, thereby replacing the governing partial differential equations by ordinary differential equations for which general solution procedures are available. A important example of this dimensional reduction procedure is beam theory, which leads to the ordinary differential equations presented in chapters 4 through 8. The reduction is based on the assumption that long, slender beams have one dimension, their span, which is much larger than the cross-sectional dimensions. Another important example of dimensional reduction is plate theory, presented in chapter 16, which transforms the three-dimensional elasticity equations into two-dimensional partial differential equations. In this case, the basic assumption is that one of the plate's geometric dimensions, its thickness, is much smaller than the other two.

The geometric dimension of a problem refers to the number of variables used to represent the displacement field: beam problems are *one-dimensional* because the displacement field is expressed in terms of a single variable along the beam's span. On the other hand, beam problems are sometimes referred to as *infinite-dimensional* because the solution of the problem requires the knowledge of the displacement field at all points, *i.e.* at an *infinite number points*, along the beam's span. To minimize

confusion, this latter situation will also be referred to as a problem with an *infinite number of degrees of freedom* for the displacement field.

Even within the framework of beam theory, closed-form solutions cannot readily be developed for many practical problems. For instance, it is arduous to find closed-form solutions for beams presenting sectional properties with arbitrary variations along their span, a situation commonly encountered for many practical aircraft structures. Consequently, considerable effort has been devoted to the development of approximate solution procedures.

In most approximate solution procedures, infinite degree of freedom problems are reduced to finite degree of freedom problems. Three main approaches are used to achieve this type of dimensional reduction. In the first approach, the solution is sought at a finite number of discrete points of the structure; this approach is essentially a *discretization procedure,* because it transforms the original problem, expressed in terms of continuous, infinite degree of freedom functions, into a discrete problem involving the values of these functions at a finite number of points. The derivatives appearing in the governing equations are then approximated using finite difference techniques. The original equations are transformed into a set of algebraic equations that is easily solved.

In the second approach, the solution of the problem is approximated by a finite sum of continuous functions, each weighted by an unknown coefficient. The solution of the problem then reduces to the determination of the unknown coefficients. It will be shown in the present chapter that the combination of this approximation technique with the energy methods developed in the previous two chapters yields powerful tools for the systematic derivation of approximate solutions.

Finally, the last approach, called the *finite element method,* combines aspects of the previous two. In this widely used approach, the solution domain is first divided into a finite number of sub-domains called *finite elements*. Within each element, the solution is then approximated by a finite number of continuous functions, based on the value of these functions at discrete points, often called *nodes*, associated with the element. The main advantage of this two-step approximation process is that many aspects of the solution procedure can be carried out at the element level, *i.e.*, by considering one single element at a time, independently of all others. The continuity of the solution across elements can be guaranteed by the fact that neighboring elements share common nodes. Here again, energy methods provide a systematic way of obtaining algebraic equations for the unknown values of the solution at the nodes. For complex problems, very large sets of linear algebraic are obtained. To a large extent, the success of the finite element method is due to the fact that computers can easily solve these large sets of equations.

This chapter focuses on the development of approximate solutions for the types of problems that are formulated in earlier chapters. The treatment begins with a re-examination of the energy methods introduced in chapter 10 with emphasis on the principle of minimum total potential energy. Specifically, several methods of deriving approximate solutions from this principle are investigated. Fundamental concepts of the calculus of variations [5, 6] are useful to streamline these formulations, which are also called variational formulations. While a general formulation of the finite

element method is beyond the scope of this book, the rudiments of the approach will be presented for beam structures as an extension of the element-oriented approach for trusses developed in section 10.7.

Finite element analysis is now a well established method, which has been the subject of intense study over the past several decades, largely because of its many successful applications. Although approximate, finite element procedures often yield very accurate and reliable solutions. Powerful commercial software tools are now widely available, and complex analysis can readily be handled on personal computers. In fact, contemporary structural analysis heavily relies on finite element analysis.

## 11.2 Rayleigh-Ritz method for beam bending

Approximate solutions of structural problems can be obtained through various approaches. The Rayleigh-Ritz approach is one of the simplest and will be introduced first. In this approach, the displacement field is represented by a linear combination of preselected displacement shapes, or shape functions, defined over the entire structure. This transforms the original, infinite dimensional problem into a finite dimensional problem. The principle of minimum total potential energy is then used to obtain an approximate solution of the problem.

### 11.2.1 Statement of the problem

Consider the simply supported beam of length $L$ subjected to a distributed transverse loading, $p_2(x_1)$, and concentrated transverse loads, $P_a$ and $P_b$, applied at locations $x_1 = a$ and $x_1 = b$, respectively, along the beam's span, as shown in fig. 11.1. The Euler-Bernoulli formulation developed in chapter 5 is used to model transverse bending deformations of the beam. Based on eq. (10.40), the strain energy stored in the beam is expressed in terms of the transverse displacement field, $\bar{u}_2(x_1)$, as

$$A = \frac{1}{2}\int_0^L H_{33}^c \left(\frac{\mathrm{d}^2\bar{u}_2}{\mathrm{d}x_1^2}\right)^2 \mathrm{d}x_1. \tag{11.1}$$

The potential of the externally applied loads is obtained from eq. (10.59), which in this case, reduces to

$$\Phi = -\int_0^L p_2\,\bar{u}_2(x_1)\,\mathrm{d}x_1 - P_a\,\bar{u}_2|_{x_1=a} - P_b\,\bar{u}_2|_{x_1=b}\,.$$

The total potential energy of the system, $\Pi = A + \Phi$, becomes

$$\Pi = \frac{1}{2}\int_0^L H_{33}^c \left(\frac{\mathrm{d}^2\bar{u}_2}{\mathrm{d}x_1^2}\right)^2 \mathrm{d}x_1 - \int_0^L p_2\,\bar{u}_2(x_1)\,\mathrm{d}x_1 - P_a\bar{u}_2(a) - P_b\bar{u}_2(b), \tag{11.2}$$

where $\bar{u}_2(x_1)$ is the unknown displacement field of the beam.

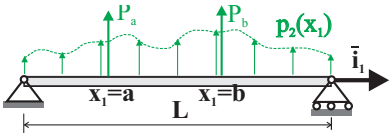


**Fig. 11.1.** Simply-supported beam subjected to distributed lateral load and.

The total potential energy is now a function of a function, $\bar{u}_2(x_1)$, *i.e.*, it is a *functional*. As mentioned earlier, this is an infinite degree of freedom problem, or a problem of infinite dimensionality because the definition of the transverse deflection field, $\bar{u}_2(x_1)$, requires the knowledge of this function for all points $0 \leq x_1 \leq L$, *i.e.*, for an infinite number of points. Rather than attempting to determine the exact solution of the problem that minimizes the total potential energy, as will be done in chapter 12, the present chapter seeks to construct approximate solutions of the problem.

### 11.2.2 Description of the Rayleigh-Ritz method

The main steps of what is known as the *Rayleigh-Ritz method* will be described here in a cursory manner. The first step of the solution procedure is to reduce the infinite degree of freedom problem into a finite degree of freedom problem. This can be done here by writing the solution for the transverse displacement field as a linear combination of $N$ suitably chosen shape functions

$$\bar{u}_2(x_1) = \sum_{i=1}^{N} h_i(x_1) q_i. \tag{11.3}$$

In this expression, the functions $h_i(x_1), i = 1, 2, \ldots, N$, are **known** functions called *shape functions*. Because the solution of the problem must satisfy the geometric boundary conditions of the problem, it is convenient to impose this condition on each of the shape functions which are otherwise arbitrarily chosen functions. The **unknown** coefficients, $q_i, i = 1, 2, \ldots, N$, are called *degrees of freedom*. Expression (11.3) now only involves $N$ unknown coefficients: it is a finite degree of freedom approximation to the exact, infinite degree of freedom solution of the problem.

The second step of the solution process is to introduce the approximate solution, eq. (11.3), into the expression for the total potential energy, eq. (11.2), and perform all indicated integrations over the span of the beam. This is now possible because the solution is expressed in terms of shape function of known analytical form. Once these integrations are performed, the total potential energy becomes a function of the degrees of freedom, $q_i, i = 1, 2, \ldots, N$, *i.e.*, $\Pi(\bar{u}_2(x_1)) = \Pi(q_1, q_2, \ldots, q_N)$. Because the expression for the total potential energy is a quadratic function of the displacement field, it now becomes a quadratic function of the degrees of freedom, $q_i, i = 1, 2, \ldots, N$.

The last step of the process is to invoke the principle of minimum total potential energy, requiring the total potential energy to be minimum. The total potential energy

is now a function of $N$ independent, unconstrained variables, and therefore calculus requires its derivatives to vanish, see eq. (10.17), leading to

$$\frac{\partial \Pi}{\partial q_i} = 0, \quad i = 1, 2, 3, \ldots, N. \tag{11.4}$$

Because the total potential energy is a quadratic expression of the degrees of freedom, its first derivatives are linear functions of the same variables, and hence, the above equations form a set of linear equations that can be solved for the values of the degrees of freedom that minimize the total potential energy.

### 11.2.3 Discussion of the Rayleigh-Ritz method

The solution obtained from eqs. (11.4) is not an exact solution. Indeed, by selecting the solution to be of the form given by eq. (11.3), the ability of the structure to deform is restricted; it can only deform in a finite number of allowable deformation shapes, $h_i(x_1)$, $i = 1, 2, \ldots, N$. In effect, the structure is made artificially stiffer than the real structure by limiting its deformation to be the linear combination of a finite number of arbitrarily preselected deformation mode shapes. Of course, the real structure is able to deform in an infinite number of deformation shapes.

In the above procedure, the shape functions are required only to satisfy the geometric boundary conditions and are otherwise arbitrary. If a different set of shape functions is selected in eq. (11.3), a different solution will be found. These remarks prompt the following question: how good is the approximate solution obtained from this process?

Let $\Pi$ be the total potential energy for the exact solution of the problem. Next, let $\widetilde{\Pi}$ be the total potential energy corresponding to an approximate solution, *i.e.*, $\widetilde{\Pi} = \Pi(q_1, q_2, \ldots, q_N)$, where $q_i$, $i = 1, 2, \ldots, N$ are the solution of the linear system defined by eqs. (11.4). Because $\Pi$ is the minimum of the exact, infinite dimensional problem, whereas $\widetilde{\Pi}$ is the minimum of the approximate, finite dimensional problem, it is clear that $\Pi \leq \widetilde{\Pi}$. As the number of degrees of freedom of the approximate solution increases, better and better solutions should be obtained and $\widetilde{\Pi} \to \Pi$, but $\widetilde{\Pi}$ always remains larger or equal to $\Pi$.

Unfortunately there is no way, short of knowing the exact solution, of ascertaining how close $\widetilde{\Pi}$ is to $\Pi$, and hence, how good the approximate solution will be. Furthermore, from a structural designer's viewpoint, a good approximation is probably a safe approximation, *i.e.*, a conservative solution, which over-estimates deflections and stresses. Unfortunately, the procedure described above guarantees only that $\Pi \leq \widetilde{\Pi}$, but little can be said about other characteristics of the solution.

In practice, this shortcoming is overcome by performing a convergence study: a series of solutions is generated that involves an increasing number of degrees of freedom. As $N$ increases, $\widetilde{\Pi} \to \Pi$ and the solution converges to the exact solution. Typically, the displacement and stress fields are monitored, and when further increase in $N$ has little effect on the solution, it is said to be converged. These statements can be made more precise using advanced mathematical concepts that are beyond the scope of this book. More details can be found in references [8, 9].

From a practical viewpoint, it is desirable to select shape functions that closely approximate the actual displacement field. This is, of course, not easily done, because the solution is, in general, unknown. From a mathematical viewpoint, the shape functions should form a *complete set of functions*. The precise mathematical definition of this concept is beyond the scope of this book, but loosely speaking, it implies that as $N \to \infty$ a series of complete functions must be able to exactly reconstruct an arbitrary continuous function. For instance, it is well known from Fourier expansion theory that an arbitrary continuous function can be represented by an infinite series of trigonometric functions; this implies that trigonometric functions form a complete set. Selecting shape function that present orthogonality properties will also simplify the solution process.

The discussion presented in the previous paragraphs underlines the importance of a judicious choice of the shape function. In the procedure described here, the principle of minimum total potential energy is used with kinematically admissible virtual displacements. This means that all virtual displacements must satisfy the constraints of the problem, and in particular, the geometric boundary conditions. Each shape function is, in fact, a virtual displacement field. In eq. (11.3), consider the case where all degrees of freedom vanish except $q_1$. Shape function $h_1(x_1)$ then becomes the only virtual displacement field and, hence, must satisfy the geometric boundary conditions. By induction, it is easy to conclude that all shape functions must then individually satisfy these conditions. It is not required, however, that the shape functions satisfy the natural boundary conditions.

The following examples will focus on approximate solutions based on polynomial and trigonometric expansions. Polynomials are, in fact, solutions of certain beam problems. Trigonometric series are often convenient to use because they enable the term-by-term satisfaction of many types of geometric boundary, and in addition, the orthogonality properties of these series simplify the calculations of the degrees of freedom.

***Example 11.1. Polynomial solution for a cantilever beam with uniform load***
Consider a cantilever beam of length $L$ and bending stiffness $H_{33}^c$, subjected to a uniform transverse loading distribution, $p_0$, as shown in fig. 11.2. This problem is treated using the classical differential equation approach in example 5.7 on page 200.

For this cantilevered beam, the geometric boundary conditions require both deflection and slope to vanish at the root of the beam: $\bar{u}_2(0) = \mathrm{d}\bar{u}_2(0)/\mathrm{d}x_1 = 0$. A monomial approximation will be selected,

$$\bar{u}_2(x_1) = q_2 x_1^2,$$

where the first two terms of the series, $q_0$ and $q_1 x_1$, cannot be used because the corresponding shape functions, 1 and $x_1$, do not satisfy the geometric boundary conditions.

Using this approximation, the total potential energy of the system, eq. (11.2), becomes

$$\Pi = \frac{1}{2}\int_0^L H_{33}^c (2q_2)^2 \,\mathrm{d}x_1 - \int_0^L p_0 q_2 x_1^2 \,\mathrm{d}x_1 = \frac{1}{2} H_{33}^c (2q_2)^2 L - p_0 q_2 \frac{L^3}{3}.$$

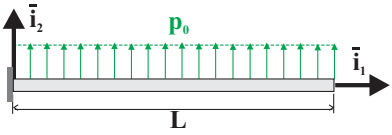


**Fig. 11.2.** Cantilevered beam subjected to a uniform lateral load.

The principle of minimum total potential energy now requires $\Pi(q_2)$ to be a minimum for the system to be in equilibrium. The necessary condition is: $\partial\Pi/\partial q_2 = 4H^c_{33}q_2L - p_0L^3/3 = 0$, and solving for $q_2$ yields $q_2 = (p_0L^2)/(12H^c_{33})$. The resulting solution for the transverse displacement field is then

$$\bar{u}_2(x_1) = \frac{p_0L^4}{12H^c_{33}}\eta^2,$$

where $\eta = x_1/L$ is the non-dimensional variable along the beam's span.

A more accurate approximate solution can be developed by adding an additional term to the approximation. To simplify the computation, it will be convenient to write the approximation as

$$\bar{u}_2(\eta) = q_2\eta^2 + q_3\eta^3,$$

where the shape functions are written in terms of the non-dimensional variable $\eta$. Performing the change of variable $x_1 = \eta L$, the strain energy in the beam, given by eq. (11.1), becomes

$$A = \frac{1}{2}\int_0^1 \frac{H^c_{33}}{L^3}(\bar{u}_2'')^2 \,\mathrm{d}\eta, \tag{11.5}$$

where the notation $(\cdot)'$ is used to indicate a derivative with respect to $\eta$. Introducing the assumed displacement field then yields the total potential energy as

$$\Pi = \frac{1}{2}\frac{H^c_{33}}{L^3}\int_0^1 (4q_2^2 + 36\eta^2q_3^2 + 24\eta q_2q_3)\,\mathrm{d}\eta - p_0L\int_0^1 (q_2\eta^2 + q_3\eta^3)\,\mathrm{d}\eta.$$

After integration, this expression becomes

$$\Pi = \frac{1}{2}\frac{H^c_{33}}{L^3}\left(4q_2^2 + \frac{36}{3}q_3^2 + \frac{24}{2}q_2q_3\right) - p_0L\left(\frac{q_2}{3} + \frac{q_3}{4}\right).$$

The total potential energy is now a function of the two degrees of freedom, $q_2$ and $q_3$, *i.e.*, $\Pi = \Pi(q_2, q_3)$. Minimization of the total potential then requires $\partial\Pi/\partial q_2 = 0$ and $\partial\Pi/\partial q_3 = 0$, yielding $(H^c_{33}/L^3)[4q_2 + 6q_3] - p_0L/3 = 0$ and $(H^c_{33}/L^3)[12q_3 + 6q_2] - p_0L/4 = 0$, respectively. These two algebraic equations form a set of linear equations; this becomes more obvious when the two equations are recast in matrix form as

$$\begin{bmatrix} 4 & 6 \\ 6 & 12 \end{bmatrix}\begin{Bmatrix} q_2 \\ q_3 \end{Bmatrix} = \frac{p_0l^4}{H^c_{33}}\begin{Bmatrix} 1/3 \\ 1/4 \end{Bmatrix}.$$

Solving this system of linear equations yields the two unknown coefficients, $q_2$ and $q_3$, and hence, the following approximate solution for the non-dimensional transverse displacement field is obtained

$$\frac{H_{33}^c \bar{u}_2(\eta)}{p_0 L^4} = \frac{1}{24}(5\eta^2 - 2\eta^3).$$

A still more accurate approximate solution can be developed by including another monomial in the approximation,

$$\bar{u}_2(\eta) = q_2\eta^2 + q_3\eta^3 + q_4\eta^4.$$

Note once again that each monomial individually satisfies the geometric boundary conditions of the problem. Introducing this assumed displacement field in the expression for the total potential energy leads to

$$\Pi = \frac{1}{2}\frac{H_{33}^c}{L^3}\int_0^1 (4q_2 + 6\eta q_3 + 12\eta^2 q_4)^2 \,\mathrm{d}\eta - p_0 L \int_0^1 (q_2\eta^2 + q_3\eta^3 + q_4\eta^4)\,\mathrm{d}\eta.$$

The first task is to expand the square under the first integral, and the second to evaluate all integrals. The total potential energy then becomes a quadratic expression of the degrees of freedom, *i.e.*, $\Pi = \Pi(q_2, q_3, q_4)$. Minimization of the total potential requires conditions (11.4), leading to a set of three simultaneous linear equations of the three degrees of freedom of the problem, $q_2$, $q_3$ and $q_4$. Here again, it is convenient to recast the resulting equations in a matrix form as

$$\begin{bmatrix} 4 & 6 & 8 \\ 6 & 12 & 18 \\ 8 & 18 & 144/5 \end{bmatrix} \begin{Bmatrix} q_2 \\ q_3 \\ q_4 \end{Bmatrix} = \frac{p_0 L^4}{H_{33}^c} \begin{Bmatrix} 1/3 \\ 1/4 \\ 1/5 \end{Bmatrix}.$$

Solving this system of linear equations yields the following approximate solution for the transverse displacement field

$$\bar{u}_2(\eta) = \frac{1}{24}\frac{p_0 L^4}{H_{33}^c}(6\eta^2 - 4\eta^3 + \eta^4).$$

Comparing this expression with that obtained in example 5.7 on page 200 using the classical differential equation approach, it appears that the exact solution of the problem has now been obtained. The principle of minimum total potential energy does not actually indicate that an exact solution has been obtained; it is only possible to ascertain this fact here because the exact solution for this problem was previously obtained by another method. If additional terms are taken in the series solution, it will be found that their coefficients are all zero. For instance, assuming a solution such as $\bar{u}_2(\eta) = q_2\eta^2 + q_3\eta^3 + q_4\eta^4 + q_5\eta^5$ will yield identical results to those found above but with $q_5 = 0$. The fact that an exact solution is found here is fortuitous; the exact solution happens to be of a polynomial form, and that same form is used for the assumed solution.

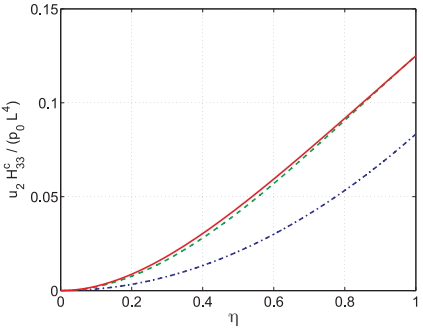


**Fig. 11.3.** Non-dimensional transverse displacement field for the cantilevered beam. Solid line: three-term polynomial solution (exact solution); dashed line: two-term approximation; dashed-dotted line: single-term approximation.

It is interesting to compare the solutions obtained from the three approximations investigated here. Figure 11.3 shows the non-dimensional transverse displacement fields, $\bar{u}_2 H^c_{33}/(p_0 L^4)$, obtained with the three approximations. As expected, the single term approximation is very inaccurate; the stiffness of the beam is overestimated because it is limited to deform into the parabolic shape implied by the shape function $x_1^2$. In fact, the tip deflection is 33% smaller than that of the exact solution. The two term approximation is noticeably better; at the tip of the beam, the transverse deflection is exact, although at all other points, the solution is not exact. The fact that the exact solution is obtained at the tip of the beam is purely fortuitous.

Although the two-term approximation produces a transverse displacement field that is in close agreement with the exact solution, as shown in fig. 11.3, the associated predictions for the internal bending moment and shear force distributions are not nearly as good. Figure 11.4 shows the distributions of non-dimensional bending moments, $M_3/(p_0 L^2)$, obtained with the three approaches. Large errors are observed over the entire span of the beam for the two approximate solutions. Furthermore, the natural boundary condition at the tip of the beam, $M_3 = 0$, is not satisfied by the approximate solutions. The same observations can be made concerning the distribution of non-dimensional shear force, $T_2/(p_0 L)$, depicted in fig. 11.5.

***Example 11.2. Simply supported beam under uniform loading***

A simply supported beam of length $L$ and bending stiffness $H^c_{33}$ is subjected to a uniformly distributed load $p_0$, as depicted in fig. 11.6. This problem is treated using the classical differential equation approach in example 5.7 on page 200, which gives the exact solution for the transverse displacement field in a simple polynomial form.

The geometric boundary conditions for this problem are $\bar{u}_2(0) = \bar{u}_2(L) = 0$, and hence, the shape functions to be selected must satisfy the conditions $h_i(0) = h_i(L) = 0$. The monomial shape functions selected in the previous example, $h_i(x_1) = x_1^i$, are not suitable for this problem because while $h_i(0) = 0^i = 0$, it is clear that $h_i(L) = L^i \neq 0$. A convenient way to satisfy this requirement is to select as the shape functions a set of periodic functions such as sine functions with

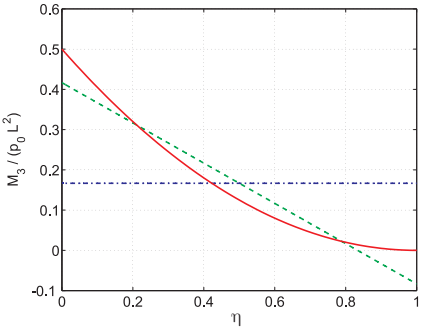


**Fig. 11.4.** Non-dimensional bending moment field for the cantilevered beam. Solid line: three-term polynomial solution (exact solution); dashed line: two-term approximation; dash-dotted line: single-term approximation.

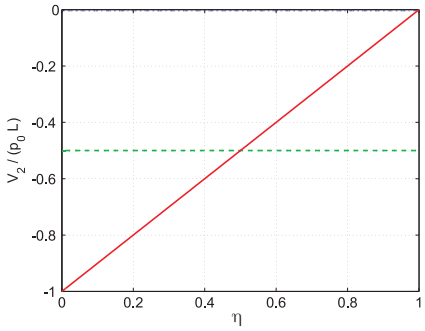


**Fig. 11.5.** Non-dimensional shear force field for the cantilevered beam. Solid line: three-term polynomial solution (exact solution); dashed line: two-term approximation; dash-dotted line: single-term approximation.

increasing wave numbers

$$\bar{u}_2(x_1) = \sum_{n=1}^{N} q_n \sin\frac{n\pi x_1}{L} = \sum_{n=1}^{N} q_n \sin n\pi\eta, \tag{11.6}$$

where $\eta = x_1/L$ is the non-dimensional variable along the beam's span.

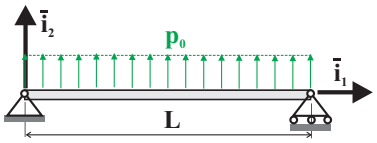


**Fig. 11.6.** Simply-supported beam subjected to a uniform lateral load.

With the help of eq. (11.5) and using the notation $(\cdot)'$ to indicate a derivative with respect to $\eta$, the strain energy in the beam becomes

$$\begin{aligned} A &= \frac{H^c_{33}}{2L^3}\int_0^1 (\bar{u}_2'')^2\,\mathrm{d}\eta = \frac{H^c_{33}}{2L^3}\int_0^1 \left[-\sum_{n=1}^{N} q_n (n\pi)^2 \sin n\pi\eta\right]^2 \mathrm{d}\eta \\ &= \frac{H^c_{33}}{2L^3}\int_0^1 \left[-\sum_{m=1}^{N} q_m (m\pi)^2 \sin m\pi\eta\right]\left[-\sum_{n=1}^{N} q_n (n\pi)^2 \sin n\pi\eta\right] \mathrm{d}\eta \\ &= \frac{H^c_{33}}{2L^3}\sum_{m=1}^{N}\sum_{n=1}^{N} q_m q_n (m\pi)^2 (n\pi)^2 \int_0^1 \sin m\pi\eta \sin n\pi\eta\,\mathrm{d}\eta. \end{aligned}$$

At first glance, this expression appears to be very complicated because of the presence of the double summation. The sine functions, however, enjoy the orthogonality property stated in eq. (A.45a), and hence, the strain energy in the beam reduces to a single summation,

$$A = \frac{H_{33}^c}{4L^3} \sum_{n=1}^{N} (n\pi)^4 q_n^2.$$

The potential of the externally applied loads, $p_2(x_1) = p_0$, is the negative of the work done and can be written as

$$\Phi = -\int_0^L p_0\, \bar{u}_2 \, \mathrm{d}x_1 = -p_0 L \int_0^1 \sum_{n=1}^{N} q_n \sin n\pi\eta \, \mathrm{d}\eta = -2p_0 L \sum_{n=\mathrm{odd}}^{N} \frac{q_n}{n\pi}.$$

Note that for even wave numbers, *i.e.*, for even values of $n$, the integrals of the sine function from 0 to 1 vanish. Hence, only the odd values of $n$ remain in the expression for the potential.

The total potential energy, $\Pi$, now simply becomes a function of the degrees of freedom, $q_i$, $i = 1, 2, \ldots, N$, and the principle of minimum total potential energy requires that

$$\frac{\partial \Pi}{\partial q_i} = \frac{\partial A}{\partial q_i} + \frac{\partial \Phi}{\partial q_i} = \begin{cases} H_{33}^c/(2L^3)(i\pi)^4 q_i = 0, & i \text{ even}, \\ H_{33}^c/(2L^3)(i\pi)^4 q_i - (2p_0 L)/(i\pi) = 0, & i \text{ odd}. \end{cases}$$

This means that $q_i = 0$ for all even values of $i$, whereas $q_i = 4(p_0 L^4/H_{33}^c)/(i\pi)^5$ for all odd values of $i$. The transverse displacement field is then

$$\bar{u}_2(\eta) = \frac{4}{\pi^5} \frac{p_0 L^4}{H_{33}^c} \sum_{n=odd}^{N} \frac{1}{n^5} \sin n\pi\eta.$$

Since $|\sin(n\pi\eta)| \leq 1$, the convergence of the series is very rapid, due to the presence of the factor $n^5$ in the denominator. It is interesting to note that the exact solution of the problem given by eq. 5.48 is a simple polynomial, whereas the present approximate solution is in the form of an infinite series.

Intuitively, the maximum transverse deflection is found at the beam's mid-span, *i.e.*, at $\eta = 0.5$, where the exact solution gives $H_{33}^c \bar{u}_2(0.5)/(p_0 L^4) = 5/384 = 0.01302$. Considering a single term in the above series yields $H_{33}^c \bar{u}_2(0.5)/(p_0 L^4) = 4/\pi^5 = 0.01307$, which is only 0.39% from the exact solution. As additional terms of the series are added, the solution rapidly converges to the exact answer, as shown in fig. 11.7, which plots the relative error associated with the approximate solution as $N$ increases. Clearly, very accurate approximations are obtained with just a few terms of the series. It should be noted that the shape functions selected here each satisfy the natural boundary conditions of the problem, $M_3(0) = M_3(L) = 0$. While this is not a requirement for the solution process, it generally leads to closer agreement with the exact solution.

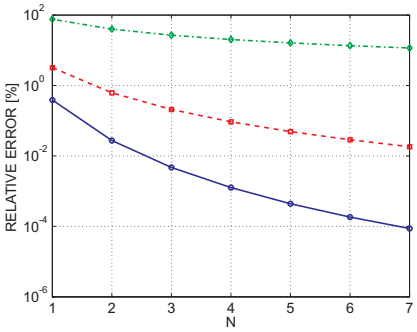


**Fig. 11.7.** Relative error of the approximate solution compared to the exact solution. Solid line: mid-span transverse displacement (○); dashed line: mid-span bending moment (□); dash-dotted line: root shear force (◊).

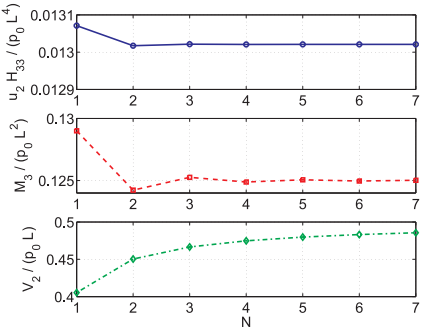


**Fig. 11.8.** Convergence of approximate solution as a function of the number of degrees of freedom. Solid line: mid-span transverse displacement (○); dashed line: mid-span bending moment (□); dash-dotted line: root shear force (◊).

Once the transverse displacement field is found, the moment distribution is readily obtained as

$$M_3(\eta) = \frac{H^c_{33}}{L^2}\bar{u}_2''(\eta) = -\frac{4}{\pi^3}p_0L^2\sum_{n=\text{odd}}^{N}\frac{1}{n^3}\sin n\pi\eta.$$

The maximum bending moment is found at the beam's mid-span, where the exact solution gives $M_3(0.5)/(p_0L^2) = -1/8 = -0.125$. Considering a single term in the series yields $M_3(0.5)/(p_0L^2) = -4/\pi^3 = -0.129$, which is 3.2% from the exact solution. As additional terms of the series are used, the error is reduced as shown in fig. 11.7, although the convergence is not nearly as rapid as that observed for the transverse deflection. Finally, the shear force distribution in the beam is obtained from eq. (5.38) as

$$V_2(\eta) = -\frac{1}{L}M_3'(\eta) = \frac{4}{\pi^2}p_0L\sum_{n=\text{odd}}^{N}\frac{1}{n^2}\cos n\pi\eta.$$

The maximum shear force is found at the end supports; for instance, at $\eta = 0$, the exact shear force is $V_2/(p_0L) = 0.5$, whereas the single term in the above series yields $V_2/(p_0L) = 4/\pi^2 = 0.405$, which is 18.9% from the exact solution. Figure 11.7 shows the reduction in error of the root shear force predictions as an increasing number of terms is used in the series.

Clearly, the convergence rates of the bending moment and shear force predictions are far slower than those observed for the transverse displacement. This is a general feature of the approximate solutions obtained with the Rayleigh-Ritz method. This is easily understood by noting that the internal forces and moments are obtained by

taking derivatives of the approximated displacement field. The bending moment is a second derivative of the displacement field, the shear force a third derivative. The accuracy of the predictions decreases as the order of the derivative increases. The results shown in fig. 11.7 clearly demonstrate this effect.

Figure 11.7 is referred to as a *convergence plot* because it demonstrates the convergence of the approximate solution to the exact solution of the problem. Such plot, however, assumes that the exact solution is known, because the relative error, the difference between the approximate and exact solutions, normalized by the exact solution, must be evaluated. In practical situations, the exact solution is not known, and hence, it is not possible to compute a relative error. In that case, approximate solutions are evaluated based on an increasing number of shape functions and are plotted against the number of degree of freedom. Figure 11.8 shows such a plot for the problem at hand. As the number of degrees of freedom increases, the solutions stabilize to a horizontal asymptote, which is presumed to be the exact solution.

If $\bar{u}_2^{(N)}$ is the approximate mid-span transverse displacement obtained with $N$ degrees of freedom, the accuracy of the approximate solution can be assessed in an ad-hoc manner by considering the following convergence criterion $(\bar{u}_2^{(N)} - \bar{u}_2^{(N-1)})/\bar{u}_2^{(N)} < \epsilon$, which compares the solutions obtained with $N-1$ and $N$ degrees of freedom; if $\epsilon$ is a small number, the satisfaction of the criterion implies that increasing the number of degrees of freedom has little effect on the solution. It is important to understand that such a criterion provides a good indication that the approximate solution is close to the exact solution, but is by no means a proof.

***Example 11.3. Discussion of the requirements for shape functions***

The Rayleigh-Ritz method presented here relies on the principle of minimum total potential energy using kinematically admissible virtual displacements. Consequently, the shape functions must satisfy the geometric boundary conditions of the problem. If these conditions are not satisfied by the shape functions, erroneous solutions will result.

Consider once again the simply supported beam of length $L$ and bending stiffness $H_{33}^c$ subjected to a uniformly distributed load $p_0$, as depicted in fig. 11.6. In view of the exact solution of this problem given by eq. (5.48), it is tempting to explore a solution in the following polynomial form with $\eta = x_1/L$

$$\bar{u}_2(\eta) = q_1\eta + q_3\eta^3 + q_4\eta^4.$$

Introducing this assumed displacement field in the expression for the total potential energy leads to

$$\Pi = \frac{1}{2}\frac{H_{33}^c}{L^3}\int_0^1 36(q_3\eta + 2q_4\eta^2)^2\,\mathrm{d}\eta - p_0 L\int_0^1 (q_1\eta + q_3\eta^3 + q_4\eta^4)\,\mathrm{d}\eta.$$

Performing all integrations and imposing the conditions (11.4) for the minimization of the total potential energy leads to the following set of linear equations

$$\begin{bmatrix} 0 & 0 & 0 \\ 0 & 12 & 18 \\ 0 & 18 & 144/5 \end{bmatrix} \begin{Bmatrix} q_1 \\ q_3 \\ q_4 \end{Bmatrix} = \frac{p_0 L^4}{H_{33}^c} \begin{Bmatrix} 1/2 \\ 1/4 \\ 1/5 \end{Bmatrix}.$$

Obviously, it is not possible to solve this linear system because the system matrix is singular: indeed, first row and column vanish. This arises because the first shape function, $\eta$, represents a rigid body motion for the beam corresponding to a rotation of the beam about the left support.

By definition, rigid body motions generate no strains, and hence, no strain energy. Indeed, the associated curvature of the beam is $\kappa_3 = \bar{u}_2''/L^2 = (\eta)''/L^2 = 0$, and hence, the first degree of freedom, $q_1$, does not appear in the expression for the strain energy, resulting in the vanishing of the first row and column of the system matrix. Of course, selecting this rigid body motion as a shape function is not correct, because this rigid body motion does not satisfy the geometric boundary condition $h(\eta = 1) = 0$.

Consider next a solution of the following form: $\bar{u}_2(\eta) = q_3\eta^3 + q_4\eta^4$, in which the rigid body mode is ignored. Proceeding as above will lead to a system of two linear equations for degrees of freedom $q_3$ and $q_4$. The corresponding system of equations is obtained by eliminating the first row and column of the above system, which is then readily solved for the unknowns and leads to the following approximate solution: $H^c_{33}\bar{u}_2(\eta)/(p_0L^4) = (12\eta^3 - 7\eta^4)/72$. This solution is obviously incorrect because it violates the geometric boundary condition at the beam's tip: $H^c_{33}\bar{u}_2(\eta = 1)/(p_0L^4) = 5/72 \neq 0$. Clearly, when deriving approximate solutions using the principle of minimum total potential energy, the solution process is unaware of the geometric boundary conditions applied to the problem unless they are specifically imposed on each of the shape functions.

The exact solution of the problem, see eq. (5.48), can be written as $H^c_{33}\bar{u}_2/(p_0L^4) = (\eta - 2\eta^3 + \eta^4)/24$. Note that the individual terms, $\eta$, $\eta^3$, and $\eta^4$, do not satisfy the geometric boundary conditions, while the complete solution does: $\bar{u}_2(0) = \bar{u}_2(1) = 0$. It is interesting to factor the exact solution as $H^c_{33}\bar{u}_2/(p_0L^4) = \eta(1-\eta)(1+\eta-\eta^2)/24$, which now shows the satisfaction of the geometric boundary conditions, $\bar{u}_2(0) = \bar{u}_2(1) = 0$.

This suggests that the following polynomial approximation is suitable for the application of the principle of minimum total potential energy to simply supported beam problems: $\bar{u}_2(\eta) = \eta(1-\eta)q_1 + \eta^2(1-\eta)q_2 + \eta^3(1-\eta)q_3 + \ldots$, where the shape functions are selected as

$$h_i = \eta(1-\eta)\,\eta^{i-1}, \quad i = 1, 2, \ldots, N. \tag{11.7}$$

Clearly, each shape function now individually satisfies the requirements $h_i(0) = h_i(1) = 0$ for all values of $i$. It will be left to the reader to verify that good solutions are obtained with the above polynomial shape functions, and for $N = 3$, the exact solution is recovered.

Consider next a beam clamped at both end. The associated geometric boundary conditions are $\bar{u}_2(0) = \bar{u}_2'(0) = 0$, and $\bar{u}_2(1) = \bar{u}_2'(1) = 0$. Note that the sine functions, $h_i(\eta) = \sin i\pi\eta$, are not admissible because although $h_i(0) = h_i(1) = 0$, the slope is not zero: $h_i'(0) \neq 0$ and $h_i'(1) \neq 0$. Using cosine functions, $h_i(\eta) = \cos i\pi\eta$, is not valid either, because $h_i(0) \neq 0$ and $h_i(1) \neq 0$, although $h_i'(0) = h_i'(1) = 0$. By analogy to the polynomial shape functions proposed in eq. (11.7) for

simply supported beams, a suitable set of shape functions for a beam clamped at both ends is

$$h_i = \eta^2(1-\eta)^2\,\eta^{i-1}, \quad i = 1, 2, \ldots, N. \tag{11.8}$$

If trigonometric shape functions are desired, it is easy to verify that the following expressions satisfy the geometric boundary conditions

$$h_i = \cos(i-1)\pi\eta - \cos(i+1)\pi\eta, \quad i = 1, 2, \ldots, N. \tag{11.9}$$

It will be left to the reader to combine the shape function given in the previous equations to find suitable shape functions to analyze problems involving a combination of the boundary conditions discussed above, for example, a cantilevered beam with a tip support.

***Example 11.4. Simply supported beam with concentrated load***
Consider now a simply supported beam of length $L$ subjected to a concentrated load $P$ at a distance $\alpha L$ from its root, as shown in fig. 11.9. This problem is treated using the classical differential equation approach in example 5.5 on page 197, and then again in example 5.6 on page 199 by first evaluating the bending moment distribution. The concentrated load introduces a discontinuity in the shear force diagram which complicates the classical differential equation approach by requiring the solution to be separately computed over two regions of the beam.

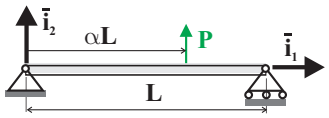


**Fig. 11.9.** Simply-supported beam subjected to a concentrated transverse load.

For this problem, the sine series,

$$\bar{u}_2(\eta) = \sum_{n=1}^{N} q_n \sin n\pi\eta,$$

used in example 11.2 is suitable because each sine function satisfies the geometric boundary conditions. The total potential energy of the system now becomes

$$\Pi = \frac{H^c_{33}}{2L^3}\int_0^1 \left[-\sum_{n=1}^{N} q_n (n\pi)^2 \sin n\pi\eta\right]^2 \mathrm{d}\eta - P\sum_{n=1}^{N} q_n \sin n\pi\alpha.$$

Rather than performing the integrals indicated in this expression, it is also possible to first write the conditions for minimization of the total potential energy, eqs. (11.4). This then leads to

$$\frac{\partial \Pi}{\partial q_i} = \frac{H^c_{33}}{2L^3}\int_0^1 2\left[\sum_{n=1}^{N} q_n (n\pi)^2 \sin n\pi\eta\right]\left[(i\pi)^2 \sin i\pi\eta\right]\,\mathrm{d}\eta - P\sin i\pi\alpha = 0,$$

where the order of the partial derivative and integral operators have been interchanged according to Leibniz' integral rule. Rearranging the individual terms then yields

$$\frac{H^c_{33}}{L^3}(i\pi)^2\left[\sum_{n=1}^{N} q_n(n\pi)^2\int_0^1 \sin n\pi\eta \sin i\pi\eta \,\mathrm{d}\eta\right] - P\sin i\pi\alpha = 0.$$

Again, because the sine functions enjoy the orthogonality properties expressed by eq. (A.45a), the integral reduces to $\delta_{ni}/2$, where $\delta_{ni}$ is the Kronecker delta defined in eq. (A.44). Because the Kronecker delta vanishes for all values of $n \neq i$, only a single term of the sum remains and the above expression reduces to

$$\frac{H^c_{33}}{2L^3}(i\pi)^4 q_i - P\sin i\pi\alpha = 0, \quad i = 1, 2, \ldots N.$$

These equations are readily solved to find $q_i$, and the transverse deflection field is now

$$\bar{u}_2(x_1) = \frac{2}{\pi^4}\frac{PL^3}{H^c_{33}}\sum_{n=1}^{N}\frac{1}{n^4}\sin n\pi\alpha \sin n\pi\eta.$$

Figure 11.10 shows the transverse displacement field calculated using the above series for $N$ = 1, 3 and 24, when $\alpha = 0.25$. Note the very rapid convergence of the results to the exact solution provided by eq. (5.51).

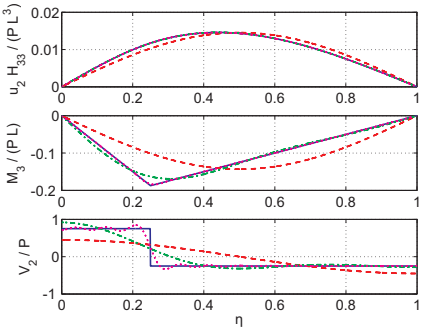


**Fig. 11.10.** Simply-supported beam subjected to a concentrated transverse load. Top figure: transverse displacement, $\bar{u}_2 H^c_{33}/(PL^3)$; middle figure: bending moment, $M_3/(PL)$; lower figure: shear force, $V_2/P$. Exact solution: solid line; single term solution: dashed line; three-term solution: dash-dotted line; 24-term solution: dotted line.

The bending moment and shear force distributions can be obtained from derivatives of the displacement field and are also shown in fig. 11.10. As expected, the convergence rates for the predictions of the internal bending moment and shear force distributions are slower than those observed for the displacement field.

The shear force distribution presents a discontinuity at the location of application of the concentrated force. The approximate solution is, of course, unable to capture

this discontinuity, because the displacement field is assumed to be the superposition of continuous, trigonometric functions; the bending moment and shear force distributions, obtained by successive derivatives of the displacement field, are continuous functions as well. Even when $N = 24$, large errors are still observed near the discontinuity of the shear force. The slow convergence of Fourier series near a discontinuity is known as the Gibbs phenomenon.

***Example 11.5. Cantilever beam with tip support***

Consider a cantilevered beam of length $L$ with a tip support, subjected to a uniformly distributed load, $p_0$, as shown in fig. 11.11. This problem is treated using the classical differential equation approach in example 5.11 on page 205. Unlike the previous examples, this problem is hyperstatic, but this does not affect the Rayleigh-Ritz approximation procedure.

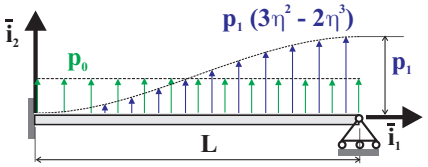


**Fig. 11.11.** Cantilever beam with tip support subjected to two different loading conditions.

In view of the discussion presented in example 11.3, an appropriate set of shape functions that satisfy the geometric boundary conditions for this problem is given by $h_i = \eta^2(1-\eta)\eta^{i-1}$, $i = 1, 2, \ldots, N$. Two terms of this series will be used for this problem

$$\bar{u}_2(\eta) = \eta^2(1-\eta)\, q_1 + \eta^2(1-\eta)\eta\, q_2.$$

The total potential energy of the system is now evaluated using the approximate solution to find

$$\Pi = \frac{1}{2}\frac{H^c_{33}}{L^3}\int_0^1 \left[(2-6\eta)q_1 + (6\eta - 12\eta^2)q_2\right]^2 \mathrm{d}\eta$$
$$-p_0 L \int_0^1 \left[(\eta^2-\eta^3)q_1 + (\eta^3-\eta^4)q_2\right] \mathrm{d}\eta.$$

After expanding the square under the first integral, and evaluating all integrals, the total potential energy becomes a quadratic expression of the degrees of freedom.

Minimization of the total potential leads to the conditions given in eq. (11.4), and the following set of linear equations results

$$\begin{bmatrix} 4 & 4 \\ 4 & 24/5 \end{bmatrix} \begin{Bmatrix} q_1 \\ q_2 \end{Bmatrix} = \frac{p_0 L^4}{H^c_{33}} \begin{Bmatrix} 1/12 \\ 1/20 \end{Bmatrix}.$$

Solving this system of linear equations yields the following approximate solution for the transverse displacement field

$$\bar{u}_2(\eta) = \frac{1}{48}\frac{p_0 L^4}{H_{33}^c}\eta^2(1-\eta)(3-2\eta).$$

In fact, this is the exact solution of the problem, as can be ascertained by comparing this result to the exact solution given in eq. (5.61).

It is often the case that a particular structural problem must be solved for a variety of loading conditions. For instance, the stresses in an aircraft wing must be computed for level flight loading, but also for a variety of maneuver cases. The procedure developed here provides an elegant solution to this problem because if only the loading is changed, only the external potential energy must be recalculated. To illustrate, let the same beam be subjected to a new transverse distributed load, $p_2(\eta) = p_1(3\eta^2 - 2\eta^3)$, depicted in fig. 11.11. The total potential energy of the system is now evaluated as

$$\Pi = \frac{1}{2}\frac{H_{33}^c}{L^3}\int_0^1 \left[(2-6\eta)q_1 + (6\eta - 12\eta^2)q_2\right]^2 \mathrm{d}\eta$$
$$-p_0 L\int_0^1 (3\eta^2 - 2\eta^3)\left[(\eta^2-\eta^3)q_1 + (\eta^3-\eta^4)q_2\right]\mathrm{d}\eta.$$

Note that the expression for the strain energy in the structure is unchanged, and the only difference is in the potential of the externally applied load. Proceeding as before, the following set of linear equations for the degrees of freedom, $q_1$ and $q_2$, is found

$$\begin{bmatrix} 4 & 4 \\ 4 & 24/5 \end{bmatrix}\begin{Bmatrix} q_1 \\ q_2 \end{Bmatrix} = \frac{p_0 L^4}{H_{33}^c}\begin{Bmatrix} 11/210 \\ 1/28 \end{Bmatrix}.$$

Comparing this system of equations to that obtained above, it is clear that changing the externally applied load only modifies the right-hand side of the equations, which, for obvious reasons, is often called the *load array*. Within the framework of this approach, different loading cases are associated with different load arrays. The left-hand side system matrix needs to be inverted only once, and multiplication of the inverse by the various different load arrays then yields the desired approximate solutions for each of the loading cases. For the loading case at hand, the approximate solution is

$$\bar{u}_2(\eta) = \frac{1}{1680}\frac{p_1 L^4}{H_{33}^c}\eta^2(1-\eta)(57-35\eta).$$

The exact solution of the problem can be obtained using the classical differential equation approach as $\bar{u}_2 = p_1 L^4/H_{33}^c\,\eta^2(1-\eta)(2\eta^4 - 5\eta^3 - 5\eta^2 - 5\eta + 24)/840$. It is left to the reader to compare the exact and approximate solutions of this problem. If necessary, the approximation could be improved by increasing the number of degrees of freedom.

***Example 11.6. Simply supported beam with two elastic springs***

A simply supported beam of span $L$ is supported by two springs of stiffness constant $k$ located at stations equidistant from the two ends, and it is subjected to a uniform transverse loading, $p_0$, as depicted in fig. 11.12. To simplify the formulation of the shape functions, it will be convenient to locate the origin of the axes at the beam's

mid-span. The springs are located at stations $x_1 = \pm(1-2\alpha)L/2 = \pm\beta L/2$, where $\beta = 1 - 2\alpha$ is the non-dimensional location of the spring. The two springs model intermediate supports for the beam that are not infinitely rigid, but rather, present a flexibility that is modeled by the spring stiffness constant $k$; as $k$ approaches infinity, these intermediate supports become rigid supports.

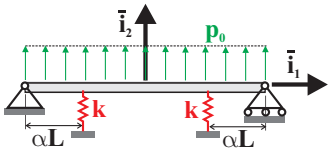


**Fig. 11.12.** Simply-supported beam with two elastic springs.

This hyperstatic problem is treated using the classical differential equation approach in example 5.13 on page 208. When using the Rayleigh-Ritz method, springs are treated as elastic components much as the beam itself. The strain energy in the structure is now the sum of the strain energy due to bending of the beam, $A_b$, and that due to deformation of the springs, $A_s$. The total strain energy of the structure becomes

$$A = A_b + A_s = \frac{1}{2}\int_0^L H_{33}^c \left(\frac{\mathrm{d}^2\bar{u}_2}{\mathrm{d}x_1^2}\right)^2 \mathrm{d}x_1 + \frac{1}{2}k\bar{u}_2^2\Big|_{-\beta L/2} + \frac{1}{2}k\bar{u}_2^2\Big|_{\beta L/2},$$

where the last two terms represent the strain energy in the springs computed using eq. (10.21).

For this problem, an approximate solution of the following form will be used

$$\bar{u}_2(\eta) = (1-\eta^2)q_1 + (1-\eta^2)\eta^2 q_2 + (1-\eta^2)\eta^4 q_3,$$

where $\eta = 2x_1/L$ is the non-dimensional variable along the beam's span. In view of the symmetry of the problem, only the even powers of $\eta$ are included. The strain energy of the structure now becomes

$$A = \frac{1}{2}\frac{8H_{33}^c}{L^3}\int_{-1}^{+1}\left[-2q_1 + (2-12\eta^2)q_2 + (12\eta^2 - 30\eta^4)q_3\right]^2 \mathrm{d}\eta$$
$$+ \frac{1}{2}k(1-\beta^2)^2\left(q_1 + \beta^2 q_2 + \beta^4 q_3\right)^2 + \frac{1}{2}k(1-\beta^2)^2\left(q_1 + \beta^2 q_2 + \beta^4 q_3\right)^2.$$

Note that the strain energies for the left and right springs are identical because of the symmetry of the problem. The potential energy of the externally applied load can be evaluated as is done in the previous examples.

After expanding the square under the first integral and evaluating all integrals, the total potential energy becomes a quadratic expression of the three degrees of freedom, *i.e.*, $\Pi = \Pi(q_1, q_2, q_3)$. Minimization of the total potential energy leads to eqs. (11.4), and finally, to the following set of linear equations

$$\left[16\begin{bmatrix}4 & 4 & 4\\ 4 & \frac{84}{5} & \frac{1956}{105}\\ 4 & \frac{1956}{105} & \frac{8172}{315}\end{bmatrix}+2\bar{k}(1-\beta^2)^2\begin{bmatrix}1 & \beta^2 & \beta^4\\ \beta^2 & \beta^4 & \beta^6\\ \beta^4 & \beta^6 & \beta^8\end{bmatrix}\right]\begin{Bmatrix}q_1\\ q_2\\ q_3\end{Bmatrix}=\frac{2p_0L^4}{H_{33}^c}\begin{Bmatrix}\frac{1}{3}\\ \frac{1}{15}\\ \frac{1}{35}\end{Bmatrix},$$

where $\bar{k}=kL^3/H_{33}^c$ is the non-dimensional spring stiffness constant.

Figure 11.13 shows the transverse displacement field for $\alpha=0.3$ and $\bar{k}=10^2$; a good correlation with the exact solution, see eq. (5.65), is obtained with the three-term approximate solution derived here. As the stiffness constant increases, the approximation becomes increasingly poorer, as shown in fig. 11.14, which gives the transverse displacement field for $\alpha=0.3$ and $\bar{k}=10^4$. To remedy the situation, a larger number of degrees of freedom would be needed in the approximate solution.

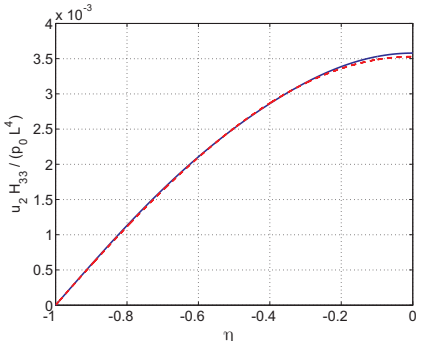


**Fig. 11.13.** Transverse displacement over left half-span of beam under uniform load for $\bar{k}=10^2$. Solid line: exact solution; dashed line: three-term approximate solution.

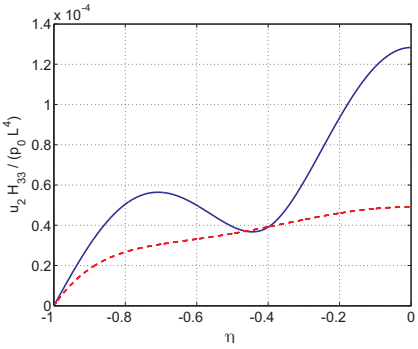


**Fig. 11.14.** Transverse displacement over left half-span of beam under uniform load for $\bar{k}=10^4$. Solid line: exact solution; dashed line: three-term approximate solution.

It is left to the reader to compute the bending moment and shear force distributions in the beam. Intuitively, the shear force distribution presents a discontinuity at the location of the spring, and the discrete change in the shear force from the right to the left of the spring equals the force in the spring. The approximate solution developed here is based on continuous shape functions, and hence, very slow convergence should be expected for the approximate shear force distribution.

### 11.2.4 Problems

**Problem 11.1. Beam with various end conditions**

Consider a beam of length $L$ extending from $\eta=0$ to $\eta=1$, where $\eta=x_1/L$. At each end of the beam, the boundary conditions could be cantilevered, simply-supported, or free, for a total of nine possible combinations. *(1)* Write a set of polynomial shape functions that is suitable for each of the nine cases. *(2)* If the beam of length $L$ extends from $\eta=-1$ to $\eta=1$, where $\eta=2x_1/L$, write the corresponding shape functions for each case.

**Problem 11.2. Cantilever with tip load: polynomial solution**
Consider a cantilever beam of length $L$ and bending stiffness $H_{33}^c$ subjected to a transverse concentrated load, $P$, acting at the beam's tip. *(1)* Construct a one-term monomial solution, $\bar{u}_2(\eta) = \eta^2 q_1$, and compare the computed tip displacement to the exact value of $PL^3/(3H_{33}^c)$. *(2)* Construct a two-term monomial solution, $\bar{u}_2(\eta) = \eta^2 q_1 + \eta^3 q_2$, and compare this with the exact value. *(3)* Compute the bending moment $M_3$ and the shear $V_2$ at the root using the two-term solution and compare these values to the exact values, which can readily be determined from statics.

**Problem 11.3. Cantilever with tip load: trigonometric solution**
Consider a cantilever beam of length $L$ and bending stiffness $H_{33}^c$ subjected to a transverse concentrated load, $P$, acting at the beam's tip. *(1)* Explain why the series, $\bar{u}_2(\eta) = \sum_{i=1}^{N} q_i(1-\cos i\pi\eta/2)$, provides a good approximate solution. *(2)* Compute an approximate solution to the problem based on this series for arbitrary $N$. *(3)* Compare your approximate solution with $N$ = 1 and 2 with the exact solution at the beam's tip. *(4)* Compare the root bending moments computed from the approximate solutions with the exact solution computed directly from statics.

**Problem 11.4. Cantilever beam with elliptical pressure load**
Consider a cantilever beam of length $L$ and bending stiffness $H_{33}^c$ subjected to a transverse distributed load $p_2(\eta) = p_0\sqrt{1-\eta^2}$ that simulates the aerodynamic load acting on an aircraft wing of semi-span $L$. *(1)* Develop a one-term approximate solution and compare the tip deflection with the exact result determined using the unit load method. *(2)* Repeat the development for a two-term solution. Hint: follow the approach and shape functions used in example 11.1

**Problem 11.5. Cantilever with tip support and rotational tip spring**
Consider a cantilever beam of length $L$ and bending stiffness $H_{33}^c$ featuring a pinned tip support and rotational spring of stiffness constant $k$, as shown in fig. 11.15. *(1)* Develop a three-term approximate solution. Use the non-dimensional tip rotational spring stiffness constant $\bar{k} = kL/H_{33}^c$. Hint: follow the approach and shape functions used in example 11.5.

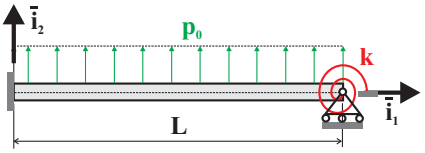


**Fig. 11.15.** Cantilevered beam with tip support and rotational spring under uniform load.

## 11.3 The strong and weak statements of equilibrium

When dealing with elastic structures, Newtonian equilibrium conditions typically are in the form of differential equations which impose the vanishing of the sums of all forces and moments on a differential element of the structure. This direct application of Newton's law leads to equilibrium equations that are referred to the *strong statement of equilibrium*. Equations (1.4) represent the strong statement of equilibrium

for a three-dimensional solid, and the strong statement of equilibrium for a beam under axial loads is given by eq. (5.18). In the next section, the *weak statement of the equilibrium* will be developed for a beam under axial loading. The term "weak" does not imply a less rigorous formulation, but rather refers to the fact that solutions may be found with less demanding, or *weaker continuity requirements*.

### 11.3.1 The weak form for beams under axial loads

Consider a beam fixed at one end and subjected to distributed axial loads, $p_1(x_1)$, and a concentrated load, $P_1$, at the free end as depicted in fig 11.16. In section 5.4, the differential equation of equilibrium of a beam under axial loads is derived as eq. (5.18) which holds for all points over the span of the beam, *i.e.*, for $0 \leq x_1 \leq L$. At the loaded end of the beam, equilibrium requires the internal force to equal the externally applied load, $N_1(L) = P_1$. These two equilibrium requirements, one applicable over the entire span of the beam the other at its tip, are known as the *strong statement of equilibrium*,

$$\frac{\mathrm{d}N_1}{\mathrm{d}x_1} = -p_1, \quad \text{for} \quad 0 \leq x_1 \leq L, \tag{11.10a}$$

$$N_1 = P_1, \quad \text{for} \quad x_1 = L. \tag{11.10b}$$

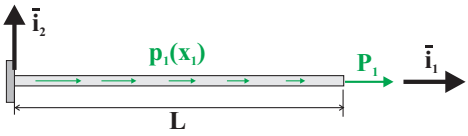


**Fig. 11.16.** Beam subjected to distributed axial load and tip load.

The following statement is now constructed

$$\int_0^L w(x_1) \left[ p_1 + \frac{\mathrm{d}N_1}{\mathrm{d}x_1} \right] \mathrm{d}x_1 + w(L) \left[ P_1 - N_1 \right]_{x_1 = L} = 0, \tag{11.11}$$

where $w(x_1)$ is an arbitrary function referred to as a *weighting function* or *test function*. If the beam is in equilibrium, eqs. (11.10) must hold, and therefore, eq. (11.11) is satisfied *for all arbitrary functions* $w(x_1)$. Indeed, the two bracketed terms, when set equal to zero, express the equilibrium equations of the problem.

Next, an integration by parts is performed on the first term appearing in the integral

$$\int_0^L w(x_1) \frac{\mathrm{d}N_1}{\mathrm{d}x_1} \, \mathrm{d}x_1 = - \int_0^L \frac{\mathrm{d}w}{\mathrm{d}x_1} N_1 \, \mathrm{d}x_1 + \left[ w N_1 \right]_0^L , \tag{11.12}$$

and introducing this result into eq. (11.11) leads to

$$-\int_0^L \frac{\mathrm{d}w}{\mathrm{d}x_1} N_1 \, \mathrm{d}x_1 + \int_0^L w p_1 \, \mathrm{d}x_1 + w(L)P_1 - w(0)N_1(0) = 0. \tag{11.13}$$

The last term in this statement is the product of the root reaction force, $N_1(0)$, by the value of the test function at the same location, $w(0)$. To eliminate the reaction force from the formulation, the test function is required to vanish at the beam's root, $w(0) = 0$. The statement now reduces to

$$\begin{gathered} -\int_0^L \frac{\mathrm{d}w}{\mathrm{d}x_1} N_1 \, \mathrm{d}x_1 + \int_0^L w p_1 \, \mathrm{d}x_1 + w(L)P_1 = 0, \\ \textit{for all arbitrary } w(x_1) \textit{ such that } w(0) = 0. \end{gathered} \tag{11.14}$$

This integral is known as the *weak statement of equilibrium*. The strong statement, eq. (11.10), implies the weak statement, eq. (11.14). On the other hand, it is easily shown that the weak statement implies the strong statement. Indeed, the weak statement implies eq. (11.13), which in turn, implies eq. (11.11) by reversing the integration by parts process. Finally, the strong statement of equilibrium is implied by eq. (11.11) because if the test function, $w(x_1)$, is entirely arbitrary, the bracketed terms must vanish.

In summary, the strong statement, eq. (11.10), and the weak statement, eq. (11.14), are two entirely equivalent statements that both express the equilibrium conditions for the beam under axial loads. The weak statement of equilibrium is often referred to as a *variational* statement.

### Comparison of the strong and weak statements

At this point, it is not clear what the advantages the weak statement might present over the strong statement. If the goal is to determine the *exact* solution for the internal forces and transverse displacement fields, little difference exists between these two entirely equivalent statements. If the goal, however, is to develop approximate solutions, the weak statement provides significant advantages.

When using the strong statement, it is necessary for the derivative of the axial force to exists because it appears in this statement. Consequently, the axial force must be continuous to use the strong statement. When using the weak statement, however, the only requirement is for the product of axial force by the derivative of the weighting function be integrable over the beam's span. Hence, the weak statement can be used with an axial force field that satisfies weaker continuity requirements.

The integration by parts is an essential part of the derivation of the weak statement of equilibrium. It is responsible for the decreased (or weakened) continuity requirement for the axial forces, but this is achieved at the expense of increasing the continuity requirements on the test function. The boundary terms generated by the integration by parts also affect the formulation of the boundary conditions of the problem.

**Sign conventions**

The particular sign convention employed in this development deserves further comment. When formulating the weak statement in eq. (11.11), the bracketed expressions must both vanish, and therefore, an arbitrary sign can be assigned to each expression. Either positive or negative sign is possible, but to simplify the development, the following sign convention will be adopted. Each bracketed equilibrium equations appearing in the weak statement, eq. (11.11), will be constructed using a positive sign for the products of the test functions by externally applied loads acting in a positive axis direction. For instance, the term under the integral is written as $+w(x_1)\,[p_1 + \ldots]$ and the boundary terms as $+w(L)\,[P_1 + \ldots]$.

**Geometric boundary conditions**

In the preceding development, the test function is chosen to satisfy the condition $w(0) = 0$. This choice eliminates the reaction force at the root of the beam from the weak statement of equilibrium. Reaction forces are the forces that appear at the locations where geometric boundary conditions are enforced. More generally, *geometric boundary conditions*, sometimes referred to as *essential boundary conditions*, are defined as those boundary conditions that restrict allowable displacements, such as the clamping of the beam at a point. For the problem depicted in fig. 11.16, the geometric boundary condition is $\bar{u}_1(0) = 0$, and the associated reaction force is the root reaction force, $N_1(0)$. If the test function is chosen to satisfy the geometric boundary condition, $w(0) = 0$, the corresponding reaction force is eliminated from the weak statement of equilibrium.

**Beam fixed at both ends**

To further illustrate the concept of geometric boundary conditions, consider a beam fixed at both ends and subjected to a distributed axial load $p_1(x_1)$. The differential equation of equilibrium is still given by eq. (5.18), however, because the beam is fixed at both ends, no additional equilibrium conditions can be stated at these ends. The following statement is now constructed

$$\int_0^L w(x_1) \left[ \frac{\mathrm{d}N_1}{\mathrm{d}x_1} + p_1 \right] \mathrm{d}x_1 = 0,$$

that must be satisfied *for all arbitrary functions* $w(x_1)$. Next, an integration by parts is performed on the first term appearing in the integral, and the above statement becomes

$$-\int_0^L \frac{\mathrm{d}w}{\mathrm{d}x_1} N_1 \,\mathrm{d}x_1 + \int_0^L w p_1 \,\mathrm{d}x_1 + [wN_1]_0^L = 0.$$

Because $w(x_1)$ is an entirely arbitrary function, it is chosen to vanish at the points where *geometric boundary conditions* are imposed, *i.e.*, $w(0) = w(L) = 0$. The above statement then reduces to

$$-\int_0^L \frac{\mathrm{d}w}{\mathrm{d}x_1} N_1 \, \mathrm{d}x_1 + \int_0^L w p_1 \, \mathrm{d}x_1 = 0,$$

*for all arbitrary* $w(x_1)$ *such that* $w(0) = w(L) = 0$.

This integral is the weak statement of equilibrium for this problem.

### Concentrated loads at an interior point

In the previous cases, a concentrated load, $P_1$, is applied at the beam's tip, and is introduced in the strong statement as an equilibrium condition at that location. Concentrated loads, however, may also be applied at any point along the span of the beam. To illustrate this situation, consider a beam fixed at both ends, subjected to a distributed axial load, $p_1(x_1)$, and a concentrated axial load, $P_1$, applied at location $x_1 = \alpha L$, as shown in fig. 11.17.

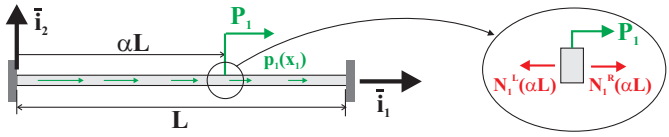


**Fig. 11.17.** Beam fixed at both ends and subjected to distributed axial load and concentrated load.

For this configuration, the presence of the concentrated load, $P_1$, creates a discontinuity in the axial loading applied along the beam, and consequently, the strong statement of equilibrium can no longer be formulated as a single differential equation over the entire span of the beam. Instead, the strong statement, eq. (11.10a), must be split into two separate differential equations over the left and right portions of the beam, leading to

$$\frac{\mathrm{d}N_1^L}{\mathrm{d}x_1} = -p_1, \quad 0 \leq x_1 \leq \alpha L, \tag{11.15a}$$

$$\frac{\mathrm{d}N_1^R}{\mathrm{d}x_1} = -p_1, \quad \alpha L \leq x_1 \leq L, \tag{11.15b}$$

$$N_1^R(\alpha L) + P_1 - N_1^L(\alpha L) = 0, \tag{11.15c}$$

where the symbols $N_1^L$ and $N_1^R$ denote the axial forces over the left and right portions of the beam, respectively. Equation (11.15c) expresses axial force equilibrium at the point of application of the concentrated load, as illustrated in the expanded detail shown in fig. 11.17. The boundary conditions at the ends are both geometric constraints, $\bar{u}_1(0) = \bar{u}_1(L) = 0$.

A weak statement of equilibrium is now constructed

$$\int_0^{\alpha L} w(x_1) \left[ p_1 + \frac{\mathrm{d}N_1^L}{\mathrm{d}x_1} \right] \mathrm{d}x_1 + \int_{\alpha L}^L w(x_1) \left[ p_1 + \frac{\mathrm{d}N_1^R}{\mathrm{d}x_1} \right] \mathrm{d}x_1 + w(\alpha L) \left[ N_1^R(\alpha L) + P_1 - N_1^L(\alpha L) \right] = 0,$$

that must be satisfied for all arbitrary $w(x_1)$. As before, the bracketed expressions are simply the equilibrium equations of the problems, eqs. (11.15).

Next, an integration by parts is performed for the terms involving the derivatives of the axial force to find

$$-\int_0^{\alpha L} \frac{\mathrm{d}w}{\mathrm{d}x_1} N_1^L \mathrm{d}x_1 + \left[wN_1^L\right]_0^{\alpha L} - \int_{\alpha L}^{L} \frac{\mathrm{d}w}{\mathrm{d}x_1} N_1^R \mathrm{d}x_1 + \left[wN_1^R\right]_{\alpha L}^{L} + \int_0^L p_1 \mathrm{d}x_1 + w(\alpha L)\left[N_1^R(\alpha L) + P_1 - N_1^L(\alpha L)\right] = 0.$$

Because the test function is arbitrary, it can be chosen to satisfy the geometric boundary conditions, $w(0) = w(L) = 0$, and then all boundary terms vanish except for $w(\alpha L)P_1$. The two integral can be recombined to yield the following statement

$$-\int_0^L \frac{\mathrm{d}w}{\mathrm{d}x_1} N_1 \mathrm{d}x_1 + \int_0^L p_1 \mathrm{d}x_1 + w(\alpha L)P_1 = 0, \quad \textit{for all arbitrary } w(x_1) \textit{ such that } w(0) = w(L) = 0. \tag{11.16}$$

Because the derivatives of the axial force have been eliminated through the integration by parts, it is no longer necessary to distinguish between the left and right portions of the beam, as is the case for the strong statement, see eqs. (11.15).

The weak statement of equilibrium for the present configuration is very similar to that obtained for a beam with an axial tip load, see in eq. (11.14). For the present configuration, the applied concentrated load is multiplied by the test function evaluated at the point of application of the concentrated load. For the strong formulation, the discontinuity of the axial force requires splitting the problem into two separate portions, see eqs. (11.15). In the weak formulation, the continuity requirement on the axial force is relaxed and the presence of concentrated loads has little effect on the weak statement of equilibrium, see eq. (11.16).

### 11.3.2 Approximate solutions for beams under axial loads

The weak statement of equilibrium takes the form of a weighted integral that is particularly well suited for obtaining approximate solutions. In the case of the axially loaded beam examined above, the product of the axial force distribution by the test function needs to be integrable over of the beam's span and the test functions must satisfy the geometric boundary conditions. These are weaker requirements than those imposed by the differential equation in the strong statement of equilibrium.

At this point, a subtle but important distinction must be made. While the strong and weak statements of equilibrium are equivalent (meaning that one can be derived from the other), not all solutions to the weak statement are solutions to the strong statement. In particular, those solutions that do not meet the continuity requirements imposed by the strong statement may, in fact, be acceptable solutions to the weak form. In this sense, these solutions, while exactly satisfying the weak form, are nonetheless approximate solutions to the strong form. This versatility makes the weak form attractive for developing approximate solutions.

As discussed in chapter 3, the solution of elasticity problems requires the simultaneous solution of three groups of equations: the strain-displacement equations, the constitutive laws, and the equilibrium equations. The weak and strong statements of equilibrium are shown in section 11.3.1 to be entirely equivalent to Newton's law. Both strain-displacement equations and constitutive laws must be added to the weak statement to solve general elasticity problems. For a beam under axial loading, the constitutive law is given by eq. (5.16) as $N_1 = S\,\bar{\epsilon}_1$, and the strain-displacement relationship by eq. (5.6) as $\bar{\epsilon}_1 = \mathrm{d}\bar{u}_1/\mathrm{d}x_1$. Substituting these equations into the weak statement of equilibrium, eq. (11.14), yields

$$-\int_0^L \frac{\mathrm{d}w}{\mathrm{d}x_1} S \frac{\mathrm{d}\bar{u}_1}{\mathrm{d}x_1}\,\mathrm{d}x_1 + \int_0^L w p_1\,\mathrm{d}x_1 + w(L)P_1 = 0. \tag{11.17}$$

Note that the use of the strong statement of equilibrium leads to a second order differential equation for the axial displacement field, see eq. (5.19), whereas only first order derivatives of the same displacement field appear in the above statement, implying weaker continuity requirements.

An approximate solution of the problem is now selected in the following form

$$\bar{u}_1(x_1) = \sum_{i=1}^{N} h_i(x_1) q_i, \tag{11.18}$$

where the $h_i(x_1)$, $i = 1, 2, \ldots, N$, are known shape functions, and $q_i$, $i = 1, 2, \ldots, N$, unknown degrees of freedom. This approximation is identical to that used earlier in the Rayleigh-Ritz method, see eq. (11.3). Here again, the shape functions must individually satisfy the geometric boundary conditions.

The weak statement of equilibrium, see eq. (11.14), also involves a set of arbitrary functions, $w(x_1)$, which must satisfy the geometric boundary conditions. In a similar manner, these test functions can be approximated as

$$w(x_1) = \sum_{i=1}^{N} g_i(x_1) w_i, \tag{11.19}$$

where the $g_i(x_1)$, $i = 1, 2, \ldots, N$, are known shape functions, and $w_i$, $i = 1, 2, \ldots, N$, a set of *arbitrary coefficients*.

The test functions, $w(x_1)$, must satisfy the geometric boundary conditions. If each of the shape functions, $g_i(x_1)$, individually satisfies the same conditions, the coefficients, $w_i$, become *entirely arbitrary coefficients*, *i.e.*, are not subjected to any restriction.

The shape functions, $h_i(x_1)$, used to approximate the axial displacement field in eq. (11.18), and $g_i(x_1)$, used to approximate the test functions must all satisfy the geometric boundary conditions, but are otherwise arbitrary and unrelated. It is possible, and often convenient, to select $h_i(x_1) = g_i(x_1)$ but this is not a requirement. When selecting $h_i(x_1) = g_i(x_1)$, the procedure is called *Galerkin's method*.

***Example 11.7. Beam under a uniform axial load***

Consider the uniform, cantilevered beam of length $L$ subjected to a uniform axial loading, $p_1(x_1) = p_0$, as depicted in fig. 11.16. For simplicity, no concentrated load is applied to the beam, *i.e.*, $P_1 = 0$. The solution of this problem presented in section 5.4 is based on the strong statement of equilibrium.

The solution of the same problem will now be derived with the help of the weak statement of equilibrium, eq. (11.17), which is now written as

$$-\int_0^L \frac{\mathrm{d}w}{\mathrm{d}x_1} S \frac{\mathrm{d}\bar{u}_1}{\mathrm{d}x_1}\,\mathrm{d}x_1 + \int_0^L w p_0\,\mathrm{d}x_1 = 0. \tag{11.20}$$

This statement must vanish for all arbitrary functions, $w(x_1)$, that satisfy the geometric boundary condition, $w(0) = 0$. A suitable approximation to the solution, see eq. (11.18), is selected as

$$\bar{u}_1(x_1) = x_1 q_1 + x_1^2 q_2, \tag{11.21}$$

where $h_1(x_1) = x_1$ and $h_2(x_1) = x_1^2$ are the shape functions, and $q_1$ and $q_2$ the two degrees of freedom. The two shape functions individually satisfy the geometric boundary condition. Next, the test functions are approximated in the form of eq. (11.19), using shape functions $g_1(x_1) = x_1$ and $g_2(x_1) = x_1^2$ as

$$w(x_1) = x_1 w_1 + x_1^2 w_2. \tag{11.22}$$

Note that $h_1 = g_1$ and $h_2 = g_2$, *i.e.*, Galerkin's method is used here.

Given these approximations, separate expressions of the weak statement can be written for test functions $h_1$ and $h_2$ as

$$\begin{aligned} -\int_0^L 1\; S(q_1 + 2q_2 x_1)\,\mathrm{d}x_1 + \int_0^L p_0 x_1\,\mathrm{d}x_1 = 0, \\ -\int_0^L 2x_1 S(q_1 + 2q_2 x_1)\,\mathrm{d}x_1 + \int_0^L p_0 x_1^2\,\mathrm{d}x_1 = 0, \end{aligned}$$

respectively. The weak statement must be satisfied for each of the two test functions, $h_1$ and $h_2$, because because coefficients $w_1$ and $w_2$ are entirely arbitrary. Also, for this reason, the number of test functions must be equal to the number of shape functions.

After carrying out the integrations, these two equations are cast in the following matrix form

$$S \begin{bmatrix} 1 & 1 \\ 1 & 4/3 \end{bmatrix} \begin{Bmatrix} q_1 \\ Lq_2 \end{Bmatrix} = p_0 L \begin{Bmatrix} 1/2 \\ 1/3 \end{Bmatrix}.$$

Solving this set of linear equations yields $q_1 = p_0 L/S$ and $Lq_2 = -p_0 L/(2S)$, and the axial displacement field now becomes

$$\bar{u}_1(x_1) = \frac{p_0 L^2}{S}\left(\eta - \frac{1}{2}\eta^2\right), \tag{11.23}$$

where $\eta = x_1/L$ is a non-dimensional variable along the beam's span.

The solution is identical to that found with the strong equilibrium statement, eq. (5.26). Nevertheless, the solution processes for the two approaches are strikingly different. The strong equilibrium statement leads to a second order differential equation that must be solved to obtain the axial displacement. On the other hand, solution of the problem based on the weak statement involves the evaluation of integrals over the beam's span and the solution of a set of linear, algebraic equations. In this case, the two solutions are identical because the approximate solution selected for this example is, in fact, the exact solution.

***Example 11.8. Bar with a concentrated axial load***

Consider the bar fixed at both ends and carrying a concentrated axial load, $P_1$, at location $x_1 = \alpha L$, as shown in fig. 11.17. An exact solution of this problem using the classical differential equation approach developed in section 5.4 will require separate axial displacement fields to be evaluated over the left and right portions of the beam, denoted $\bar{u}_1^L(x_1)$ and $\bar{u}_1^R(x_1)$, respectively. Boundary conditions are used at the two fixed ends, and at the point of application of the concentrated load, two compatibility conditions must be imposed between the two separate solutions. The first compatibility condition is the continuity of displacement, $\bar{u}_1^L(\alpha L) = \bar{u}_1^R(\alpha L)$ and the second is the equilibrium condition, $N_1^L(\alpha L) = P_1 + N_1^R(\alpha L)$.

The weak statement given by eq. (11.16) reduces the solution process to the evaluation of a much simpler integral form over the beam's span. A single degree of freedom approximation is selected for this problem, $\bar{u}_1(\eta) = q_1 h_1(\eta)$, with the following shape function,

$$h_1(\eta) = \begin{cases} \eta/\alpha, & 0 \le \eta \le \alpha, \\ (1-\eta)/(1-\alpha), & \alpha \le \eta \le 1, \end{cases}$$

where $\eta = x_1/L$ is the non-dimensional variable along the beam's span. As required, this shape function satisfies the geometric boundary conditions of the problem. Using Galerkin's method, the test function is selected to be identical to the shape function, $g_1(\eta) = h_1(\eta)$, and $w(\eta) = w_1 g_1(\eta)$. The weak statement, eq. (11.16), becomes

$$-\int_0^L \frac{\mathrm{d}w}{\mathrm{d}x_1} S \frac{\mathrm{d}\bar{u}_1}{\mathrm{d}x_1}\,\mathrm{d}x_1 + w(\alpha L)P_1 =$$
$$-\int_0^1 w' \frac{S}{L}\bar{u}_1'\mathrm{d}\eta + w(\alpha L)P_1 = w_1\left[-\frac{S}{L}q_1\frac{1}{\alpha(1-\alpha)} + P_1\right] = 0,$$

where the notation $(\cdot)'$ is used to indicate a differentiation with respect to $\eta$.

Since coefficient $w_1$ is entirely arbitrary, the bracketed expression must vanish, leading to $q_1 = \alpha(1-\alpha)P_1 L/S$, and finally

$$\bar{u}_1(\eta) = \frac{P_1 L}{S}\begin{cases} (1-\alpha)\eta, & 0 \le \eta \le \alpha, \\ \alpha(1-\eta), & \alpha \le \eta \le 1. \end{cases}$$

The axial force is given by $N_1 = S\mathrm{d}\bar{u}_1/\mathrm{d}x_1 = S\bar{u}_1'/L$ and this leads to

$$N_1(\eta) = P_1 \begin{cases} (1-\alpha), & 0 \le \eta \le \alpha, \\ -\alpha, & \alpha \le \eta \le 1. \end{cases}$$

This solution consists of a linearly varying displacement in each portion of the beam. The axial strain, $\bar{\epsilon}_1$, and the axial force, $N_1$ are constant with each portion of the beam. At $\eta = \alpha$, the axial force is discontinuous, $N_1^L(\alpha L) = P_1 + N_1^R(\alpha L)$, as required by equilibrium. A complete solution of the problem using the classical differential equation approach will reveal that the present solution is, in fact, the exact solution of the problem.

***Example 11.9. Beam under a uniform axial load: a more formal presentation***
In the previous examples, Galerkin's method is used to solve simple problems that only required limited algebraic manipulations. As the number of degrees of freedom increases, a more systematic approach will be needed to obtain a streamlined procedure. A compact matrix notation will be introduced; in particular, the important concepts of stiffness matrix and load array will enable a more formal presentation of Galerkin's method. Furthermore, this matrix algebra presentation of the method is readily implemented on computers.

The polynomial forms used for approximate displacements in the previous examples will be used here again, see eq. (11.21) for the assumed solution and eq. (11.22) for the assumed test functions. The degrees of freedom of the problem are $q_1$ and $q_2$, whereas $w_1$ and $w_2$ are arbitrary coefficients. With these approximations, the weak statement of equilibrium, eq. (11.20), becomes

$$-\int_0^L S(w_1 + 2w_2x_1)(q_1 + 2q_2x_1)\,\mathrm{d}x_1 + \int_0^L p_0(w_1x_1 + w_2x_1^2)\,\mathrm{d}x_1 = 0.$$

Expansion and integration then leads to

$$-S\left(w_1q_1L + 2w_1q_2\frac{L^2}{2} + 2w_2q_1\frac{L^2}{2} + 4w_2q_2\frac{L^3}{3}\right) + p_0\left(w_1\frac{L^2}{2} + w_2\frac{L^3}{3}\right) = 0.$$

It is customary to write this equation in a matrix form as

$$-\{w_1, w_2\}\ SL\begin{bmatrix} 1 & L \\ L & 4L^2/3 \end{bmatrix}\begin{Bmatrix} q_1 \\ q_2 \end{Bmatrix} + \{w_1, w_2\}\, p_0L^2\ \begin{Bmatrix} 1/2 \\ L/3 \end{Bmatrix} = 0. \qquad (11.24)$$

The $2 \times 2$ matrix of stiffness coefficients is called the *stiffness matrix*, $\underline{\underline{K}}$, and the array of loading coefficients the *load array*, $\underline{Q}$, which are defined as

$$\underline{\underline{K}} = SL\begin{bmatrix} 1 & L \\ L & 4L^2/3 \end{bmatrix}, \quad \underline{Q} = p_0L^2\begin{Bmatrix} 1/2 \\ L/3 \end{Bmatrix}.$$

The array of degrees of freedom is called the *solution array*, $\underline{q}$, and the array of arbitrary coefficients the *test array*, $\underline{w}$,

$$\underline{q} = \begin{Bmatrix} q_1 \\ q_2 \end{Bmatrix}, \quad \underline{w} = \begin{Bmatrix} w_1 \\ w_2 \end{Bmatrix}.$$

With these definitions, the weak statement, eq. (11.24), takes the following compact form

$$\underline{w}^T \left[ \underline{\underline{K}}\, \underline{q} - \underline{Q} \right] = 0. \tag{11.25}$$

Coefficients $w_1$ and $w_2$ are entirely arbitrary, *i.e.*, can be assigned any value. In particular, the following choices will be used here: $\underline{w}^T = \{1, 0\}$ and $\underline{w}^T = \{0, 1\}$, leading to

$$\{1, 0\} \left[ \underline{\underline{K}}\, \underline{q} - \underline{Q} \right] = 0, \quad \{0, 1\} \left[ \underline{\underline{K}}\, \underline{q} - \underline{Q} \right] = 0.$$

Combining these two equations yields

$$\underline{\underline{I}} \left[ \underline{\underline{K}}\, \underline{q} - \underline{Q} \right] = \underline{0},$$

where $\underline{\underline{I}}$ is the $2 \times 2$ identity matrix. Of course, because the identity matrix is never singular, it can be dropped to yield a set of algebraic equations for the solution array

$$\underline{\underline{K}}\, \underline{q} = \underline{Q}. \tag{11.26}$$

The solution of this equation is simply $\underline{q} = \underline{\underline{K}}^{-1} \underline{Q}$, or

$$\begin{Bmatrix} q_1 \\ q_2 \end{Bmatrix} = \frac{1}{SL} \begin{bmatrix} 1 & L \\ L & 4L^2/3 \end{bmatrix}^{-1} p_0 L^2 \begin{Bmatrix} 1/2 \\ L/3 \end{Bmatrix},$$

which yields the solution array as $q_1 = p_0 L/S$, and $q_2 = -p_0/(2S)$. Substituting these coefficients into the assumed solution, eq. (11.21), leads to

$$\bar{u}_1 = \frac{p_0 L}{S}\, x_1 - \frac{p_0}{2S}\, x_1^2 = \frac{p_0 L^2}{S} \left( \eta - \frac{1}{2} \eta^2 \right),$$

where $\eta = x_1/L$ is a non-dimensional variable along the beam's span. As expected, this solution is identical to that obtained in the previous example 11.8.

***Example 11.10. Tapered beam under centrifugal load***

In the previous examples, the solutions developed based on the weak statement of equilibrium are exact solutions. This occurs because the assumed form of the solution could represent the exact solution. In general, the exact solution is not known, and the assumed form of the solution cannot represent the exact solution.

Consider a helicopter blade of length $L$ rotating at an angular velocity $\Omega$ about axis $\bar{\imath}_2$, as depicted in fig. 11.18. This problem is treated using the classical differential equation approach in example 5.2 on page 184. The rotor blade is homogeneous and its cross-section tapers linearly from an area $\mathcal{A}_0$ at the root to $\mathcal{A}_1 = \mathcal{A}_0/2$ at the tip, and hence, its axial stiffness is $S = E\mathcal{A}(x_1) = \mathcal{A}_0\ (1 - x_1/2L)$.

For this problem, the weak statement of equilibrium becomes

$$-\int_0^L \frac{\mathrm{d}w}{\mathrm{d}x_1} S(x_1) \frac{\mathrm{d}\bar{u}_1}{\mathrm{d}x_1}\, \mathrm{d}x_1 + \int_0^L w \rho \mathcal{A}(x_1) \Omega^2 x_1\, \mathrm{d}x_1 = 0.$$

Introducing the non-dimensional span variable, $\eta = x_1/L$, then leads to

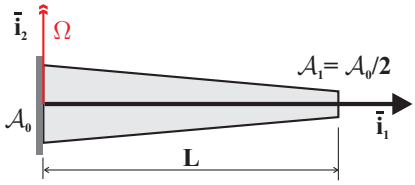


**Fig. 11.18.** A helicopter blade rotating at an angular speed $\Omega$.

$$-\frac{E\mathcal{A}_0}{L}\int_0^1 w'\left(1-\frac{\eta}{2}\right)\bar{u}_1'\,\mathrm{d}\eta+\rho\mathcal{A}_0\Omega^2L^2\int_0^1 w\left(\eta-\frac{\eta^2}{2}\right)\mathrm{d}\eta=0,$$

where the notation $(\cdot)'$ indicates a derivative with respect to $\eta$.

An approximate solution for the axial displacement field is assumed in the following simple polynomial form, which satisfies the only geometric boundary condition of the problem, $\bar{u}_1(0)=0$,

$$\bar{u}_1(\eta)=q_1\eta+q_2\eta^2. \tag{11.27}$$

Using Galerkin's method, an identical form is selected for the weighting function, $w(\eta)=w_1\eta+w_2\eta^2$, and the weak statement becomes

$$-\frac{E\mathcal{A}_0}{L}\int_0^1 (w_1+2w_2\eta)(1-\frac{\eta}{2})(q_1+2q_2\eta)\,\mathrm{d}\eta$$
$$+\rho\mathcal{A}_0\Omega^2L^2\int_0^1 (w_1\eta+w_2\eta^2)\left(\eta-\frac{\eta^2}{2}\right)\mathrm{d}\eta=0.$$

After expansion and integration, this expression can be recast into a matrix form following a procedure similar to that used in example 11.9, leading to

$$-\left\{w_1,w_2\right\}\frac{E\mathcal{A}_0}{L}\begin{bmatrix}3/4 & 2/3\\ 2/3 & 5/6\end{bmatrix}\begin{Bmatrix}q_1\\ q_2\end{Bmatrix}+\left\{w_1,w_2\right\}\rho\mathcal{A}_0\Omega^2L^2\begin{Bmatrix}5/24\\ 3/20\end{Bmatrix}=0.$$

As before, it is convenient to define a stiffness matrix, $\underline{\underline{K}}$, and a loading array, $\underline{Q}$, as

$$\underline{\underline{K}}=\frac{E\mathcal{A}_0}{L}\begin{bmatrix}3/4 & 2/3\\ 2/3 & 5/6\end{bmatrix},\quad\text{and}\quad\underline{Q}=\rho\mathcal{A}_0\Omega^2L^2\begin{Bmatrix}5/24\\ 3/20\end{Bmatrix}.$$

With these definitions, the weak statement is again in the form of eq. (11.25).

Following the same steps as those detailed in the previous example, the weak statement then leads to a set of linear equations, eq. (11.26). These can be solved to yield the solution array

$$\begin{Bmatrix}q_1\\ q_2\end{Bmatrix}=\underline{\underline{K}}^{-1}\underline{Q}=\frac{L}{E\mathcal{A}_0}\begin{bmatrix}3/4 & 2/3\\ 2/3 & 5/6\end{bmatrix}^{-1}\rho\mathcal{A}_0\Omega^2L^2\begin{Bmatrix}5/24\\ 3/20\end{Bmatrix}.$$

Inverting the $2\times 2$ stiffness matrix yields the degrees of freedom as $q_1=53\rho\Omega^2L^3/(130E)$ and $q_2=-19\rho\Omega^2L^3/(130E)$. Introducing these coefficients into the assumed solution, eq. (11.27), leads to

$$\bar{u}_1 = \frac{\rho\Omega^2 L^3}{E}\left(\frac{53}{130}\,\eta - \frac{19}{130}\,\eta^2\right). \tag{11.28}$$

This solution is clearly different from that obtained based on the strong statement of equilibrium, eq. (5.27). Indeed, eq. (5.27) is an *exact solution* of the problem, whereas eq. (11.28) is *an approximate solution*. The approximation is introduced by assuming the form of the solution and weighting function in eq. (11.27).

Clearly, the assumed polynomial form of the solution cannot possibly represent the exact solution of the problem, eq. (5.27), which involves transcendental functions. Furthermore, the weak statement, eq. (11.14), requires the vanishing of an integral for all arbitrary choices of the test function, but the two polynomials selected here to represent the test function cannot possibly represent all arbitrary choices of this function.

Within the framework of this approximation, the solution process determines the degrees of freedom, $q_1$ and $q_2$, which provide the "best overall match" with the exact solution. Detailed mathematical analysis of the solution procedure [8, 9] can be used to prove that under certain restrictions, the approximate solution does converge to the exact solution as the number of degrees of freedom increases.

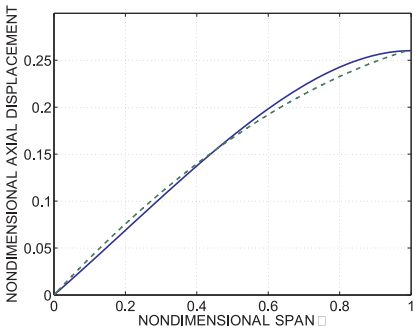


**Fig. 11.19.** Non-dimensional axial displacement, $\bar{u}_1 E/(\rho\mathcal{A}_0^2 L^3)$, versus $\eta$. Strong statement of equilibrium: solid line; weak statement: dashed line.

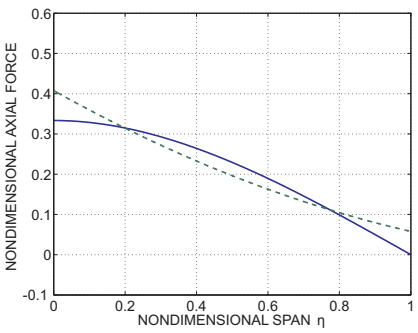


**Fig. 11.20.** Non-dimensional axial force, $N_1/(\rho\mathcal{A}_0\Omega^2 L^2)$, versus $\eta$. Strong statement of equilibrium: solid line; weak statement: dashed line.

Although only two unknown coefficients are used here, it is interesting to note that the approximate solution is in close agreement with the exact solution, as shown in fig. 11.19, which depicts the distribution of non-dimensional axial displacement over the beam's span. Table 11.1 compares the predictions of the two approaches at two locations along the span of the blade.

Finally, the axial force in the blade is obtained by introducing eq. (11.28) into eq. (5.16) to find

$$N_1 = \frac{\rho\mathcal{A}_0\Omega^2 L^2}{260}\left(106 - 129\eta + 38\eta^2\right). \tag{11.29}$$

**Table 11.1.** Comparison of the exact and approximate solutions.

| | $\bar{u}_1 E/(\rho\Omega^2 L^3)$ $\eta = 0.8$ | $\bar{u}_1 E/(\rho\Omega^2 L^3)$ $\eta = 1.0$ | $N_1/(\rho\mathcal{A}_0\Omega^2 L^2)$ $\eta = 0.5$ | $N_1/(\rho\mathcal{A}_0\Omega^2 L^2)$ $\eta = 0.8$ |
|---|---|---|---|---|
| Strong statement | 0.2426 | 0.2601 | 0.2292 | 0.0987 |
| Weak statement | 0.2326 | 0.2615 | 0.1962 | 0.1043 |
| Error (%) | -4.1% | 0.54% | -14% | 5.6% |

Figure 11.20 compares the axial forces predicted by the two approaches. This result is, of course, different from that obtained from the strong statement, eq. (5.28). The two solutions, however, are in reasonable agreement, as shown in fig. 11.20, which depicts the distribution of non-dimensional axial force along the span of the blade. Table 11.1 lists the predictions of the two approaches at two locations along the span of the blade.

### 11.3.3 Problems

**Problem 11.6. Rotating helicopter blade with tip mass**
A helicopter blade of length $L$ and with a tip mass $M_0$ is rotating at an angular velocity $\Omega$ about axis $\bar{\imath}_2$, see fig 11.21. The blade is homogeneous and its cross-section linearly tapers from an area $\mathcal{A}_0$ at the root to $\mathcal{A}_1$ at the tip so that $\mathcal{A}(x_1) = \mathcal{A}_0 + (\mathcal{A}_1 - \mathcal{A}_0)x_1/L$. Select $\mathcal{A}_0 = 2\mathcal{A}_1$. The tip mass $M_0 = \zeta\rho\mathcal{A}_0 L$, where $\zeta = 0.2$ and $\rho$ is the material mass density. *(1)* Solve the governing differential equations of this problem to find the axial displacement $\bar{u}(x_1)$ and the axial load $N_1(x_1)$. *(2)* Find an approximate solution for the axial displacement $\bar{u}_1(x_1)$ using a weak formulation. Select the following forms for the displacement field, $\bar{u}_1(x_1) = q_1 x_1 + q_2 x_1^2$, and weighting function, $w(x_1) = w_1 x_1 + w_2 x_1^2$. *(3)* Determine the axial force $N_1(x_1)$. *(4)* On the same graph, plot the non-dimensional displacement fields for the exact and approximate solutions. *(5)* On the same graph, plot the non-dimensional axial force for the exact and approximate solutions. *(6)* How would you improve the approximate solution?
**Hint**: A mass $M$ rotating about axis $\bar{\imath}_2$ at an angular velocity $\Omega$ is subjected to a centrifugal force $F_c = M\Omega^2 r$, where $r$ is the distance between the mass and the axis of rotation. Hence, the helicopter blade is subjected to an axial load per unit span $p_1(x_1) = \rho\mathcal{A}(x_1)\Omega^2 x_1$, where $\rho$ is the material density. In a similar way, the tip mass $M_0$ creates a concentrated tip force $M_0\Omega^2 L$.

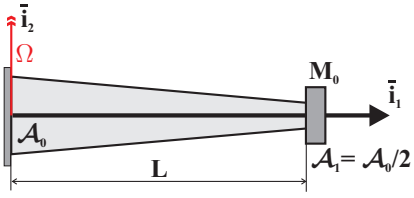


**Fig. 11.21.** A helicopter blade with a tip mass rotating at an angular speed $\Omega$.

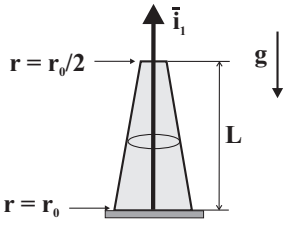


**Fig. 11.22.** Tapered beam subjected to gravity loads

**Problem 11.7. Tapered beam under gravity load**
Consider the tapered beam of circular cross-section subjected to gravity loads, as shown in fig. 11.22. The root section is of radius $r_0$, whereas the tip section has a radius $r_0/2$. The radius linearly tapers along the length of the beam, $r(x_1) = r_0[1-x_1/(2L)]$. The acceleration of gravity is $g$, the material Young's modulus $E$, and the material density $\rho$. *(1)* Solve the governing differential equations of this problem to find the axial displacement $\bar{u}(x_1)$ and the axial load $N_1(x_1)$. *(2)* Find an approximate solution of the problem using a weak formulation. Select the following forms for the displacement field $\bar{u}_1(x_1) = q_1 x_1 + q_2 x_1^2$ and test function $w(x_1) = w_1\, x_1 + w_2\, x_1^2$. *(3)* On the same graph, plot the non-dimensional displacement fields for the exact and approximate solutions. *(4)* On the same graph, plot the non-dimensional axial force for the exact and approximate solutions.

**Problem 11.8. Tapered beam with mid-span axial load**
Consider the axially loaded beam shown in fig. 11.17, but assume now that the beam is tapered uniformly from a radius, $r_0$, at $x_1 = 0$ to a radius, $r_0/2$, at the right end, $x_1 = L$. The concentrated axial load, $P_1$, is applied at $x_1 = \alpha L$. *(1)* Using the same assumed linear form for the axial displacement field used in example 11.8, develop an approximate solution for the axial displacement, $\bar{u}_1(x_1)$ in each portion of the beam. *(2)* Calculate the axial force, $N_1$, in each portion of the beam. *(3)* Determine if equilibrium is satisfied at the load point by this approximate solution and comment on your results.

### 11.3.4 The weak form for beams under transverse loads

The differential equation of equilibrium of a cantilever beam subjected to distributed transverse loading and a concentrated transverse tip load, $P_2$, as shown in fig. 11.23, is derived in section 5.5.3, and the equilibrium equation is given by eq. (5.39). This equation holds at all points over the span of the beam, *i.e.*, for $0 \le x_1 \le L$.

At the loaded tip of the beam, equilibrium requires the shear force to equal the applied transverse load, $V_2(L) = P_2$, and the bending moment must vanish, $M_3 = 0$. These three equilibrium requirements are summarized as

$$\frac{\mathrm{d}^2 M_3}{\mathrm{d}x_1^2} = p_2, \quad \text{for} \quad 0 \le x_1 \le L, \tag{11.30a}$$

$$V_2 = P_2, \quad M_3 = 0, \quad \text{for} \quad x_1 = L, \tag{11.30b}$$

and are known as the *strong statement of equilibrium* for this problem.

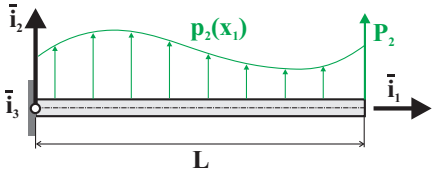


**Fig. 11.23.** Beam subjected to transverse loads.

These three equilibrium equations are used to construct the following integral statement using the sign convention described in section 11.3.1

$$-\int_0^L w(x_1)\left[\frac{\mathrm{d}^2 M_3}{\mathrm{d}x_1^2}-p_2\right]\mathrm{d}x_1+w(L)\left[P_2-V_2\right]_L+\frac{\mathrm{d}w(L)}{\mathrm{d}x_1}\left[0-M_3\right]_L=0. \tag{11.31}$$

The second boundary equilibrium equation is multiplied by the derivative of the test function to preserve the dimensionality of the overall equation. If the beam is in equilibrium, eqs. (11.30) hold, and eq. (11.31) must be satisfied *for all arbitrary functions* $w(x_1)$.

Next, to reduce or weaken the continuity requirements on the bending moment distribution and to reveal the boundary conditions, an integration by parts is performed on the first term appearing in the integral

$$\int_0^L w(x_1)\frac{\mathrm{d}^2 M_3}{\mathrm{d}x_1^2}\,\mathrm{d}x_1=-\int_0^L \frac{\mathrm{d}w}{\mathrm{d}x_1}\frac{\mathrm{d}M_3}{\mathrm{d}x_1}\,\mathrm{d}x_1+\left[w\frac{\mathrm{d}M_3}{\mathrm{d}x_1}\right]_0^L.$$

The integration by parts is repeated for the first term on the right-hand side of the equation and eq. (5.38) is introduced in the boundary term to find

$$\int_0^L w(x_1)\frac{\mathrm{d}^2 M_3}{\mathrm{d}x_1^2}\,\mathrm{d}x_1=\int_0^L \frac{\mathrm{d}^2 w}{\mathrm{d}x_1^2}\,M_3\,\mathrm{d}x_1-\left[\frac{\mathrm{d}w}{\mathrm{d}x_1}\,M_3\right]_0^L-\left[wV_2\right]_0^L. \tag{11.32}$$

Introducing this result into eq. (11.31) leads to

$$-\int_0^L \frac{\mathrm{d}^2 w}{\mathrm{d}x_1^2}\,M_3\,\mathrm{d}x_1+\int_0^L wp_2\,\mathrm{d}x_1+w(L)P_2+\frac{\mathrm{d}w}{\mathrm{d}x_1}(0)\,M_3(0)+w(0)V_2(0)=0. \tag{11.33}$$

At the root, the beam is clamped, giving rise to two geometric boundary conditions, $\bar{u}_2(0)=0$ and $\mathrm{d}\bar{u}_2(0)/\mathrm{d}x_1=0$. Since $w(x_1)$ is an entirely arbitrary function, it is possible to choose $w(0)=\mathrm{d}w/\mathrm{d}x_1(0)=0$. This choice causes $w(x_1)$ to satisfy the geometric boundary conditions and eliminates the root reaction force and moment from the formulation. This leads to

$$\begin{gathered}-\int_0^L \frac{\mathrm{d}^2 w}{\mathrm{d}x_1^2}M_3\,\mathrm{d}x_1+\int_0^L wp_2\,\mathrm{d}x_1+w(L)P_2=0,\\ \textit{for all arbitrary } w(x_1) \textit{ such that } w(0)=\mathrm{d}w/\mathrm{d}x_1(0)=0.\end{gathered} \tag{11.34}$$

This integral is known as the *weak statement of equilibrium*. The strong statement, eq. (11.30), implies the weak statement, eq. (11.34). On the other hand, it is easily shown that the weak statement implies the strong statement. Indeed, the weak statement implies eq. (11.33), which in turn, implies eq. (11.31) by reversing the integration by parts processes. Finally, the strong statement of equilibrium is implied by eq. (11.31) because this equation must hold for all arbitrary choices of the test function, $w(x_1)$.

The above reasoning still holds if different boundary conditions are imposed to the problem. The test function, or its derivative, must vanish at those locations where the transverse displacement, or rotation, of the beam are prescribed, respectively. More generally, the integral appearing in the weak statement must vanish for all test

functions that satisfy the *geometric boundary conditions*, *i.e.*, for all arbitrary test functions that vanish at the points where geometric boundary conditions are applied. As before, these are also referred to as the *essential boundary conditions*.

In summary, the strong statement, eq. (11.30), and the weak statement, eq. (11.34), are two entirely equivalent statements that both express the equilibrium conditions for the beam under transverse loads.

### Simply supported beam under a uniform load

To illustrate the effect of geometric boundary conditions on the weak form statement, consider a simply supported beam subjected to a distributed transverse load $p_2(x_1) = p_0$, as depicted in fig 11.24 and treated earlier in example 11.2. The differential equilibrium equation is still given by eq. (5.39), and the equilibrium conditions at the ends of the beam are $M_3(0) = M_3(L) = 0$.

The following statement is now constructed using the sign convention defined in section 11.3.1

$$-\int_0^L w(x_1)\left[\frac{\mathrm{d}^2 M_3}{\mathrm{d}x_1^2} - p_0\right]\mathrm{d}x_1 - \left[\frac{\mathrm{d}w}{\mathrm{d}x_1}\,M_3\right]_0^L = 0. \tag{11.35}$$

that is satisfied *for all arbitrary functions*, $w(x_1)$. The last term is a statement of moment equilibrium at the ends, *i.e.*, $M_3(0) = M_3(L) = 0$, while $\bar{u}_2(0) = \bar{u}_2(L) = 0$ are the geometric boundary conditions.

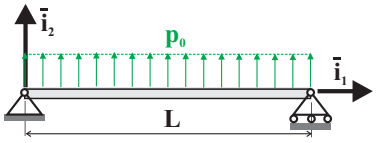


**Fig. 11.24.** Simply supported beam under a uniform transverse load.

Next, two integrations by parts are performed on the first term appearing in the integral, and the above statement becomes

$$-\int_0^L \frac{\mathrm{d}^2 w}{\mathrm{d}x_1^2} M_3\,\mathrm{d}x_1 + \int_0^L w p_0\,\mathrm{d}x_1 + \left[\frac{\mathrm{d}w}{\mathrm{d}x_1} M_3\right]_0^L + [wV_2]_0^L - \left[\frac{\mathrm{d}w}{\mathrm{d}x_1} M_3\right]_0^L = 0.$$

Since $w(x_1)$ is an entirely arbitrary function, it is selected to vanish at the points where *geometric boundary conditions* are applied, *i.e.*, $w(0) = w(L) = 0$, to yield

$$-\int_0^L \frac{\mathrm{d}^2 w}{\mathrm{d}x_1^2}\,M_3\,\mathrm{d}x_1 + \int_0^L w p_0\,\mathrm{d}x_1 = 0,$$
$$\textit{for all arbitrary } w(x_1) \textit{ such that } w(0) = w(L) = 0.$$

This integral is the weak statement of equilibrium for this problem.

**Simply supported beam under a concentrated load**

Consider the simply supported beam subjected to a concentrated load, $P$, applied at location $x_1 = \alpha L$, as shown in fig. 11.25. When using the classical differential equation approach, the beam must be split into two portions, one to the left, the other to the right of the point of application of the concentrated load, as is done in example 5.5 on page 197. Superscripts $(\cdot)^L$ and $(\cdot)^R$ will be used to indicate quantities associated with the left and right portions of the beam, respectively.

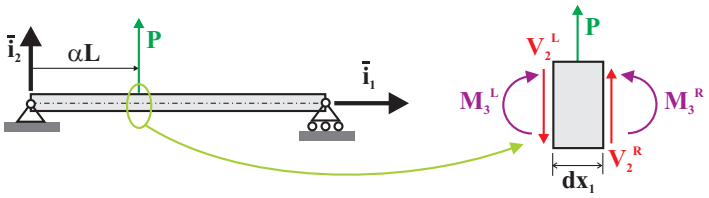


**Fig. 11.25.** Simply supported beam with one concentrated load.

At the point of application of the concentrated load, two conditions arise, $M_3^L = M_3^R$ and $V_2^R + P - V_2^L = 0$, corresponding to moment and vertical force equilibrium equations of the differential element shown in fig 11.25, respectively. The geometric boundary conditions of the problem are $\bar{u}_2(0) = \bar{u}_2(L) = 0$.

The strong statement of equilibrium for this problem is

$$\frac{\mathrm{d}^2 M_3^L}{\mathrm{d}x_1^2} = 0, \quad \text{for} \quad 0 \le x_1 \le \alpha L,$$
$$\frac{\mathrm{d}^2 M_3^R}{\mathrm{d}x_1^2} = 0, \quad \text{for} \quad \alpha L \le x_1 \le L.$$

Equilibrium conditions at the beam's root and tip are $M_3^L = 0$ and $M_3^R = 0$, respectively, and at $x_1 = \alpha L$, $M_3^L = M_3^R$ and $V_2^R + P - V_2^L = 0$.

The following statement is now constructed,

$$-\int_0^{\alpha L} w(x_1) \left[\frac{\mathrm{d}^2 M_3^L}{\mathrm{d}x_1^2}\right] \mathrm{d}x_1 - \int_{\alpha L}^{L} w(x_1) \left[\frac{\mathrm{d}^2 M_3^R}{\mathrm{d}x_1^2}\right] \mathrm{d}x_1$$
$$+\frac{\mathrm{d}w(\alpha L)}{\mathrm{d}x_1} \left[M_3^R - M_3^L\right] + w(\alpha L) \left[V_2^R + P - V_2^L\right] - \left[\frac{\mathrm{d}w}{\mathrm{d}x_1} M_3\right]_0^L = 0.$$

Each of the bracketed terms represents one the equilibrium equations of the problem. If the beam is in equilibrium, the above statement is satisfied *for all arbitrary functions*, $w(x_1)$.

Next, two integrations by parts are performed on the first two integrals to weaken the continuity requirements on the bending moment distribution and reveal the remaining boundary conditions, leading to

$$
\begin{aligned}
&-\int_0^{\alpha L} \frac{\mathrm{d}^2 w}{\mathrm{d}x_1^2} M_3^L \,\mathrm{d}x_1 + \left[\frac{\mathrm{d}w}{\mathrm{d}x_1} M_3\right]_0^{\alpha L} + \left[w V_2^L\right]_0^{\alpha L} \\
&-\int_{\alpha L}^{L} \frac{\mathrm{d}^2 w}{\mathrm{d}x_1^2} M_3^R \,\mathrm{d}x_1 + \left[\frac{\mathrm{d}w}{\mathrm{d}x_1} M_3\right]_{\alpha L}^{L} + \left[w V_2^R\right]_{\alpha L}^{L} \\
&+\frac{\mathrm{d}w(\alpha L)}{\mathrm{d}x_1}\left[M_3^R - M_3^L\right] + w(\alpha L)\left[V_2^R + P - V_2^L\right] - \left[\frac{\mathrm{d}w}{\mathrm{d}x_1}\, M_3\right]_0^{L} = 0.
\end{aligned}
$$

The first two integrals can be combined and many of the boundary terms cancel out, leaving the following statement

$$
-\int_0^{\alpha L} \frac{\mathrm{d}^2 w}{\mathrm{d}x_1^2} M_3 \,\mathrm{d}x_1 + w(\alpha L) P - w(0) V_2^L(0) + w(L) V_2^R(L) = 0.
$$

Because $w(x_1)$ is an entirely arbitrary function, it can be chosen to satisfy the geometric boundary conditions, $w(0) = w(L) = 0$, thereby eliminating the reaction forces at the two end supports from the formulation. The only remaining terms are

$$
-\int_0^{L} \frac{\mathrm{d}^2 w}{\mathrm{d}x_1^2}\, M_3 \,\mathrm{d}x_1 + w(\alpha L) P = 0.
$$

This is the weak statement of equilibrium for the problem. In contrast with the strong statement of equilibrium, it is not necessary to write two distinct statements over the left and right portions of the beam, because the continuity requirements for the bending moment distribution have been weakened.

### 11.3.5 Approximate solutions for beams under transverse loads

Approximate solutions for the transverse displacement field of a beam under transverse loads can be developed from the weak statement of equilibrium in a manner similar to that used for axially loaded beams in section 11.3.2. Because the objective is to determine the displacement field, the equilibrium equations must be expressed first in terms of sectional strains using the sectional constitutive laws, eq. (5.37), then in terms of transverse displacement using the strain-displacement relationship, eq. (5.6).

The weak statement of equilibrium, eq. (11.34), applied to the cantilever beam shown in fig. 11.23 can now be written as

$$
-\int_0^{L} \frac{\mathrm{d}^2 w}{\mathrm{d}x_1^2} H_{33} \frac{\mathrm{d}^2 \bar{u}_2}{\mathrm{d}x_1^2} \,\mathrm{d}x_1 + \int_0^{L} w p_2 \,\mathrm{d}x_1 + w(L) P_2 = 0. \tag{11.36}
$$

Because the beam is cantilevered, this integral must vanish for all arbitrary test functions that satisfy the geometric boundary conditions, $w(0) = \mathrm{d}w(0)/\mathrm{d}x_1 = 0$.

At this point, the continuity requirements on the test function and displacement field are identical. Whereas the strong statement of equilibrium leads to a fourth order differential equation for the displacement field, see eq. (5.40), the weak statement

involves only second order derivatives for both the transverse displacement field and test functions.

Approximate solutions for the transverse displacement field are constructed as before,

$$\bar{u}_2(x_1) = \sum_{i=0}^{N} q_i h_i(x_1), \tag{11.37}$$

where the assumed shape functions, $h_i(x_1)$, must individually satisfy the geometric boundary conditions. Similarly, the test functions will be approximated as

$$w(x_1) = \sum_{i=0}^{N} w_i g_i(x_1), \tag{11.38}$$

where the assumed shape functions, $g_i(x_1)$, must also individually satisfy the geometric boundary conditions. Otherwise, the two sets of shape functions are unrelated. In Galerkin's method, both sets of shape functions are selected to be identical, *i.e.*, $h_i(x_1) = g_i(x_1)$.

***Example 11.11. Simply supported beam under a uniform load***

Consider a simply supported, uniform beam of length $L$ subjected to a uniform transverse loading $p_2(x_1) = p_0$, as depicted in fig. 11.24. The exact solution of this problem, based on the classical differential equation approach, is presented in example 5.4 on page 196.

An approximate solution of the same problem will now be derived using the weak statement of equilibrium, eq. (11.36),

$$-\int_0^L \frac{\mathrm{d}^2 w}{\mathrm{d}x_1^2} H_{33} \frac{\mathrm{d}^2 \bar{u}_2}{\mathrm{d}x_1^2}\, \mathrm{d}x_1 + \int_0^L w p_0\, \mathrm{d}x_1 = 0.$$

This integral must vanish for all test functions that satisfy the geometric boundary conditions, $w(0) = w(L) = 0$.

Using Galerkin's method, the transverse displacement field and test function are assumed to be of the following respective forms

$$\bar{u}_2(x_1) = q_1 \sin\frac{\pi x_1}{L} + q_3 \sin\frac{3\pi x_1}{L}, \quad w(x_1) = w_1 \sin\frac{\pi x_1}{L} + w_3 \sin\frac{3\pi x_1}{L},$$

where $q_1$ and $q_3$ are two degrees of freedom, and $w_1$ and $w_3$ two arbitrary coefficients. The selection of sine functions for the shape functions guarantees the satisfaction of the geometric boundary conditions of the problem. With these approximations, the weak statement becomes

$$\begin{aligned} -\int_0^L &\left[-w_1 \left(\frac{\pi}{L}\right)^2 \sin\frac{\pi x_1}{L} - w_3 \left(\frac{3\pi}{L}\right)^2 \sin\frac{3\pi x_1}{L}\right] \\ &H_{33} \left[-q_1 \left(\frac{\pi}{L}\right)^2 \sin\frac{\pi x_1}{L} - q_3 \left(\frac{3\pi}{L}\right)^2 \sin\frac{3\pi x_1}{L}\right] \mathrm{d}x_1 \\ +\int_0^L & p_0 \left(w_1 \sin\frac{\pi x_1}{L} + w_3 \sin\frac{3\pi x_1}{L}\right) \mathrm{d}x_1 = 0. \end{aligned}$$

After expanding, integrating, and using the orthogonality properties of the sine functions, see eqs. (A.45a), this equation can be recast into a matrix form as

$$-\{w_1, w_2\}\frac{\pi^4 H_{33}}{2L^3}\begin{bmatrix}1 & 0\\ 0 & 81\end{bmatrix}\begin{Bmatrix}q_1\\ q_3\end{Bmatrix}+\{w_1, w_2\}\frac{2p_0 L}{\pi}\begin{Bmatrix}1\\ 1/3\end{Bmatrix}=0.$$

If the stiffness matrix, $\underline{\underline{K}}$, and the load array, $\underline{Q}$, are defined as

$$\underline{\underline{K}}=\frac{\pi^4 H_{33}}{2L^3}\begin{bmatrix}1 & 0\\ 0 & 81\end{bmatrix},\quad \text{and}\quad \underline{Q}=\frac{2p_0 L}{\pi}\begin{Bmatrix}1\\ 1/3\end{Bmatrix},$$

respectively, the weak statement can again be written in the form of eq. (11.25), leading to a set of linear equations, eq. (11.26). These can be solved for the solution array to find

$$\begin{Bmatrix}q_1\\ q_3\end{Bmatrix}=\frac{2L^3}{\pi^4 H_{33}}\begin{bmatrix}1 & 0\\ 0 & 81\end{bmatrix}^{-1}\frac{2p_0 L}{\pi}\begin{Bmatrix}1\\ 1/3\end{Bmatrix}.$$

The degrees of freedom are then $q_1 = 4p_0L^4/(\pi^5 H_{33})$ and $q_3 = 4p_0L^4/(243\pi^5 H_{33})$. Introducing these coefficients into the assumed solution leads to

$$\bar{u}_2=\frac{4p_0L^4}{\pi^5 H_{33}}\left(\sin\frac{\pi x_1}{L}+\frac{1}{243}\sin\frac{3\pi x_1}{L}\right). \tag{11.39}$$

This solution is clearly different from that obtained from the classical differential equation approach, eq. (5.48), which is the exact solution of the problem, whereas eq. (11.39) is an approximate solution.

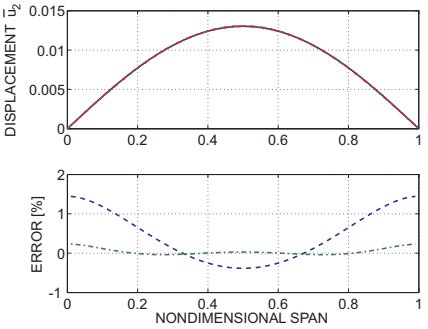


**Fig. 11.26.** Top figure: transverse displacement $\bar{u}_2$; bottom figure: error. Exact solution: solid line; Approximate solution: dashed line (*case 1*), dash-dotted line (*case 2*).

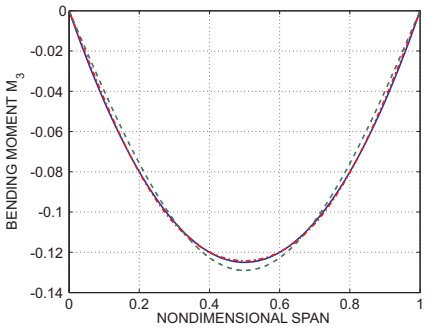


**Fig. 11.27.** Bending moment $M_3$ versus non-dimensional span. Exact solution: solid line; Approximate solution: dashed line (*case 1*), dash-dotted line (*case 2*).

Figure 11.26 depicts the distribution of non-dimensional transverse displacement $\bar{u}_2 H_{33}/(p_0 L^4)$ over the span of the beam for both exact and approximate solutions. Two approximate solutions are shown: *Case 1* includes only the term $\sin \pi x_1/L$ in

eq. (11.39), whereas *Case 2* includes both terms. At the scale of the figure, the exact and approximate solutions are indistinguishable. The lower portion of the figure shows the discrepancy between the approximate and exact solutions. The excellent agreement between the various solutions is also apparent in table 11.2.

**Table 11.2.** Comparison of the exact and approximate solutions at the quarter- and mid-points.

| | $\bar{u}_2 H_{33}/(p_0 L^4)$ $\eta = 0.25$ | $\bar{u}_2 H_{33}/(p_0 L^4)$ $\eta = 0.5$ | $M_3/(p_0 L^2)$ $\eta = 0.25$ | $M_3/(p_0 L^2)$ $\eta = 0.5$ |
|---|---|---|---|---|
| Exact solution | 0.009277 | 0.01302 | 0.09375 | 0.125 |
| Approximation (*Case 1*) | 0.009243 | 0.01307 | 0.09122 | 0.129 |
| Relative error | -0.4% | 0.4% | -2.7% | 3.2% |
| Approximation (*Case 2*) | 0.009281 | 0.01302 | 0.0946 | 0.124 |
| Relative error | 0.04% | -0.03% | 0.9% | -0.8% |

Finally, the bending moment distribution is obtained by introducing eq. (11.39) into eq. (5.37) to find

$$M_3 = -\frac{4p_0 L^2}{\pi^3}\left(\sin\frac{\pi x_1}{L} + \frac{1}{27}\sin\frac{3\pi x_1}{L}\right). \tag{11.40}$$

Figure 11.27 compares the bending moments predicted by the two approaches. Here again, excellent agreement is observed between the various solutions, as confirmed by table 11.2.

### 11.3.6 Problems

**Problem 11.9. Uniformly loaded simply supported beam**
Consider a simply supported, uniform beam of length $L$ subjected to a uniform transverse loading $p_2(x_1) = p_0$, as depicted previously in fig. 11.24. *(1)* Solve the governing differential equations of this problem to find the transverse displacement $\bar{u}_2(x_1)$, the bending moment $M_3(x_1)$, and the shear force $V_2(x_1)$. *(2)* Find an approximate solution of the problem using a weak formulation. Select the following forms for the displacement field $\bar{u}_2(x_1) = \sum_{i=1}^{N} q_i \sin(2i-1)\pi x_1/L$ and test function $w(x_1) = \sum_{i=1}^{N} w_i \sin(2i-1)\pi x_1/L$. *(3)* Plot the exact and approximate transverse displacement fields $\bar{u}_2(x_1)$ on the same plot. For the approximate solutions use $N = 1$, 2, 3, 4, and 5. *(4)* Plot the exact and approximate bending moments $M_3(x_1)$ on the same plot. *(5)* Plot the exact and approximate shear forces $V_2(x_1)$ on the same plot.

**Problem 11.10. Simply supported beam with concentrated load**
Consider a simply supported beam with a concentrated load, $P$, applied at a point $x_1 = \alpha L$ from the left support as illustrated in fig. 5.23 on page 197. This configuration is solved using the classical differential equation approach in example 5.5, and the transverse displacement is found to be given by eq. (5.51). The solution presents a discontinuity in the transverse shear force, and solutions are developed separately for the portions of the beam to the left and right of the concentrated load. Using the weak statement, it is possible to develop a single expression that approximates the deflection over the entire span of the beam, because the continuity

requirements associated with this approach are lower than those required for the differential equation approach. *(1)* Find an approximate solution of the problem using a weak formulation. Select the following forms for the displacement field $\bar{u}_2(x_1) = \sum_{i=1}^{N} q_i \sin i\pi x_1/L$ and test function $w(x_1) = \sum_{i=1}^{N} w_i \sin i\pi x_1/L$. *(2)* On one graph, plot the exact and approximate transverse displacement fields, $H_{33}^c \bar{u}_2(x_1)/(PL^3)$. For the approximate solutions, use $N =$ 1, 2, 3, 4, and 5. *(3)* On one graph, plot the exact and approximate bending moment distributions, $M_3(x_1)/(PL)$. *(4)* On one graph, plot the exact and approximate shear force diagrams, $V_2(x_1)/P$.

### 11.3.7 Equivalence with energy principles

The weak statement of equilibrium developed in the previous sections is equivalent to the statement of equilibrium cast in the form of the principle of virtual work developed in chapter 9 and recast in terms of work and energy in chapter 10. This equivalence will be demonstrated in the following sections. Consequently, it is clear that all approaches are equally valid, and all lead to effective ways of developing approximate solutions to structural problems.

#### The principle of virtual work

The weak statement of equilibrium is introduced in section 11.3.1 through a purely mathematical process, and consequently, its physical interpretation is not clear at this point. In particular, this approach is based on the introduction of a test or weighting function, $w(x_1)$, that is entirely arbitrary except that it must satisfy the geometric boundary conditions for the problem.

To help cast the weak statement of equilibrium in a more physical framework, the test functions are now interpreted as follows

$$w(x_1) \equiv \delta u(x_1), \tag{11.41}$$

where the right-hand side can be read as: *arbitrary variation in displacement* or, using the concepts introduced in chapter 9, as *virtual displacement*. The equivalence stated in eq. (11.41) is purely a matter of notation: the test functions are arbitrary functions that must satisfy only the geometric boundary conditions, and equivalently, the virtual displacements defined in section 9.3.4, are arbitrary displacements that must satisfy only the geometric boundary conditions. The two notations are entirely equivalent, although virtual displacements afford a more direct physical interpretation.

In chapter 9, the principle of virtual work for a single particle is introduced by using an arbitrary fictitious displacement, $\underline{s}$, multiplying the strong statement of equilibrium, $\sum \underline{F} = 0$, to find $(\sum \underline{F}) \cdot \underline{s} = 0$, see eq. (9.8). Later in that chapter, the concept of virtual displacement is introduced by setting $\underline{s} = \delta \underline{u}$, see eq. (9.13), leading to a more physical interpretation of the principle of virtual work based on the concepts of internal and external virtual work. A similar thought process is followed here. The weak statement of equilibrium is introduced by using an arbitrary test function (equivalent to the arbitrary fictitious displacement, $\underline{s}$), multiplying the

strong statement of equilibrium of the problem. The weak statement of equilibrium is difficult to interpret physically, but by introducing the virtual displacement defined in eq. (11.41) it will become possible establish the equivalence of the weak statement of equilibrium with the principle of virtual work.

**Beam under axial load**

To illustrate this equivalence, the equilibrium of an axially loaded beam examined in section 11.3.1 will now be recast using virtual displacements rather than weighting functions. Introducing this notation into the weak statement of equilibrium, eq. (11.14), yields

$$-\int_0^L \frac{\mathrm{d}\delta\bar{u}_1}{\mathrm{d}x_1} N_1 \,\mathrm{d}x_1 + \int_0^L \delta\bar{u}_1 p_1 \,\mathrm{d}x_1 + \delta\bar{u}_1(L) P_1 = 0, \tag{11.42}$$

*for all arbitrary $\delta\bar{u}_1$ satisfying the geometric boundary conditions.*

The first integral in this statement can be written as $-\int_0^L N_1 \delta\bar{\epsilon}_1 \,\mathrm{d}x_1$ and represents the internal virtual work, $\delta W_I$, in a beam subjected to axial loads only, see eq. (9.79a).

The last two terms in this equation are the product of forces by virtual displacements and hence, are naturally interpreted as virtual work quantities. More specifically, the last term is the work done by the concentrated tip force, $P_1$, acting through a virtual displacement, $\delta\bar{u}_1(L)$. Similarly, the middle term is the work done by the distributed axial load, $p_1(x_1)\mathrm{d}x_1$, acting through the virtual axial displacement, $\delta\bar{u}_1(x_1)$; the integral then sums up the virtual work done by the force distributed all along the beam's span to find the total virtual work done by the distributed force. The sum of these two terms defines the virtual work done by the externally applied loads acting on the beam, and following the notation in chapter 9, it is called the external virtual work, $\delta W_E$.

With these interpretations, eq. (11.42) is recast in a more physically meaningful manner as

$$\delta W_I + \delta W_E = \delta W = 0, \tag{11.43}$$

which is immediately recognized as a restatement of the principal of virtual work. The principle of work is therefore entirely equivalent to the weak statement of equilibrium, which in turn, is entirely equivalent to the equilibrium conditions for the beam.

**Beam under transverse load**

In a similar manner, a more physical interpretation of the weak statement of equilibrium for beams under transverse loads given by eq. (11.34) can be obtained by introducing virtual transverse displacements, $\delta\bar{u}_2(x_1)$, in place of test functions, $w(x_1)$. This leads to

$$-\int_0^L \frac{\mathrm{d}^2\delta\bar{u}_2}{\mathrm{d}x_1^2} M_3 \,\mathrm{d}x_1 + \int_0^L \delta\bar{u}_2 p_2 \,\mathrm{d}x_1 + \delta\bar{u}_2(L)P_2 = 0, \tag{11.44}$$

*for all arbitrary $\delta\bar{u}_2$ satisfying the geometric boundary conditions.*

The first integral in this statement can be written as $-\int_0^L M_3\delta\kappa_3 \,\mathrm{d}x_1$ and represents the internal virtual work, $\delta W_I$, in a beam subjected to transverse loads only, see eq. (9.79a).

Using the same reasoning as before, the second and third terms in eq. (11.44) represent the virtual work done by the applied distributed transverse load, $p_2$, and concentrated tip load, $P_2$. This is the total work done by the externally applied loads, $\delta W_E$.

In summary, eq. (11.44) can now be restated as, $\delta W_I + \delta W_E = \delta W = 0$, which is simply a statement of the principal of virtual work. Although the expressions of the principle of virtual work for beams under axial and transverse loads, eqs. (11.42) and (11.44), respectively, are different, their physical interpretation is identical.

**Approximate solutions**

Approximate solutions for beam problems can be obtained from the principle of virtual work by following a procedure identical to that used with the weak statement of equilibrium in section 11.3.2. Consider, for instance, the beam under a uniform axial load treated in example 11.7. The principal of virtual work can be written for this problem as

$$\delta W = -\int_0^L \frac{\mathrm{d}\delta\bar{u}_1}{\mathrm{d}x_1} S \frac{\mathrm{d}\bar{u}_1}{\mathrm{d}x_1} \,\mathrm{d}x_1 + \int_0^L \delta\bar{u}_1(x_1) p_0 \,\mathrm{d}x_1 = 0.$$

The following forms are then assumed for the solution, $\bar{u}_1(x_1)$, and for the virtual displacements, $\delta\bar{u}_1(x_1)$,

$$\bar{u}_1(x_1) = q_1 x_1 + q_2 x_1^2; \quad \delta\bar{u}_1(x_1) = \delta q_1 x_1 + \delta q_2 x_1^2, \tag{11.45}$$

where $q_1$ and $q_2$ are two unknown coefficients, and $\delta q_1$ and $\delta q_2$ are arbitrary virtual coefficients since the virtual displacement is itself arbitrary.

These expressions should be compared with eq. (11.21). The only difference is one of notation: $w_1 = \delta q_1$ and $w_2 = \delta q_2$. The rest of the procedure is identical to that outlined in section 11.3.4, and identical results are obtained.

A similar approach can also be taken for bending of a beam subjected to transverse loads as treated in section 11.3.5.

### 11.3.8 The principle of minimum total potential energy

The principle of virtual work is solely a statement of equilibrium. Equations (11.42) and (11.44) are statements of this principle for beams under axial and transverse loads, respectively, and do not involve the beam's sectional strains or stiffness characteristics. Clearly, the principle is unaware of the strain-displacement relationships

and constitutive laws. These two sets of equations will now be combined with the principle of virtual work.

Consider an axially loaded beam. Introducing the axial constitutive law, eq. (5.16), and the axial strain-displacement relationship, eq. (5.6), into eq. (11.42) yields

$$-\int_0^L \frac{\mathrm{d}\,\delta\bar{u}_1}{\mathrm{d}x_1} S \frac{\mathrm{d}\bar{u}_1}{\mathrm{d}x_1}\,\mathrm{d}x_1 + \int_0^L \delta\bar{u}_1(x_1) p_1\,\mathrm{d}x_1 + \delta\bar{u}_1(L) P_1 = 0. \tag{11.46}$$

The beam is now assumed to be made of a linearly elastic material, resulting in the sectional constitutive law give by eq. (5.16). Hence, the developments that follow apply only to linearly elastic materials, whereas the principle of virtual work, which is equivalent to Newton's law, is not limited by any such restrictions.

The last two terms in eq. (11.46) can still be interpreted as the virtual work done by the externally applied loads, whereas the first term is the virtual work done by the internal axial forces. As observed before, the variational operator, $\delta$, and the derivative operator, $\mathrm{d}$, commute, and hence, the internal virtual work can be manipulated as follows

$$\begin{aligned}\int_0^L \left(\frac{\mathrm{d}\delta\bar{u}_1}{\mathrm{d}x_1}\right) S \frac{\mathrm{d}\bar{u}_1}{\mathrm{d}x_1}\,\mathrm{d}x_1 &= \int_0^L \delta\left(\frac{\mathrm{d}\bar{u}_1}{\mathrm{d}x_1}\right) S \frac{\mathrm{d}\bar{u}_1}{\mathrm{d}x_1}\,\mathrm{d}x_1 \\ &= \int_0^L \delta\left[\frac{1}{2} S \left(\frac{\mathrm{d}\bar{u}_1}{\mathrm{d}x_1}\right)^2\right]\,\mathrm{d}x_1 = \delta\int_0^L \frac{1}{2} S\bar{\epsilon}_1^2\,\mathrm{d}x_1.\end{aligned}$$

The second equality is the direct result of treating the variational operator, $\delta$, as a differential operator, and the third equality follows from the definition of the sectional axial strain, $\bar{\epsilon}_1$, see eq. (5.6). Note that in the third equality, the integral sign and the variational operator are assumed to commute, by analogy with the differential operator, which enjoys this property according to Leibnitz' integral rule.

The quantity $1/2\ S\bar{\epsilon}_1^2$ is the strain energy density function, $a(\bar{\epsilon}_1)$, defined in eq. (10.34), which represents the elastic energy stored in a deformed differential slice of the beam, as discussed in section 10.4.1. The total elastic energy stored in the deformed beam, $A(\bar{\epsilon}_1)$, is then found by integrating the strain energy density function over the beam's span. The previous equation can now be written as

$$\int_0^L \delta\left(\frac{\mathrm{d}\bar{u}_1}{\mathrm{d}x_1}\right) S \frac{\mathrm{d}\bar{u}_1}{\mathrm{d}x_1}\,\mathrm{d}x_1 = \delta\int_0^L a(\bar{\epsilon}_1)\,\mathrm{d}x_1 = \delta A(\bar{\epsilon}_1).$$

Using this result, eq. (11.46) now becomes

$$\delta A(\bar{\epsilon}_1) - \delta W_E = 0, \tag{11.47}$$

and is interpreted as follows. *A beam is in equilibrium if and only if virtual changes in the total strain energy equal the virtual work done by the externally applied loads, for all arbitrary virtual displacements that satisfy the geometric boundary conditions.*

An even more compact statement can be obtained if the externally applied loads are assumed to be conservative and can therefore be derived from a potential,

$$p_1(x_1) = -\frac{\partial \phi}{\partial \bar{u}_1} \quad \text{and} \quad P_1 = -\frac{\partial \Psi}{\partial \bar{u}_1}, \tag{11.48}$$

where $\phi$ is the *potential of the distributed loads*, and $\Psi$ the *potential of the concentrated load*. The virtual work done by the externally applied loads now becomes

$$\begin{aligned}\int_0^L p_1\, \delta\bar{u}_1(x_1)\, \mathrm{d}x_1 + P_1 \delta\bar{u}_1(L) &= -\int_0^L \frac{\partial \phi}{\partial \bar{u}_1}\, \delta\bar{u}_1(x_1)\, \mathrm{d}x_1 - \frac{\partial \Psi}{\partial \bar{u}_1}\delta\bar{u}_1(L) \\ &= -\delta\left[\int_0^L \phi\, \mathrm{d}x_1 + \Psi\right] = -\delta\Phi,\end{aligned}$$

where $\Phi$ is the *total potential of the externally applied loads*. Introducing this result in eq. (11.47) yields $\delta A(\epsilon_1) + \delta\Phi = 0$.

Finally, if the *total potential energy*, $\Pi$, of the system is defined as

$$\Pi = A + \Phi, \tag{11.49}$$

it then follows that

$$\delta\Pi = 0. \tag{11.50}$$

This result is the statement of the principle of stationary total potential energy developed in section 10.2 as principle 8. It states: *a beam is in equilibrium if and only virtual changes in the total potential energy vanish for all virtual displacements.*

For beams subjected transverse loads, the total potential energy is still given by eq. (11.49). The strain energy is now due to curvature, and the total strain energy in the beam is given by eq. (10.39). The total potential of the applied load combines the potentials of the distributed and concentrated transverse loads as follows

$$p_2(x_1) = -\frac{\partial \phi}{\partial \bar{u}_2}; \quad P_2 = -\frac{\partial \Psi}{\partial \bar{u}_2}, \tag{11.51}$$

respectively. The statement of the principle of stationary total potential energy, principle 8, remains unchanged.

### 11.3.9 Treatment of the boundary conditions

In the weak statement of equilibrium and in the principle of virtual work, the geometric and natural boundary conditions are treated in a different manner. Test functions or virtual displacements are introduced, which are required to satisfy the geometric boundary conditions. On the other hand, the natural boundary conditions are not mentioned in the statement of these principles.

Although this distinction is generally made in presentations of energy and variational principles, it is an unnecessary distinction as will be demonstrated in the following sections through a number of examples. Beams under both axial and transverse loads will be considered.

**Beams under axial loads**

Consider a cantilever beam subjected to distributed axial loads, $p_1(x_1)$, and a concentrated axial load, $P_1$, at the free end as depicted in fig 11.28. In section 11.3.1, the weak statement of equilibrium is formulated for this problem. A similar reasoning will be presented here; the concept of virtual displacements rather than that of test functions will be used. Furthermore, the treatment of the boundary conditions will be fundamentally altered.

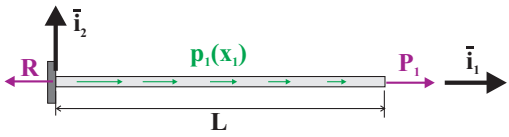


**Fig. 11.28.** Simple cantilevered beam.

The equations of equilibrium of the problem are in two parts: the differential equilibrium condition that holds for all points along the beam's span, eq. (11.10a), and the equilibrium conditions that apply at the beam's boundaries. At the beam's tip, eq. (11.10b) states that $N_1(L) = P_1$. As indicated in fig. 11.28, a reaction force, $R$, acts at the root end of the beam, and equilibrium implies $N_1(0) = R$.

The forces acting at the two ends of the beam are often regarded as being of a different nature, and distinct names are used for the two types of forces: the root force, $R$, is called a *reaction force*, whereas the tip load, $P_1$, is called an *externally applied load*. When it comes to Newton's law, however, this distinction is irrelevant: the "sum of the forces must vanish" applies to all forces including reaction forces and externally applied loads.

Equilibrium is the most fundamental condition in structural analysis, and it must always be satisfied. The two equilibrium equations, $N_1(0) = R$ and $N_1(L) = P_1$, are both correct, and equally important. In view of this discussion, the strong statement of equilibrium is recast as follows,

$$\frac{\mathrm{d}N_1}{\mathrm{d}x_1} + p_1 = 0, \quad \text{for} \quad 0 \leq x_1 \leq L, \tag{11.52a}$$

$$N_1 = R, \quad \text{for} \quad x_1 = 0, \tag{11.52b}$$

$$N_1 = P_1, \quad \text{for} \quad x_1 = L. \tag{11.52c}$$

The following integral statement can now be constructed, again using the sign convention defined in section 11.3.1

$$\int_0^L \delta\bar{u}_1 \left[\frac{\mathrm{d}N_1}{\mathrm{d}x_1} + p_1\right] \mathrm{d}x_1 + \delta\bar{u}_1(0)\left[N_1 - R\right]_0 - \delta\bar{u}_1(L)\left[N_1 - P_1\right]_L = 0,$$

where $\delta\bar{u}_1(x_1)$ is an arbitrary virtual displacement field.

If the beam is in equilibrium, eqs. (11.52) must hold, and therefore the above equation is satisfied *for all arbitrary virtual displacements*. Indeed, the three bracketed terms are simply the equilibrium equations of the problem.

Next, an integration by parts is performed on the first term appearing in the above integral, see eq. (11.12), leading to the following statement

$$-\int_0^L \delta\frac{\mathrm{d}\bar{u}_1}{\mathrm{d}x_1}N_1\,\mathrm{d}x_1+\int_0^L \delta\bar{u}_1 p_1\,\mathrm{d}x_1-\delta\bar{u}_1(0)R+\delta\bar{u}_1(L)P_1=0, \qquad (11.53)$$

*for all arbitrary virtual displacements.*

As discussed in section 11.3.7, the first integral can be interpreted as the internal virtual work, $\delta W_I$, done by the axial force acting within the beam. The last three terms form the virtual work, $\delta W_E$, done by the externally applied loads. The integral is the virtual work done by the distributed load, $p_1$, and the last two terms are the virtual work done by the root reaction and tip load, respectively.

Clearly, the above statement is, once again, a statement of the principle of virtual work. This new statement should be compared to that given in eq. (11.42). Two crucial differences can be observed. In eq. (11.53), the virtual work done by the externally applied forces includes the work done by the root reaction, and the virtual displacements are entirely arbitrary. In contrast, in eq. (11.42), the root reaction does not appear in the expression for the virtual work done by the externally applied forces, and the virtual displacements must satisfy the geometric boundary conditions but are otherwise arbitrary.

The principle of virtual work as stated in eq. (11.53) is more general than that expressed by eq. (11.42). In eq. (11.53), virtual displacements are entirely arbitrary, and hence it is always possible to select $\delta\bar{u}_1(0)=0$, *i.e.*, to restrict the virtual displacements to those that satisfy the geometric boundary conditions. The second virtual work term now vanishes, $\delta\bar{u}_1(0)R=0$, and the principle of virtual work stated by eq. (11.42) is recovered.

Clearly, the vanishing of the virtual work done by the root reaction force does by no means imply the vanishing of the reaction force itself. Restricting virtual displacements to those that satisfy the geometric boundary conditions, *i.e.*, setting $\delta\bar{u}_1(0)=0$, implies $\delta\bar{u}_1(0)R=0$ although $R\neq 0$. Restricting the virtual displacements to those that satisfy the geometric boundary conditions does, however, eliminate the reaction force from the statement of the principle of virtual work because the virtual work it performs vanishes.

This discussion underlines an important feature of the principle of virtual work as stated by eq. (11.42): because virtual displacements are restricted to those satisfying the geometric boundary conditions, the reaction forces are eliminated from the statement of the principle. This simplifies the problem because it is no longer necessary to even identify the reaction forces which therefore, do not enter the formulation of the problem. On the other hand, the principle provides no information about the reaction forces which are often quantities of primary interest to structural analysts.

At this point in the discussion, the relationship between geometric boundary conditions and reaction forces can be clarified: reaction forces are those arising from the

enforcement of geometric boundary conditions. At any point on a structure's outer surface, it is possible to prescribe either a displacement or an externally applied force. It is, however, impossible to prescribe both at the same time. If the displacement is prescribed at a point *i.e.*, a geometric boundary condition is imposed, an unknown force (the reaction force) will arise at that point. If a force is applied at a point (an externally applied force), an unknown displacement will arise at that point. The principle of virtual work as stated by eq. (11.42) will provide equations to evaluate the displacements at all points where external forces are applied, but it will yield no information concerning the reaction forces.

In contrast, the principle of virtual work stated by eq. (11.53) allows the use of any arbitrary virtual displacements, *including those that violate the geometric boundary conditions*. The reactions forces, however, must be included the formulation of the virtual work done by the externally applied loads and the *reaction forces should be treated as externally applied loads*.

This view is consistent with Newtonian mechanics: when formulating equilibrium equations, no distinction is made between externally applied loads and reaction forces. Since the principle of virtual work is entirely equivalent to Newton's law, it should also treat externally applied loads and reaction forces in identical ways. This slightly complicates problem formulations because all reaction forces must be properly identified, and the virtual work they perform must be accurately accounted for in the statement of the principle. On the other hand, the principle will then provide the necessary equations to compute these reaction forces.

This discussion mirrors the developments presented in chapter 9, where the use of kinematically admissible virtual displacements and arbitrary virtual displacements is contrasted in sections 9.5.3 and 9.5.4, respectively. Kinematically admissible virtual displacements satisfy the geometric boundary conditions, whereas arbitrary virtual displacements do not.

### Beams under transverse loads

The reasoning presented in the previous section for beams under axial loads will be repeated here for beam under transverse loads. Consider a cantilevered beam with a tip support subjected to a uniform transverse load, $p_0$, and a tip moment, $Q_T$, as depicted in fig. 11.29. In section 11.3.4, the weak statement of equilibrium is developed for this problem. A very similar reasoning will be presented here, with special attention devoted to the treatment of the boundary conditions.

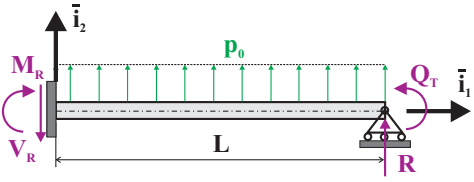


**Fig. 11.29.** Cantilevered beam with a tip support.

The differential equation of equilibrium of a beam under bending is developed in section 5.5.3, and the equilibrium equation is given by eq. (5.39). This equation holds at all points over the span of the beam, *i.e.*, for $0 \leq x_1 \leq L$.

As indicated in fig. 11.29, several reaction forces will also develop. At the beam's root, a shear reaction, $V_R$, and a bending moment, $M_R$, will appear, while at the beam's tip, a vertical force, $R$, arises. As expected, each of these forces is associated with a specific geometric boundary condition. At the beam's root, the vanishing of the displacement and rotation generates the reaction shear force, $V_R$, and moment, $M_R$, respectively, while at the beam's tip, the vanishing of the vertical displacement causes the vertical reaction, $R$. The complete set of equilibrium equations is now

$$\frac{\mathrm{d}^2 M_3}{\mathrm{d}x_1^2} = p_2, \quad \text{for} \quad 0 \leq x_1 \leq L, \tag{11.54a}$$

$$V_2 = V_R, \quad M_3 = M_R, \quad \text{for} \quad x_1 = 0, \tag{11.54b}$$

$$V_2 = R, \quad M_3 = Q_T, \quad \text{for} \quad x_1 = L. \tag{11.54c}$$

Next, the following integral statement is constructed using the sign convention defined in section 11.3.1

$$\int_0^L -\delta\bar{u}_2 \left[\frac{\mathrm{d}^2 M_3}{\mathrm{d}x_1^2} - p_2\right] \mathrm{d}x_1 + \delta\bar{u}_2(0)\left[V_2 - V_R\right]_0 + \delta\left(\frac{\mathrm{d}\bar{u}_2}{\mathrm{d}x_1}\right)_0 \left[M_3 - M_R\right]_0 - \delta\bar{u}_2(L)\left[V_2 - R\right]_L - \delta\left(\frac{\mathrm{d}\bar{u}_2}{\mathrm{d}x_1}\right)_L \left[M_3 - Q_T\right]_L = 0.$$

where $\delta\bar{u}_2(x_1)$ is an arbitrary virtual displacement field.

If the beam is in equilibrium, eqs. (11.54) must hold, and therefore, the above equation is satisfied *for all arbitrary virtual displacements*. Indeed, the five bracketed terms set equal to zero are simply the equilibrium equations of the problem.

Next, two integrations by parts are performed on the first term appearing in the above integral, and the $\delta$ and $\mathrm{d}$ operators are interchanged, see eq. (11.32), leading to the following statement

$$-\int_0^L \delta\left(\frac{\mathrm{d}^2\bar{u}_2}{\mathrm{d}x_1^2}\right) M_3 \,\mathrm{d}x_1 + \int_0^L \delta\bar{u}_2 p_2 \,\mathrm{d}x_1 - \delta\bar{u}_2(0)V_R - \delta\left(\frac{\mathrm{d}\bar{u}_2}{\mathrm{d}x_1}\right)_0 M_R + \delta\bar{u}_2(L)R + \delta\left(\frac{\mathrm{d}\bar{u}_2}{\mathrm{d}x_1}\right)_L Q_T = 0, \tag{11.55}$$

*for all arbitrary virtual displacements.*

As discussed in section 11.3.7, the first integral can be interpreted as the virtual work, $\delta W_I$, done by the bending moment acting within in the beam. The remaining five terms form the virtual work, $\delta W_E$, done by the externally applied loads. The integral is the virtual work done by the distributed load, $p_2$, and the last four terms are the virtual work done by the root reaction shear force, root reaction bending moment, tip reaction and applied tip moment, respectively.

The above statement once again expresses the principle of virtual work and should be compared to that given by eq. (11.44). Here again, two crucial differences are observed. In eq. (11.55), the virtual work done by the externally applied forces includes the work done by all reaction forces and moments, and the virtual displacements are entirely arbitrary. In contrast, in eq. (11.44), the reaction forces and moments do not appear in the expression for the virtual work done by the externally applied forces, because the virtual displacements must satisfy the geometric boundary conditions and are therefore zero at the reaction points.

It is easy to derive statement (11.44) from eq. (11.55). Indeed, in eq. (11.55), virtual displacements are entirely arbitrary, and hence, it is always possible to select $\delta\bar{u}_2(0) = \delta\left(\mathrm{d}\bar{u}_2(0)/\mathrm{d}x_1\right) = \delta\bar{u}_2(L) = 0$, *i.e.*, to restrict the virtual displacements to those that satisfy the geometric boundary conditions. Introducing these three conditions into eq. (11.55) then leads to statement (11.44).

Restricting the virtual displacements to only those that satisfy the geometric boundary conditions implies that the reaction forces and moments no longer appear in the statement of the principle of virtual work, because the virtual work they performs does vanish.

In summary, the principle of virtual work stated by eq. (11.53) allows the use of any arbitrary virtual displacements, *including those that violate the geometric boundary conditions*. The reactions forces and moments, however, must be included in the statement of the virtual work done by the externally applied loads, *i.e.*, *reaction forces and moments should be treated as externally applied loads*.

***Example 11.12. Cantilevered beam with tip support. Case 1***

To illustrate the treatment of the boundary conditions discussed in the previous sections, consider a cantilevered beam with a tip support, subjected to a uniform transverse load, $p_0$, as depicted in fig. 11.29. The tip moment, $Q_T$, will be set to zero in this example. The geometric boundary conditions for this problem are $\bar{u}_2(0) = \mathrm{d}\bar{u}_2/\mathrm{d}x_1(0) = \bar{u}_2(L) = 0$. This problem is treated in example 5.11 on page 205 using the classical differential equation approach.

The principle of virtual work will be used to find an approximate solution of this problem, starting with the following assumed displacement field

$$\bar{u}_2(\eta) = h_1(\eta)q_1 + h_2(\eta)q_3 + h_3(\eta)q_3 = \eta^2(1-\eta)q_1 + \eta^2(1-\eta)\eta q_2 + \eta^2 q_3, \quad (11.56)$$

where $\eta = x_1/L$ is the non-dimensional variable along the beam's span. Note that the first two shape functions, $h_1 = \eta^2(1-\eta)$ and $h_2 = \eta^2(1-\eta)\eta$, satisfy all three boundary conditions, whereas the last shape function, $h_3 = \eta^2$, satisfies the first two, but not the last, because $h_3(1) = 1 \neq 0$. Consequently, the appropriate statement of the principle of virtual work is

$$-\int_0^L \delta\left(\frac{\mathrm{d}^2\bar{u}_2}{\mathrm{d}x_1^2}\right) M_3 \,\mathrm{d}x_1 + \int_0^L \delta\bar{u}_2 p_2 \,\mathrm{d}x_1 + \delta\bar{u}_2(L)R = 0.$$

Because all shape functions satisfy the two geometric boundary conditions at the beam's root, the virtual work done by the root reaction force and bending moment

vanish, and hence, do not appear in the above statement. On the other hand, because one of the shape functions violates the geometric boundary condition at the beam's tip, the virtual work done by the tip reaction force does not vanish and must be included in the principle.

Introducing the assumed displacement field along with the moment-curvature expression, $M_3 = H_{33}^c \bar{u}_2''/L^2$, and using Galerkin's approach then leads to

$$
\begin{aligned}
&-\frac{H_{33}^c}{L^3}\int_0^1 \left[h_1''\delta q_1 + h_2''\delta q_2 + h_3''\delta q_3\right]\left[h_1'' q_1 + h_2'' q_2 + h_3'' q_3\right]\,\mathrm{d}\eta \\
&+ p_0 L \int_0^1 \left[(\eta^2-\eta^3)\delta q_1 + (\eta^3-\eta^4)\delta q_2 + \eta^2\delta q_3\right]\,\mathrm{d}\eta + \delta q_3 R = 0.
\end{aligned}
$$

Introducing the derivatives of the shape functions, $h_1'' = 2 - 6\eta$, $h_2'' = 6\eta - 12\eta^2$, and $h_3'' = 2$, and evaluating all integrals leads to

$$
-\left\{\delta q_1, \delta q_2, \delta q_3\right\}\frac{H_{33}^c}{L^3}\begin{bmatrix} 4 & 4 & -2 \\ 4 & \frac{24}{5} & -2 \\ -2 & -2 & 4 \end{bmatrix}\begin{Bmatrix} q_1 \\ q_2 \\ q_3 \end{Bmatrix} + \left\{\delta q_1, \delta q_2, \delta q_3\right\}\begin{Bmatrix} p_0 L/12 \\ p_0 L/20 \\ p_0 L/3 + R \end{Bmatrix} = 0.
$$

Because the virtual displacements are arbitrary coefficients, they can be selected as $\left\{\delta q_1, \delta q_2, \delta q_3\right\} = \left\{1, 0, 0\right\}$, $\left\{\delta q_1, \delta q_2, \delta q_3\right\} = \left\{0, 1, 0\right\}$, and $\left\{\delta q_1, \delta q_2, \delta q_3\right\} = \left\{0, 0, 1\right\}$. The resulting three equations then form a set of linear equations

$$
\frac{H_{33}^c}{L^3}\begin{bmatrix} 4 & 4 & -2 \\ 4 & \frac{24}{5} & -2 \\ -2 & -2 & 4 \end{bmatrix}\begin{Bmatrix} q_1 \\ q_2 \\ q_3 \end{Bmatrix} = \begin{Bmatrix} p_0 L/12 \\ p_0 L/20 \\ p_0 L/3 + R \end{Bmatrix}. \tag{11.57}
$$

This system is a set of three equations for four unknowns, $q_1$, $q_2$, $q_3$, and the tip reaction force, $R$.

At this point it is important to remember that the assumed solution, eq. (11.56), does not satisfy the geometric boundary condition at the beam's tip, $\bar{u}_2(1) = q_3 \neq 0$. In other words, the solution process is not "aware" of the fact that the beam's tip deflection must vanish.

To proceed further, the tip boundary condition, *i.e.*, $q_3 = 0$, must now be enforced. It then becomes possible to solve the first two equations of system (11.57) to find $q_1 = 3p_0 L^4/(48 H_{33}^c)$ and $q_2 = -2p_0 L^4/(48 H_{33}^c)$. The transverse displacement field, eq. (11.56), is found as

$$
\bar{u}_2 = \frac{1}{48}\frac{p_0 L^4}{H_{33}^c}\eta^2(1-\eta)(3-2\eta).
$$

This result matches the exact solution given by eq. (5.61).

Next, the last equation of system (11.57) is solved for the tip reaction force to yield

$$
R = -\frac{p_0 L}{3} - 2\frac{H_{33}^c}{L^3}(q_1 + q_2) = -\frac{3p_0 L}{8},
$$

which matches the exact solution, eq. (5.62). The use of a virtual displacement that does not satisfy the geometric boundary condition at the beam's tip provides an additional equation that can be solved for the reaction force, $R$.

As mentioned earlier, at any point along the beam's span, either displacement or external force can be prescribed, but not both at the same time. The structure of system (11.57) reflect this fact: it features three equations linking four variables. If the tip deflection is prescribed, $q_3 = 0$, and the remaining three variables can be found, as is done in the previous paragraph. If the tip force is prescribed, $R$ is a known quantity, and the solution of system (11.57) for $q_1$, $q_2$, and $q_3$, yields the transverse displacement field as

$$\bar{u}_2 = \frac{p_0 L^4}{48 H_{33}^c}\eta^2(1-\eta)(3-2\eta) + \frac{RL^3}{6H_{33}^c}\eta^2(3-\eta).$$

The first term corresponds to the deflection of the cantilevered beam under the uniform load, and the second is that due to the externally applied tip load, $R$. In this case, the tip support is not present, and the tip boundary condition is not imposed.

Finally, it should be noted that system (11.57) can also be used to find the response of the structure under a prescribed displacement, $\Delta$, at the tip. In this case, $q_3 = \Delta$, and the system is solved for the remaining variables to find the transverse displacement field

$$\bar{u}_2 = \frac{p_0 L^4}{48 H_{33}^c}\eta^2(1-\eta)(3-2\eta) + \frac{\Delta}{2}\eta^2(3-\eta).$$

The last equation of system (11.57) is then solved for the reaction force $R = 3p_0 L/8 + 3H_{33}^c \Delta / L^3$.

***Example 11.13. Cantilevered beam with tip support. Case 2***

Consider a cantilevered beam with a tip support subjected to a uniform transverse load, $p_0$, as depicted in fig. 11.29. The tip moment, $Q_T$, shown in the figure will again be set to zero in this example. The geometric boundary conditions for this problem are $\bar{u}_2(0) = \mathrm{d}\bar{u}_2/\mathrm{d}x_1(0) = \bar{u}_2(L) = 0$.

The principle of virtual work will be used to find an approximate solution of this problem, starting with the following assumed displacement field that is slightly different from the one used in the previous example

$$\bar{u}_2(\eta) = h_1 q_1 + h_2 q_2 + h_3 q_3 = \eta^2(1-\eta)q_1 + \eta^2(1-\eta)\eta q_2 + \eta(1-\eta)q_3, \quad (11.58)$$

where $\eta = x_1/L$ is the non-dimensional variable along the beam's span. Note that the first two shape functions, $h_1 = \eta^2(1-\eta)$ and $h_2 = \eta^2(1-\eta)\eta$, satisfy all three boundary conditions, whereas the last shape function, $h_3 = \eta(1-\eta)$, satisfies the zero deflection conditions at the beam's root and tip, but the vanishing of the root rotation is not satisfied because $h_3'(0) = 1 \neq 0$.

An appropriate statement of the principle of virtual work is, therefore,

$$-\int_0^L \delta\left(\frac{\mathrm{d}^2\bar{u}_2}{\mathrm{d}x_1^2}\right) M_3 \,\mathrm{d}x_1 + \int_0^L \delta\bar{u}_2 p_2 \,\mathrm{d}x_1 - \delta\left(\frac{\mathrm{d}\bar{u}_2}{\mathrm{d}x_1}\right)_0 M_R = 0.$$

In this case, the virtual work done by the root reaction moment must be included in the statement of the principle because the third shape function does not satisfy the zero slope condition at the beam's root.

Introducing the assumed displacement field and using Galerkin's approach then leads to

$$-\frac{H^c_{33}}{L^3}\int_0^1 \left[h_1''\delta q_1 + h_2''\delta q_2 + h_3''\delta q_3\right]\left[h_1'' q_1 + h_2'' q_2 + h_3'' q_3\right]\,\mathrm{d}\eta$$
$$+ p_0 L\int_0^1 \left[(\eta^2-\eta^3)\delta q_1 + (\eta^3-\eta^4)\delta q_2 + \eta(1-\eta)\delta q_3\right]\,\mathrm{d}\eta - \delta q_3 M_R/L = 0.$$

After introducing the derivatives of the shape functions, $h_1'' = 2-6\eta$, $h_2'' = 6\eta - 12\eta^2$, and $h_3'' = -2$, and evaluating of all integrals, the following system of equations is found

$$\frac{H^c_{33}}{L^3}\begin{bmatrix} 4 & 4 & 2 \\ 4 & \frac{24}{5} & 2 \\ 2 & 2 & 4 \end{bmatrix}\begin{Bmatrix} q_1 \\ q_2 \\ q_3 \end{Bmatrix} = \begin{Bmatrix} p_0 L/12 \\ p_0 L/20 \\ p_0 L/6 - M_R/L \end{Bmatrix}. \tag{11.59}$$

This system is a set of three equations for four unknowns, $q_1$, $q_2$, $q_3$, and the root reaction moment, $M_R$.

The assumed solution, eq. (11.58), does not satisfy one of the geometric boundary conditions at the beam's root, $\mathrm{d}\bar{u}_2(0)/\mathrm{d}x_1 = q_3/L \neq 0$. To proceed, this root boundary condition, *i.e.*, $q_3 = 0$, must now be enforced. It then becomes possible to solve the first two equations of system (11.59) to find $q_1 = 3p_0L^4/(48H^c_{33})$ and $q_2 = -2p_0L^4/(48H^c_{33})$. Once again, this leads to the exact solution for the transverse displacement field, which is given by eq. (5.61). Finally, the last equation of system (11.59) is solved for the root reaction moment, to yield

$$M_R = \frac{p_0 L^2}{6} - 2\frac{H^c_{33}}{L^3}L(q_1+q_2) = \frac{p_0 L^2}{8}.$$

Elementary statics arguments reveal that this result is exact. Clearly, the use of a virtual displacement that does not satisfy the rotation geometric boundary condition at the beam's root yields an additional equilibrium equation that can be solved for the root reaction moment, $M_R$.

If the root moment, $M_R$, is assumed to be known, system 11.59 can then be solved directly for $q_1$, $q_2$, and $q_3$. In this case, the vanishing of the root rotation is not enforced, and the problem now consists of a beam simply supported at both ends and subjected to a uniform transverse loading and the root bending moment, $M_R$. The transverse displacement field is found as

$$\bar{u}_2 = \frac{p_0 L^4}{24H^c_{33}}\eta(1-\eta)(1+\eta-\eta^2) - \frac{M_R L^2}{6H^c_{33}}\eta(1-\eta)(2-\eta).$$

The first term corresponds to the deflection of the simply supported beam under the uniform load, see eq. (5.48), and the second is that due to the externally applied root moment, $M_R$.

### 11.3.10 Summary

#### Equilibrium formulations

The three equilibrium formulations derived thus far all express the equilibrium conditions for a beam because all are derived from the weak statement of equilibrium. However, these formulations are not all equivalent.

The weak statement of equilibrium and the principle of virtual work are entirely equivalent to Newton's law and express the equilibrium conditions for the beam; they provide no information about either constitutive laws or strain-displacement relationships. Newton's law expresses the vanishing of all forces and moments acting on each differential element of the structure, and so do the weak statement of equilibrium and the principle of virtual work. Because Newton's law always applies to any structure, so do the weak statement of equilibrium and the principle of virtual work.

The principle of minimum total potential energy is the third statement of equilibrium, but both constitutive laws and strain-displacement relationships are incorporated into this principle. The principle can be expressed in a single, concise statement that encapsulates the three groups of equations required for the solution of structural problems. It is, however, important to note that *two fundamental assumptions* are made in the derivation of this principle and restrict its applicability. First, the existence of a strain energy density function is assumed and second, the externally applied loads are assumed to be conservative. These two assumptions are discussed in section 10.2. A hybrid form, principle 10, is useful when a strain energy function exists but applied loads are nonconservative and therefore cannot be derived from a potential.

#### Variational operator

In making the connection between the weak statement of equilibrium and the principle of virtual work, the variational operator, $\delta$, is introduced, and several properties of the this operator are used in this section. Clearly, this operator can be used in much the same way as the differential operator, $\mathrm{d}$, although its physical interpretation is quite different. Using the variational operator, virtual displacements are introduced in eq. (11.41) as being simply equivalent to arbitrary functions. A formal mathematical treatment of the variational operator can be found in several textbooks [6, 5] and is beyond the scope of this book.

## 11.4 Formal procedures for the derivation of approximate solutions

The examples presented in the previous sections demonstrate that approximate solutions of structural problem can be derived from either the weak statement of equilibrium, the principle of virtual work, or the principle of minimum total potential

energy. To extend this approach to more complex structures, a formal procedure for constructing approximate solutions based on these concepts is now introduced.

Approximate solutions are generally implemented in computer programs, and for this reason, it will be convenient to recast all quantities in the form of arrays or matrices to enable the systematic use of linear algebra methods.

After presentation of the basic approximation approach, procedures based on the principle of virtual work and principle of minimum total potential energy will then be described separately.

### 11.4.1 Basic approximations

The problem of a beam under axial loads will be used once again to illustrate the process. The first step of the solution procedure is to assume the displacements and virtual displacements fields to be of the following forms

$$\bar{u}_1(x_1) = \sum_{i=1}^{N} h_i(x_1) q_i, \tag{11.60a}$$

$$\delta\bar{u}_1(x_1) = \sum_{i=1}^{N} g_i(x_1) w_i, \tag{11.60b}$$

respectively, where the coefficients $q_i$, $i = 1, 2, \ldots, N$, are unknown coefficients, often called *degrees of freedom*, which determine the solution of the problem, and the coefficients $w_i$, $i = 1, 2, \ldots, N$, a set of arbitrary coefficients reflecting the arbitrary nature of the virtual displacements.

Functions $h_i(x_1)$ and $g_i(x_1)$ are sets of arbitrary functions called *shape functions*, each of which must satisfy the geometric boundary conditions of the problem. Polynomials or trigonometric functions can be selected as shape functions; transcendental functions can also be used as long as they form a set of linearly independent functions that each satisfy the geometric boundary conditions.

In Galerkin's approach, the same shape functions are selected for both displacements and virtual displacements, *i.e.*, $h_i(x_1) = g_i(x_1)$. Although this is a common and convenient choice, it is not required by any of the approaches.

Equation (11.60a) represents an approximate solution of the problem because it combines a finite number, $N$, of preselected shape functions. Each coefficient, $q_i$, indicates how much the corresponding shape function contributes to the final solution; hence, these coefficients are also called *participation factors*. If a complete series of shape functions is selected, the approximate solution should converge to the exact solution as an increasing number of shape functions is used. The finite series limit in eq. (11.60a) reduces the number of degrees of freedom from infinity to $N$ and results in an approximate solution. The same remarks can be made about the assumed form of the virtual or test displacements, eq. (11.60b).

All three principles considered here require an integral statement to hold "for all arbitrary choices of the virtual displacements that satisfy the geometric boundary conditions." This calls for virtual displacements or test functions involving an

infinite number of degrees of freedom: "for all arbitrary choices" clearly means "for an infinite number of arbitrary choices." Here again, the assumption implied by eq. (11.60b) reduces the number of choices for the virtual displacements from infinity to $N$; hence, "for all arbitrary choices" is replaced by "for $N$ arbitrary choices."

It is convenient to recast the expressions for the assumed displacements and virtual displacements, eqs. (11.60), into a matrix form as

$$\bar{u}_1(x_1) = \underline{H}^T(x_1)\underline{q}; \quad \text{and} \quad \delta\bar{u}_1(x_1) = \underline{H}^T(x_1)\underline{w}, \tag{11.61}$$

where $\underline{q} = \left\{q_1, q_2, \cdots, q_N\right\}^T$ is an array of size $N$ that stores the participation factors, and $\underline{w} = \left\{w_1, w_2, \cdots, w_N\right\}^T$ an array of arbitrary coefficients. The assumed displacements and virtual or test displacements are scalar quantities expressed as the scalar product of a row and a column array. The *displacement interpolation array*, $\underline{H}(x_1)$, also of size $N$, stores the selected shape functions,

$$\underline{H} = \left\{h_1(x_1), h_2(x_1), h_3(x_1), \cdots, h_N(x_1)\right\}^T. \tag{11.62}$$

When using Galerkin's approach, identical shape functions are chosen for both displacements and virtual displacements, leading to identical interpolation arrays for both quantities.

Next, the assumed displacements are introduced in the strain-displacement relationship for a beam under axial load, eq. (5.6), to find the corresponding axial strain distribution

$$\bar{\epsilon}_1(x_1) = \frac{\partial\bar{u}_1}{\partial x_1} = \frac{\partial}{\partial x_1}\underline{H}^T(x_1)\,\underline{q} = \underline{B}^T(x_1)\,\underline{q}. \tag{11.63}$$

The *strain interpolation array* of size $N$ is defined as

$$\underline{B}(x_1) = \left\{\frac{\mathrm{d}h_1}{\mathrm{d}x_1}, \frac{\mathrm{d}h_2}{\mathrm{d}x_1}, \frac{\mathrm{d}h_3}{\mathrm{d}x_1}, \cdots, \frac{\mathrm{d}h_N}{\mathrm{d}x_1}\right\}^T, \tag{11.64}$$

The virtual strains can be written in a similar manner as

$$\delta\bar{\epsilon}_1(x_1) = \delta\left(\frac{\mathrm{d}\bar{u}_1}{\mathrm{d}x_1}\right) = \frac{\mathrm{d}}{\mathrm{d}x_1}\delta\bar{u}_1 = \underline{B}^T(x_1)\,\underline{w}. \tag{11.65}$$

### 11.4.2 Principle of virtual work

All terms appearing in the principle of virtual work are virtual work quantities expressed as the product of forces by virtual displacements or stresses by virtual strains. In the present formalism, the virtual work is expressed as the scalar product of a row, representing forces, and a column, representing virtual displacements, *i.e.*, $\underline{F}^T\underline{d}$, where $\underline{F}$ and $\underline{d}$ represent the force and virtual displacement array, respectively. The factors of a scalar product commute, and the virtual work can be expressed as either $\underline{F}^T\underline{d}$ or as $(\underline{F}^T\underline{d})^T = \underline{d}^T\underline{F}$.

**Beam under axial load**

Consider a beam under axial loads and the corresponding statement of the principle of virtual work given by eq. (11.42), repeated here for reference

$$-\int_0^L N_1 \delta\bar{\epsilon}\, \mathrm{d}x_1 + \int_0^L \delta\bar{u}_1(x_1) p_1\, \mathrm{d}x_1 + \delta\bar{u}_1(L) P_1 = 0.$$

Introducing the approximations presented in the previous section, and using the appropriate constitutive law, $N_1 = S\bar{\epsilon}_1$, leads to

$$\begin{aligned} &-\int_0^L \left(\underline{B}^T \underline{w}\right)^T S \left(\underline{B}^T \underline{q}\right)\, \mathrm{d}x_1 + \int_0^L \left(\underline{H}^T \underline{w}\right)^T p_1\, \mathrm{d}x_1 + \left(\underline{H}^T(L)\underline{w}\right)^T P_1 \\ &= -\int_0^L \underline{w}^T \underline{B} S \underline{B}^T \underline{q}\, \mathrm{d}x_1 + \int_0^L \underline{w}^T \underline{H}\, p_1\, \mathrm{d}x_1 + \underline{w}^T \underline{H}(L)\, P_1 = 0, \end{aligned}$$

where each term in this expression evaluates to a scalar, as expected.

The arrays of coefficients, $\underline{q}$ and $\underline{w}$, do not depend on variable $x_1$ and can be extracted from the integrals, to yield

$$-\underline{w}^T \left[\int_0^L \underline{B} S \underline{B}^T\, \mathrm{d}x_1\right] \underline{q} + \underline{w}^T \left[\int_0^L \underline{H} p_1\, \mathrm{d}x_1\right] + \underline{w}^T \underline{H}(L) P_1 = 0. \quad (11.66)$$

To simplify the above equation, two important quantities are defined. First, the *stiffness matrix*, which is the bracketed matrix in the first term of the equation, is defined as

$$\underline{\underline{K}} = \int_0^L \underline{B}(x_1) S(x_1) \underline{B}^T(x_1)\, \mathrm{d}x_1, \quad (11.67)$$

and is of size $N \times N$. Each entry of the stiffness matrix is an average of the axial stiffness distribution weighted by a product of the strain interpolation array. For a given choice of the shape functions, each entry of the stiffness matrix can be obtained by integration along the beam's span. Moreover, the stiffness matrix is symmetric, $\underline{\underline{K}}^T = \underline{\underline{K}}$.

Second, the *load array* of size $N$ is defined as

$$\underline{Q} = \int_0^L \underline{H}(x_1) p_1(x_1)\, \mathrm{d}x_1 + \underline{H}(L) P_1. \quad (11.68)$$

Here again, for a given choice of the shape functions, the entries of the load array can be obtained by integration along the beam's span. Each entry of the load array corresponds to an average of the applied load distribution weighted by the displacement interpolation array.

With these two definitions, eq. (11.66) can be recast in a compact form as

$$\underline{w}^T \left[\underline{\underline{K}}\, \underline{q} - \underline{Q}\right] = \underline{0}. \quad (11.69)$$

Because the $N$ entries of the array of arbitrary coefficients, $\underline{w}$, can be selected at will, $N$ convenient choices will be used: $\underline{w} = \{1, 0, 0, \cdots, 0\}^T$, $\underline{w} = \{0, 1, 0, \cdots, 0\}^T$, $\underline{w} = \{0, 0, 1, \cdots, 0\}^T$, $\cdots$, and finally $\underline{w} = \{0, 0, 0, \cdots, 1\}^T$. Each new choice gives rise to a new equation, and this collection of $N$ equations can be written as

$$\underline{\underline{I}} \left[ \underline{\underline{K}}\, \underline{q} - \underline{Q} \right] = \underline{0},$$

where $\underline{\underline{I}}$ is the $N \times N$ identity matrix. Because the identity matrix is never singular, $N$ algebraic equations for the solution array are obtained

$$\underline{\underline{K}}\, \underline{q} = \underline{Q}. \tag{11.70}$$

This equation expresses the relationship between the externally applied loads represented by the load array, $\underline{Q}$, and the resulting structural displacements represented by the solution array, $\underline{q}$. Because the structure is assumed to behave in a linear manner, a linear relationship exists between the applied loads and the resulting displacements. In the present linear algebra formalism, this proportionality takes the form of set of linear equations.

The solution of the above set of equations is $\underline{q} = \underline{\underline{K}}^{-1} \underline{Q}$. Once the solution array is found, the displacement field follows from eq. (11.60a). Next, the strain field is evaluated with the help of eq. (11.63), and finally, the constitutive law, $N_1 = S\bar{\epsilon}_1$, yields the internal force.

The general solution procedure using the principle of virtual work can be summarized by the following steps,

1. Select a set of $N$ shapes functions that satisfy the geometric boundary conditions.
2. Construct the displacement interpolation array, eq. (11.62), and strain interpolation array, eq. (11.64).
3. Compute the stiffness matrix according to eq. (11.67) and load array from eq. (11.68).
4. Solve the set of $N$ simultaneous linear equations, $\underline{\underline{K}}\, \underline{q} = \underline{Q}$, for the solution array, $\underline{q}$.
5. Determine the strain distribution from eq. (11.63), and the internal forces from the constitutive law, eq. (5.16).

From a mathematical standpoint, this procedure involves the following types of operation: integrations over the beam's span for evaluating the stiffness matrix and load array, the solution of a set of linear algebraic equations to obtain the solution array, and linear algebra operations for the determination of the strain and internal force distributions. Of course, the process becomes increasingly tedious as the number of degrees of freedom increases. All the required operations, however, are easily performed on computers using numerical integration procedures for the evaluation of the stiffness matrix and load array, and standard linear algebra software packages for all remaining operations. This makes such methods very attractive for implementation on a computer.

**Beam under transverse load**

A process nearly identical to that presented above can be developed for beams subjected to transverse loads. To start, specific forms for the transverse displacements and virtual displacements fields are assumed to be in the following form

$$\bar{u}_2(x_1) = \sum_{i=1}^{N} h_i(x_1) q_i; \quad \text{and} \quad \delta\bar{u}_2(x_1) = \sum_{i=1}^{N} h_i(x_1) w_i. \tag{11.71}$$

The displacement field can then be expressed as $\bar{u}_2(x_1) = \underline{H}^T(x_1)\underline{q}$, where the displacement interpolation array is given by eq. (11.62). Next, the curvatures are computed from eq. (5.6) to find $\kappa_3 = \underline{B}^T(x_1)\underline{q}$ where the curvature interpolation array is

$$\underline{B}(x_1) = \left\{ \frac{\mathrm{d}^2 h_1}{\mathrm{d}x_1^2}, \frac{\mathrm{d}^2 h_2}{\mathrm{d}x_1^2}, \frac{\mathrm{d}^2 h_3}{\mathrm{d}x_1^2}, \cdots \frac{\mathrm{d}^2 h_N}{\mathrm{d}x_1^2} \right\}^T. \tag{11.72}$$

The rest of the procedure mirrors that presented above for the beam under axial load with the stiffness matrix and load array defined as

$$\underline{\underline{K}} = \int_0^L \underline{B}(x_1) H_{33}(x_1) \underline{B}^T(x_1)\, \mathrm{d}x_1, \tag{11.73}$$

and

$$\underline{Q} = \int_0^L \underline{H}(x_1) p_2(x_1)\, \mathrm{d}x_1 + \underline{H}(L) P_2, \tag{11.74}$$

respectively.

It is interesting to note that the entire solution process can be automated once the particular shape functions have been selected. For instance, example 11.7 is an axial load problem and is characterized by a displacement interpolation array $\underline{H}(x_1) = \left\{x_1, x_1^2\right\}^T$ and corresponding strain interpolation array $\underline{B}(x_1) = \left\{1, 2x_1\right\}^T$. On the other hand, example 11.11 is a transverse load (bending) problem with corresponding quantities $\underline{H}(x_1) = \left\{\sin \pi x_1/L, \sin 3\pi x_1/L\right\}^T$ and $\underline{B}(x_1) = -(\pi/L)^2 \left\{\sin \pi x_1/L, 9 \sin 3\pi x_1/L\right\}^T$. The remaining solution steps are identical for both problems.

### 11.4.3 The principle of minimum total potential energy

A formal solution procedure can also be developed based on the principle of minimum total potential energy to obtain approximate solutions of structural problem. The methodology closely mirrors that used in conjunction with the principle of virtual work for axially loaded beams and for beams under transverse loads.

Axially loaded beams will be considered first. The first step of the solution procedure is to assume a specific form for the displacement field

$$\bar{u}_1(x_1) = \sum_{i=1}^{N} h_i(x_1)\, q_i = \underline{H}^T \underline{q}.$$

Next, the strains are expressed in terms of the assumed displacements, resulting in eq. (11.63), with the strain interpolation array defined in eq. (11.64). Using these, the total strain energy in the beam can now be written as

$$\begin{aligned} A(\bar{\epsilon}_1) &= \frac{1}{2}\int_0^L S\bar{\epsilon}_1^2 \,\mathrm{d}x_1 = \frac{1}{2}\int_0^L S(\underline{B}^T\underline{q})^T(\underline{B}^T\underline{q})\mathrm{d}x_1 \\ &= \frac{1}{2}\,\underline{q}^T\left[\int_0^L S\,\underline{B}\,\underline{B}^T\,\mathrm{d}x_1\right]\underline{q} = \frac{1}{2}\,\underline{q}^T\,\underline{\underline{K}}\,\underline{q}, \end{aligned} \tag{11.75}$$

where the stiffness matrix is identical to that defined in eq. (11.67).

Next, the total potential of the externally applied loads becomes

$$\Phi = \int_0^L \phi\,\mathrm{d}x_1 + \Psi = -\left[\int_0^L \underline{H}^T(x_1)p_1(x_1)\,\mathrm{d}x_1\right]\underline{q} - \underline{H}^T(L)P_1\underline{q} = -\underline{Q}^T\underline{q}. \tag{11.76}$$

Here again, the load array, $\underline{Q}$, is the same as that found earlier, eq. (11.68). The total potential energy of the system, $\Pi = A + \Phi$, can now be written as

$$\Pi(\underline{q}) = \frac{1}{2}\,\underline{q}^T\,\underline{\underline{K}}\,\underline{q} - \underline{Q}^T\underline{q}. \tag{11.77}$$

According to the principle of stationary total potential energy, principle 8, expressed by eq. (10.17), the derivatives of the total potential energy with respect to the degrees of freedom, $\underline{q}$, must vanish, leading to

$$\frac{\partial \Pi}{\partial \underline{q}} = \frac{\partial}{\partial \underline{q}}\left(\frac{1}{2}\,\underline{q}^T\,\underline{\underline{K}}\,\underline{q} - \underline{Q}^T\underline{q}\right) = \underline{\underline{K}}\,\underline{q} - \underline{Q} = \underline{0}. \tag{11.78}$$

where eqs. (A.29) and (A.27) are used to compute the derivatives of the strain energy and potential of the externally applied loads, respectively. The final equilibrium equations of the problem are

$$\underline{\underline{K}}\,\underline{q} - \underline{Q} = \underline{0}. \tag{11.79}$$

The general solution procedure using the principle of minimum total potential energy can be summarized by the following steps.

1. Select $N$ shapes functions that satisfy the geometric boundary conditions.
2. Construct the displacement interpolation array, eq. (11.62), and strain interpolation array, eq. (11.64).
3. Compute the stiffness matrix according to eq. (11.67) and load array from eq. (11.68).
4. Compute the total potential of the externally applied loads, $\Phi(\underline{q}) = -\underline{q}^T\underline{Q}$, where the load array, $\underline{Q}$, is given by eq. (11.68).

5. Solve the set of $N$ simultaneous linear equations, $\underline{\underline{K}}\,\underline{q} = \underline{Q}$, for the solution array, $\underline{q}$.
6. Determine the strain distribution from eq. (11.63), and the internal forces from the constitutive law, eq. (5.16).

Clearly, the solution procedures based on the principle of virtual work and principle of minimum total potential energy are closely related. Although the physical interpretation of the intermediate quantities is different, the major elements of the two procedures, the stiffness matrix and load array, are identical, and so are the final solutions.

The general method presented here for beams under axial loads can be readily applied to beams subjected to transverse loads by using the appropriate expressions for the stiffness matrix, eq. (11.73), and load array, eq. (11.74).

When the structural system to be analyzed comprises several elastic components, such as beams and springs, the strain energies of the various elastic elements are simply added together to find the total strain energy. This additive property of strain energy is one of the key simplifications inherent to variational and energy methods.

Consider, for instance, a cantilevered beam with a spring of stiffness constant $k$ connected to the ground at location $x_1 = \alpha L$. The elastic components of the system are the beam and spring, and the total strain energy can be written as

$$A = \frac{1}{2}\int_0^L H_{33}\left(\frac{\mathrm{d}^2\bar{u}_2}{\mathrm{d}x_1^2}\right)^2 \mathrm{d}x_1 + \frac{1}{2}\,k\bar{u}_2^2(\alpha L),$$

where the first term corresponds to the strain energy stored in the beam, and the second represents that stored in the spring. The stiffness matrix is now $\underline{\underline{K}} = \underline{\underline{K}}_b + \underline{\underline{K}}_s$, where $\underline{\underline{K}}_b$ is associated with the strain energy of the beam and $K_s$ with that stored in the spring. Matrix $\underline{\underline{K}}_b$ is given by eq. (11.73), and the strain energy in the spring gives rise to $\underline{\underline{K}}_s$

$$\begin{aligned}\frac{1}{2}\,k\,\bar{u}_2^2(\alpha L) &= \frac{1}{2}k(\underline{H}^T(\alpha L)\underline{q})^T(\underline{H}^T(\alpha L)\underline{q}) \\ &= \frac{1}{2}\,\underline{q}^T\left[\underline{H}(\alpha L)k\underline{H}^T(\alpha L)\right]\,\underline{q} = \frac{1}{2}\,\underline{q}^T\underline{\underline{K}}_s\,\underline{q}.\end{aligned}$$

Several examples will now be used to illustrate the formal solution procedure for beams under transverse loading.

***Example 11.14. Simply supported beam with two elastic spring supports***

Figure 5.31 on page 208 depicts a simply supported beam of span $L$ supported by two spring of stiffness constant $k$ located at stations $x_1 = \alpha L$ and $(1-\alpha)L$, and subjected to a uniform transverse loading $p_0$. The exact solution of this problem is obtained using the classical differential equation approach in example 5.13 on page 208. This problem will now be analyzed with the principle of minimum total potential energy.

The system under consideration consists of an elastic beam and two elastic spring. The strain energy for beam in bending is given by eq. (10.39), and the strain

energy for the springs is $A_s = 1/2\, k\bar{u}_2^2(\alpha L) + 1/2\, k\bar{u}_2^2[(1-\alpha)L]$. The strain energy for the entire system is then the sum to the strain energies for the various components of the system

$$A = \frac{1}{2}\int_0^L H_{33}^c \left(\frac{\mathrm{d}^2\bar{u}_2}{\mathrm{d}x_1^2}\right)^2 \mathrm{d}x_1 + \frac{1}{2}k\bar{u}_2^2(\alpha L) + \frac{1}{2}k\bar{u}_2^2((1-\alpha)L).$$

Next, the displacement interpolation array is selected as

$$\underline{H} = \left\{\sin\pi\eta,\ \sin 3\pi\eta,\ \sin 5\pi\eta\right\}^T,$$

where $\eta = x_1/L$ is a non-dimensional span variable. The shape functions each satisfy the geometric boundary conditions $h_i(0) = h_i(1) = 0$.

The corresponding strain interpolation array becomes

$$\underline{B} = -\pi^2\left\{\sin\pi\eta,\ 3^2\sin 3\pi\eta,\ 5^2\sin 5\pi\eta\right\}^T.$$

and the stiffness matrix for the beam is then

$$\underline{\underline{K}}_b = \frac{H_{33}^c}{L^3}\int_0^1 \underline{B}(\eta)\underline{B}^T(\eta)\,\mathrm{d}\eta = \frac{H_{33}^c\pi^4}{2L^3}\begin{bmatrix}1 & 0 & 0\\ 0 & 3^4 & 0\\ 0 & 0 & 5^4\end{bmatrix} \tag{11.80}$$

The stiffness matrix associated with the springs is

$$\begin{aligned}\underline{\underline{K}}_s =& k\,\underline{H}(\alpha)\,\underline{H}^T(\alpha) + k\,\underline{H}(1-\alpha)\,\underline{H}^T(1-\alpha)\\ =& 2k\begin{bmatrix}\sin^2\pi\alpha & \sin\pi\alpha\,\sin 3\pi\alpha & \sin\pi\alpha\,\sin 5\pi\alpha\\ \sin 3\pi\alpha\,\sin\pi\alpha & \sin^2 3\pi\alpha & \sin 3\pi\alpha\,\sin 5\pi\alpha\\ \sin 5\pi\alpha\,\sin\pi\alpha & \sin 5\pi\alpha\,\sin 3\pi\alpha & \sin^2 5\pi\alpha\end{bmatrix}.\end{aligned}$$

Finally, the stiffness matrix for the entire structure, $\underline{\underline{K}} = \underline{\underline{K}}_b + \underline{\underline{K}}_s$, becomes

$$\underline{\underline{K}} = \frac{H_{33}^c}{L^3}\begin{bmatrix}\pi^4/2 + 2\bar{k}\sin^2\pi\alpha & 2\bar{k}\sin\pi\alpha\,\sin 3\pi\alpha & 2\bar{k}\sin\pi\alpha\,\sin 5\pi\alpha\\ 2\bar{k}\sin 3\pi\alpha\,\sin\pi\alpha & 3^4\pi^4/2 + 2\bar{k}\sin^2 3\pi\alpha & 2\bar{k}\sin 3\pi\alpha\,\sin 5\pi\alpha\\ 2\bar{k}\sin 5\pi\alpha\,\sin\pi\alpha & 2\bar{k}\sin 5\pi\alpha\,\sin 3\pi\alpha & 5^4\pi^4/2 + 2\bar{k}\sin^2 5\pi\alpha\end{bmatrix},$$

where $\bar{k} = kL^3/H_{33}^c$ is the non-dimensional spring stiffness constant.

Next, the load array associated with the uniform transverse load is computed as

$$\underline{Q} = p_0 L\int_0^1 \underline{H}(\eta)\,\mathrm{d}\eta = \frac{2p_0 L}{\pi}\left\{1, 1/3, 1/5\right\}^T.$$

The solution of this problem is obtained by solving the linear set of equations $\underline{\underline{K}}\,\underline{q} = \underline{Q}$ to find the solution array. This step is most easily performed numerically because the inversion of the $3 \times 3$ stiffness matrix is a rather arduous task to do by hand.

If a single shape function is selected, *i.e.*, if $\underline{H} = \left\{\sin\pi\eta\right\}^T$, then $\underline{q}$ and $\underline{Q}$ contain only a single term and $\underline{\underline{K}}$ is a $1 \times 1$ matrix leading to

$$q_1 = \frac{p_0 L^4}{H^c_{33}} \frac{2}{\pi(\pi^4/2 + 2\bar{k}\sin^2\pi\alpha)}.$$

The exact solution of the problem, given by eq. (5.65), will now be compared with this approximate solution. Three cases, denoted *cases 1, 2*, and *3* correspond to the following displacement interpolation arrays: $\underline{H} = \{\sin\pi\eta\}^T$, $\underline{H} = \{\sin\pi\eta, \sin 3\pi\eta\}^T$, and $\underline{H} = \{\sin\pi\eta, \sin 3\pi\eta, \sin 5\pi\eta\}^T$, respectively.

Figure 11.30 shows the non-dimensional transverse displacement $\bar{u}_2 H^c_{33}/(p_0 L^4)$ for the exact and approximate solutions with the following choice of the parameters: $\alpha = 0.3$ and $\bar{k} = 10^4$. Due to the symmetry of the problem, the solution is presented over a half-span only. Excellent correlation is observed between the exact and approximate solutions. At the scale of the figure, the predictions for *cases 2* and *3* are in close agreement with the exact solution. Table 11.3 quantifies the observed errors for the various approximations.

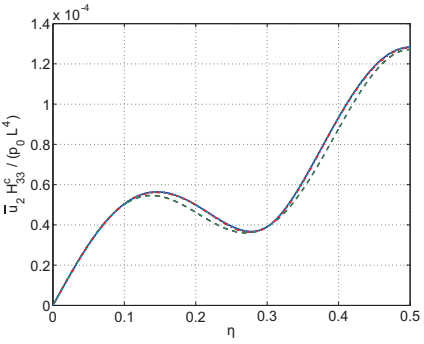


**Fig. 11.30.** Transverse displacement $\bar{u}_2 H^c_{33}/(p_0 L^4)$ for the exact and approximate solutions versus non-dimensional span. Exact solution: solid line; approximate solution *case 1*: dashed line, *case 2*: dash-dotted line, *case 3*: dotted line.

The exact distribution of bending moment is given by eq. (5.66), and fig. 11.31 depicts the non-dimensional bending moment $M_3/(p_0 L^2)$ for the various solutions. Note that the exact solution presents a cusp at $\eta = 0.3$. This feature is not reproduced by the approximate solutions that consist of a sum of smooth functions. As the number of degrees of freedom increases, the quality of the approximation improves, as detailed in table 11.3. The errors in bending moment predictions are much larger than those observed for the transverse displacements.

Finally, fig. 11.32 shows the non-dimensional shear force $V_2/(p_0 L)$ for the exact solution, eq. (5.67), and the approximate solutions. The exact shear force distribution presents a discontinuity at $\eta = 0.3$ corresponding to the concentrated force the spring applies to the beam. Here again, this feature cannot be reproduced by the approximate solutions that consist of a sum of smooth functions. As the number of degrees of freedom increases, the approximate solution converges to shear force value corresponding to the average of the exact shear forces to the left and right of

**Table 11.3.** Comparison of the exact and approximate solutions.

| | Exact solution | *Case 1* error | *Case 2* error | *Case 3* error |
|---|---|---|---|---|
| Transverse displacement $[10^{-05}]$ | | | | |
| $\eta = 0.15$ | 5.6351 | 3.9% | -0.50% | -0.050% |
| $\eta = 0.30$ | 3.9068 | 0.03% | 0.003% | 0.0001% |
| $\eta = 0.45$ | 11.882 | -2.6% | -0.3% | -0.08% |
| Bending moment $[10^{-03}]$ | | | | |
| $\eta = 0.15$ | -5.1476 | -1.9% | -7.5% | 3.6% |
| $\eta = 0.30$ | 12.205 | -42.% | -19.% | -14.% |
| $\eta = 0.45$ | -6.5452 | 6.1% | -3.6% | 2.4% |
| Shearing force $[10^{-02}]$ | | | | |
| $\eta = 0.15$ | -4.0683 | 64.% | -4.9% | 5.7% |
| $\eta = 0.30$ | 0.9320 | -160.% | 14.% | 35.% |
| $\eta = 0.45$ | 5.000 | 95.% | 6.9% | 9.75% |

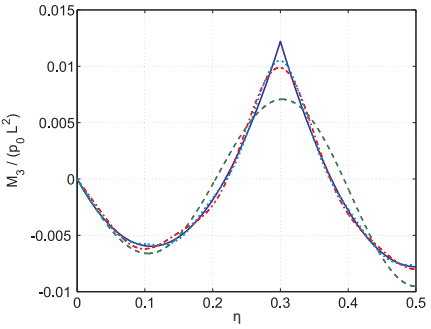


**Fig. 11.31.** Bending moment $M_3/(p_0L^2)$ for the exact and approximate solutions versus non-dimensional span. Exact solution: solid line; approximate solution *case 1*: dashed line, *case 2*: dash-dotted line, *case 3*: dotted line.

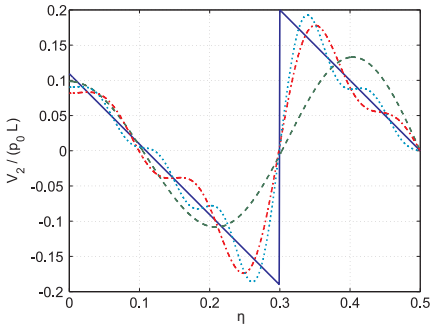


**Fig. 11.32.** Shear force $V_2/(p_0L)$ for the exact and approximate solutions versus non-dimensional span. Exact solution: solid line; approximate solution *case 1*: dashed line, *case 2*: dash-dotted line, *case 3*: dotted line.

the discontinuity. This convergence, however, is quite slow, as detailed in table 11.3. The larger errors observed in the predictions of bending moments and shear forces are expected since these quantities are obtained from higher order derivatives of the approximate displacement field.

***Example 11.15. Simply supported beam on an elastic foundation***

Consider a simply supported beam of length $L$ subjected to a uniform transverse load $p_0$ and supported by an elastic foundation of distributed stiffness constant $k$, as depicted in fig. 5.32 on page 209. The exact solution of the problem, obtained from the classical differential approach, is presented in example 5.14 on page 209.

The strain energy for the complete system is

$$A = A_b + A_{ef} = \frac{1}{2}\int_0^L H_{33}^c \left(\frac{\mathrm{d}^2\bar{u}_2}{\mathrm{d}x_1^2}\right)^2 \mathrm{d}x_1 + \frac{1}{2}\int_0^L k\bar{u}_2^2(x_1)\,\mathrm{d}x_1.$$

where the first term is the strain energy in the beam due to bending given by eq. (10.39), and the second term is the strain energy in the elastic foundation.

Here again, the displacement interpolation array is selected as $\underline{H} = \left\{\sin\pi\eta, \sin 3\pi\eta, \sin 5\pi\eta\right\}^T$, where $\eta$ is the non-dimensional variable along the beam's span. Note that each of the shape functions satisfies the geometric boundary conditions, $h_i(0) = h_i(1) = 0$. The corresponding strain interpolation array becomes $\underline{B} = -\pi^2\left[\sin\pi\eta,\ 3^2\sin 3\pi\eta,\ 5^2\sin 5\pi\eta\right]^T$.

The beam's stiffness matrix is identical to that found in the previous example, see eq. (11.80), and the stiffness matrix associated with the elastic foundation is

$$\underline{\underline{K}}_{ef} = \int_0^L k(\underline{H}^T\underline{q})^T(\underline{H}^T\underline{q})\mathrm{d}x_1 = kL\int_0^1 \underline{H}(\eta)\underline{H}^T(\eta)\,\mathrm{d}\eta = \frac{kL}{2}\begin{bmatrix}1&0&0\\0&1&0\\0&0&1\end{bmatrix}.$$

The stiffness matrix for the entire structure is now

$$\underline{\underline{K}} = \underline{\underline{K}}_b + \underline{\underline{K}}_{ef} = \frac{H_{33}^c}{L^3}\frac{1}{2}\begin{bmatrix}\pi^4+\bar{k} & 0 & 0\\ 0 & 3^4\pi^4+\bar{k} & 0\\ 0 & 0 & 5^4\pi^4+\bar{k}\end{bmatrix},$$

where $\bar{k} = kL^4/H_{33}^c$ is the non-dimensional stiffness constant of the elastic foundation and expresses this relative to the bending stiffness.

Next, the load array associated with the uniform transverse load is found as

$$\underline{Q} = p_0 L\int_0^1 \underline{H}(\eta)\,\mathrm{d}\eta = \frac{2p_0L}{\pi}\left\{1, 1/3, 1/5\right\}^T.$$

The solution of the problem is then obtained by solving the linear set of equations $\underline{\underline{K}}\,\underline{q} = \underline{Q}$. The solution for the transverse displacement is

$$\bar{u}_2(\eta) = \frac{4}{\pi}\frac{p_0L^4}{H_{33}^c}\left[\frac{\sin\pi\eta}{\pi^4+\bar{k}} + \frac{\sin 3\pi\eta}{3(3^4\pi^4+\bar{k})} + \frac{\sin 5\pi\eta}{5(5^4\pi^4+\bar{k})}\right].$$

The exact solution of the problem, given by eq. (5.71), will now be compared with the above approximate solution. *Case 1* and *2*, corresponding to the displacement interpolation arrays $\underline{H} = \left\{\sin\pi\eta, \sin 3\pi\eta\right\}^T$, and $\underline{H} = \left\{\sin\pi\eta, \sin 3\pi\eta, \sin 5\pi\eta\right\}^T$, respectively, will be examined. Figure 11.33 shows the non-dimensional transverse displacement, $\bar{u}_2 H_{33}^c/(p_0L^4)$, for the exact and approximate solutions when $\bar{k} = 8\times 10^3$. Good correlation is observed and quantitative results are listed in table 11.4.

The exact distribution of bending moment is given by eq. (5.72), and fig. 11.34 depicts the non-dimensional bending moment, $M_3/(p_0L^2)$, for the various solutions. Here again, the errors in bending moment predictions are much larger than those observed for those of the transverse displacement. As the number of degrees of freedom increases, the quality of the approximation improves, as shown in table 11.4.

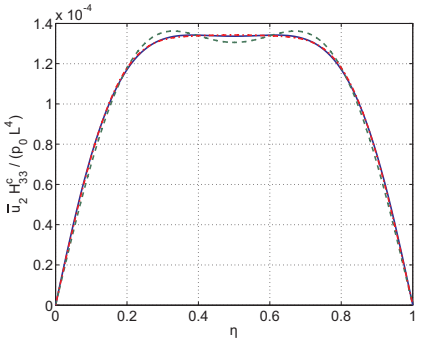


**Fig. 11.33.** Transverse displacement $\bar{u}_2 H^c_{33}/(p_0 L^4)$ for the exact and approximate solutions versus non-dimensional span. Exact solution: solid line; approximate solution *case 1*: dashed line, *case 2*: dash-dotted line.

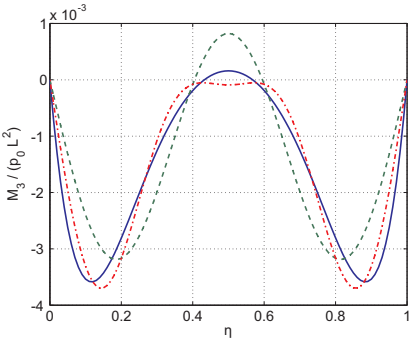


**Fig. 11.34.** Bending moment $M_3/(p_0 L^2)$ for the exact and approximate solutions versus non-dimensional span. Exact solution: solid line; approximate solution *case 1*: dashed line, *case 2*: dash-dotted line.

**Table 11.4.** Comparison of the exact and approximate solutions.

| | Exact solution | *Case 1* error | *Case 2* error |
|---|---|---|---|
| Transverse displacement $\eta = 0.50$ | $1.3364 \times 10^{-4}$ | -2.3% | 0.4% |
| Bending moment $\eta = 0.10$ | $-3.5381 \times 10^{-3}$ | -32.% | -6.4% |

### 11.4.4 Problems

**Problem 11.11. Cantilever with nonuniform bending stiffness**
Consider the cantilevered beam subjected to a tip load $P$ as shown in fig. 11.35. The bending stiffness of the beam's left half is $3H_0$, while that of the right half is $H_0$, as shown in the figure. Develop an approximate solution for the transverse deflection of the entire beam using the principle of minimum total potential energy with a two-term polynomial. Compare your solution at the tip with the exact solution computed using the unit load method.

**Problem 11.12. Simply-supported beam with nonuniform bending stiffness**
Consider the cantilever beam shown in fig. 11.35 but now assume that both ends are simply supported instead. The bending stiffness of the beam's right half is $H_0$ while that of the left half is $\beta H_0$ where $\beta = 3$. Develop an approximate solution for the transverse deflection of the entire beam using the principle of minimum total potential energy with a two-term trigonometric approximate solution. Compare your solution at the mid-span with the exact solution computed using the unit load method.

**Problem 11.13. Simply-supported beam with two mid-span springs**
A simply supported beam of span $L$ is supported by two spring of stiffness $k$ located at stations $x_1 = \alpha L$ and $(1-\alpha)L$, and is subjected to a uniform transverse loading $p_0$, as depicted in fig. 11.36. *(1)* Find the exact solution of the problem from the solution of the governing

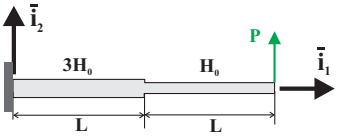


**Fig. 11.35.** Cantilevered beam with nonuniform bending stiffness.

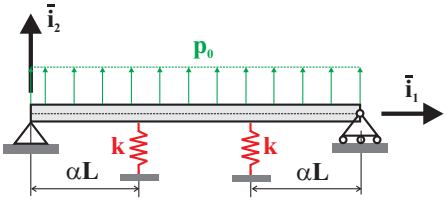


**Fig. 11.36.** Simply supported beam with two mid-span springs.

differential equation and associated boundary conditions. *(2)* Find approximate displacement solutions for the problem using the principle of minimum total potential energy with the following assumed shape functions: $h_i(x_1) = \sin(2i-1)\pi x_1/L$. Construct 5 separate solutions for $n = 1, 2, 3$ term approximations. *(3)* On a single graph, plot the exact solution and the 3 approximate solutions. Also construct a single plot of the error in maximum displacement for each of the 3 cases. Use $\bar{k} = kL^3/H_{33}^c = 10^4$ and $\alpha = 0.3$. *(4)* Find the bending moment distribution for each of the approximate solutions. On a single graph, plot the exact solution and the approximate solutions. Also construct a single plot of the error in maximum bending moment for each of the 3 cases. *(5)* Check the overall equilibrium of the problem for both the exact and approximate solutions. In view of the symmetry of the problem, overall equilibrium implies $p_0 L = 2R + 2k\bar{u}_2(L/3)$, where $R$ is the reaction at either end of the beam, and $k\bar{u}_2(L/3)$ the force either elastic spring. Comment on your results. *(6)* Based on a simple free body diagram, show that for the exact solution the shear force presents a discontinuity at the elastic springs. What happens in your approximate solution? Comment and explain your results. On a single graph, plot the exact solution and the approximate shear force distribution. Quantify the error in maximum bending moment as the number of terms in the approximate solution increases.

### Problem 11.14. Simply-supported beam with two mid-span springs

Consider a simply supported, uniform beam of length $L$ with two end point torsional springs of stiffness $k_1$ and a mid-span spring of stiffness $k_2$. The beam, shown in fig. 11.37, is subjected to a uniform transverse loading $p_2(x_1) = p_0$. *(1)* Solve the governing differential equations of this problem to find the transverse displacement $\bar{u}_2(x_1)$, the bending moment $M_3(x_1)$, and the shear force $V_2(x_1)$. *(2)* Find an approximate solution of the problem using the principle of minimum total potential energy. Select the following form for the displacement field: $\bar{u}_2(x_1) = q_1 \sin \pi x_1/L + q_3 \sin \pi 3x_1/L$. *(3)* On the same graph, plot the exact and approximate transverse displacement fields, $H_{33}^c \bar{u}_2/(p_0 L^4)$. *(4)* On the same graph, plot the exact and approximate bending moment distributions, $M_3/(p_0 L^2)$. *(5)* On the same graph, plot the exact and approximate shear force distributions, $V_2/(p_0 L)$. *(6)* Explain why the approximation is so poor. Hint: look at the bending moment plots. It will be convenient to work with non-dimensional spring stiffnesses $\bar{k}_1 = k_1 L/H_{33}^c$ and $\bar{k}_2 = k_2 L^3/H_{33}^c$. For your plots, select $\bar{k}_1 = 10.0$ and $\bar{k}_2 = 100.0$.

### Problem 11.15. Two parallel simply supported beams with interconnecting springs

Figure 11.38 depicts a system consisting of two simply supported beams connected by two elastic springs of stiffness $k$. The upper and lower beam have the same bending stiffness $H_{33}$ and the upper beam is subjected to a uniform load distribution $p_0$. *(1)* Find the exact solution of the problem. Determine the deflection and bending moment distributions in the upper

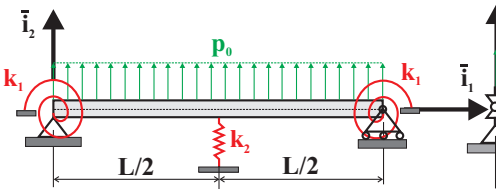


**Fig. 11.37.** Simply supported beam with mid-span and end point springs.

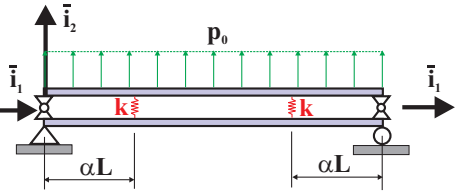


**Fig. 11.38.** Two simply supported beams with interconnecting springs.

and lower beams and the force in the connecting springs. *(2)* Find an approximate solution of the problem based on the principle of minimum total potential energy. Used the following interpolation array $\underline{H} = \{\sin\pi\eta, \sin 3\pi\eta, \sin 5\pi\eta\}^T$, where $\eta = x_1/L$, for the upper and lower beams. This gives a total of six degrees of freedom. *(3)* Plot the exact and approximate displacements for the upper and lower beams on the same graph. *(4)* Plot the exact and approximate bending moments for the upper and lower beams on the same graph.

Use the following data for the plots: $\alpha = 0.3$, $\bar{k} = kL^3/H_{33}^c = 10, 100, 1000$.

### Problem 11.16. Simply supported beam with variable bending stiffness

A simply supported beam of span $L$ is subjected to forces of magnitude $P$ located at stations $x_1 = \alpha L$ and $(1-\alpha)L$, as depicted in fig. 11.39. The beam has a bending stiffness $H_0$ and is reinforced in its central portion where its bending stiffness is $H_1$. *(1)* Find the exact solution of the problem from the solution of the governing differential equation and associated boundary conditions. *(2)* Use the principle of minimum total potential energy to find approximate solutions for this problem using the following shape functions: $h_i(x_1) = \sin(2i-1)\pi x_1/L$ using the first 1, 2 and 3 terms. On a single graph, plot the exact solution and the 3 approximate solutions. Also, construct a single plot of the error in maximum displacement for the 3 approximate solutions. Use $H_1/H_0 = 2$ and $\alpha = 0.3$. *(3)* Find the bending moment distribution for the problem. On a single graph, plot the exact solution and the 3 approximate solutions using. Also, construct a single plot of the error in maximum bending moment for the approximate solutions. *(4)* Based on a simple free body diagram, show that for the exact solution the shear force presents a discontinuity at the point of application of the transverse loads $P$. What happens in your approximate solution? Comment and explain your results. On a single graph, plot the exact solution and the approximate shear force distribution for the approximate solutions.

### Problem 11.17. Cross-supported beams

The lower beam depicted in fig. 11.40 is of length $2L$ and is simply supported at both ends. The upper beam of length $L + a$ is cantilevered from **C**, supported by the lower beam at point **A**, and subjected to a uniform transverse loading $p_0$. Both upper and lower beams have a uniform bending stiffness $H_0$. *(1)* Find the exact solution for the transverse deflection of the lower beam under a mid-span concentrated load. Show that the lower beam can be replaced by a spring of stiffness $k_{\text{eq}} = 6H_0/L^3$. *(2)* Find the exact solution for the transverse deflection of the upper beam from the governing differential equation and associated boundary conditions. Replace the lower beam by the equivalent spring of stiffness constant given above. Model the interaction between the upper beam and equivalent spring by a force $X$, yet unknown. The magnitude of this force is found by equating the displacements of the upper beam and spring at point **A**. *(3)* Find an approximate displacement solution for the upper beam. Use the principle of minimum total potential energy with the following assumed shape functions: $h_i(x_1) = x_1^{2+i}$. Use $L/a = 2$. On a single graph, plot the exact and approximate solutions

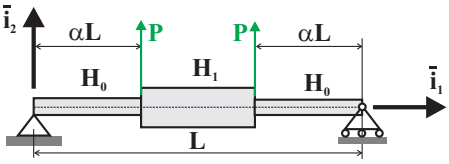


**Fig. 11.39.** Simply supported beam with variable bending stiffness.

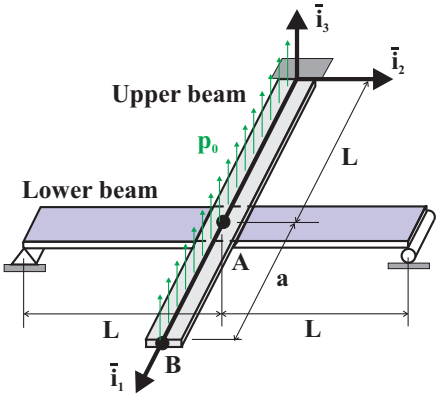


**Fig. 11.40.** Simply supported beam with cantilever beam crossed and pinned at midspans.

for 3 cases with the first 1, 2, 3 and 4 terms. Quantify the error in maximum displacement for each case. *(4)* Find the approximate bending moment distribution for the problem. On a single graph, plot the exact and approximate solutions for each case. Quantify the error in maximum bending moment for each case. *(5)* Based on a simple free body diagram, show that for the exact solution the shear force presents a discontinuity at point $A$. What happens in your approximate solution? Comment and explain your results. On a single graph, plot the exact and approximate shear force distributions for each case. Quantify the error in maximum shear force for each case.

### Problem 11.18. Cantilever beam with uniform load and spring

The cantilever beam depicted in fig. 11.41 is of length $L$, uniform bending stiffness, $H^c_{33} = H_0$, and is subjected to a uniform distributed load $p_0$. A spring of stiffness $k$ is connected to the beam at a distance $a$ from its root. *(1)* Find the exact solution of the problem from the solution of the governing differential equations and associated boundary conditions for the cantilever beam. It will be necessary to solve the problem in two parts for the segments to the right and left of the spring using the continuity conditions at this point. It will be convenient to define the non-dimensional spring constant $\bar{k} = ka^3/H_0$ *(2)* Find an approximate displacement solution for the beam. Use the principle of minimum total potential energy with the following shape functions: $h_i(x_1) = x_1^{2+i}$. Use $L/a = 3$ and $\bar{k} = 100$. On a single graph, plot the exact and approximate solutions using the first 1, 2, 3 and 4 terms. Quantify the error in maximum displacement for each case. *(3)* Find the approximate bending moment distribution for the problem. On a single graph, plot the exact and approximate solutions for each case. Quantify the error in maximum bending moment for each case. *(4)* Based on a simple free body diagram, show that for the exact solution the shear force presents a discontinuity at the connection point for the spring. What happens in your approximate solution? Comment and explain your results. On a single graph, plot the exact and approximate shear force distributions for each case. Quantify the error in maximum shear force for each case.

### Problem 11.19. Simply supported beam on elastic foundation

Consider the simply supported beam of length $L$ depicted in fig. 11.42. The beam rests on an elastic foundation of stiffness $k$ and is subjected to a concentrated load $P$ acting

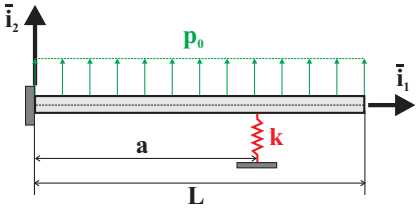


**Fig. 11.41.** Cantilever beam with uniform load and spring at intermediate point.

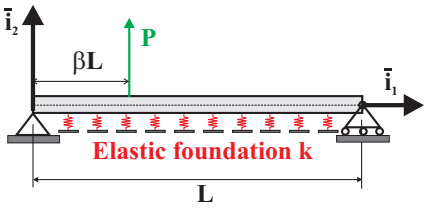


**Fig. 11.42.** Beam with elastic foundation subjected to a concentrated load.

at a distance $\beta L$ from the left support. Use the principle of minimum total potential energy to find an approximate solution for this problem using the following shape functions: $h_i(x_1) = \sin(2i-1)\pi x_1/L$. *(1)* Find the exact solution of the problem from the solution of the governing differential equation and associated boundary conditions. *(2)* Find the approximate displacement solution for the problem. On a single graph, plot the exact solution and the approximate solutions using 1, 2 and 3 terms in the shape function series. Quantify the error in maximum displacement for each case. Use $\bar{k} = kL^4/H_{33}^c = 8\ 10^3$ and $\beta = 0.5$. *(3)* Find the approximate bending moment distribution for the problem. On a single graph, plot the exact solution and the approximate solutions for each case. Quantify the error in maximum bending moment for each case. *(4)* Based on a simple free body diagram, show that for the exact solution the shear force presents a discontinuity at point of application of the load. What happens in your approximate solution? Comment and explain your results. On a single graph, plot the exact solution and the approximate shear force distribution for each case. Quantify the error in maximum bending moment for each case.

## 11.5 A finite element formulation for beams

In the previous sections, approximate solutions for the axial and lateral transverse displacement fields of beams are developed using both the weak statement of equilibrium, and work and energy methods. In each case, the starting point of the approach is the selection of shape functions used to approximate the beam's displacement field; typically, these shape functions are required to satisfy the geometric boundary conditions. For the simple problems considered thus far, the selection of appropriate shape functions is a relatively simple task because geometric boundary conditions are typically imposed at one or both ends of the beam.

In practice, however, a variety of more complex problem must be solved. Typical beam structures involve multiple supports or sectional properties with span-wise variations. Furthermore, loading conditions often involve complex distributed loads or multiple concentrated forces. In such cases, the classical differential equation approach becomes very tedious, if not impossible to manage, and more often than not, no closed-form solutions exist to practical problems of interest. Even the approximate solution procedures presented earlier in this chapter become more difficult to apply because the selection of a set of suitable shape function becomes very arduous. Furthermore, discrete supports or applied concentrated loads generate discontinuities

in the solution. If continuous shape functions are used, the resulting approximate solutions are expected to yield poor accuracy in the neighborhood of the discontinuities.

The work and energy methods developed earlier lack the generality required to solve the various types of problems listed above. The main reason for this weakness is that the selection of the shape functions is problem dependent. Indeed, the presence of specific boundary conditions, multiple supports, or applied concentrated loads impacts the choice of suitable shape functions. Many of these problems stem from the fact that the shape functions used thus far are continuous functions defined over the entire span of the beam.

To overcome these deficiencies, the complete beam structure is first broken into a finite number of short segments, and simple polynomial shape functions are used to approximate the beam's displacement over that segment only. Of course, appropriate conditions must be imposed to preserve the continuity of the displacement and rotation fields between neighboring segments. These segments are commonly called *finite elements*; the complete structure is said to be divided in a number of finite elements. The approach outlined here is called the *finite element method.*

The approach to be presented here is very similar to that developed in section 10.7 for planar trusses. When dealing with trusses, each bar is a finite element, and within this element, the strain field is assumed to be constant. A stiffness matrix and a load array are then computed for each bar, and the contributions of all bars are then assembled into a global problem. The finite element method for beams follows the same pattern, although a preliminary discretization step is required. Because the displacement and strain fields vary within each element, a procedure must be devised to approximate theses fields within each element.

To underline the close connection between the finite element method for trusses developed in section 10.7 and that for beams, the notation used here echoes that used for truss problems.

The finite element formulation for beam bending is based on the Euler-Bernoulli assumptions presented in chapter 5 and for simplicity, axial deformations are ignored. Figure 11.43 depicts the problem under investigation. The axis of the bean coincides with axis $\bar{\imath}_1$, and plane $(\bar{\imath}_1, \bar{\imath}_2)$ is a plane of symmetry of the problem. Consequently, the beam deflects in the transverse direction along axis $\bar{\imath}_2$, and the cross-section rotates about axis $\bar{\imath}_3$. The transverse displacement field is denoted $\bar{u}_2(x_1)$, and the cross-sectional rotation field is denoted $\Phi_3(x_1)$. The beam is subjected to distributed loads and concentrated forces. Of course, the method can be generalized to deal with three-dimensional, anisotropic, curved beams with unsymmetrical cross-sections under arbitrary loading, but this is beyond the scope of this introductory treatment.

### 11.5.1 General description of the problem

In the first step of the approach, the beam is subdivided into a number of segments or finite elements, as depicted in fig. 11.43. Two neighboring elements are connected together at common point called a *node*. The illustration shown in fig. 11.43 depicts

seven finite elements and the eight nodes that connect them. While nodes can be located at any span-wise location along the axis of the beam, it will be convenient to locate nodes at the locations of the supports, and at the points of application of the concentrated loads. As illustrated in fig. 11.43, nodes 1, 6 and 8 are located at the supports, while the locations of nodes 3 and 5 coincide with the point of applications of the two concentrated forces. Additional node locations are selected to create a nearly uniform distribution of nodes along the beam's span.

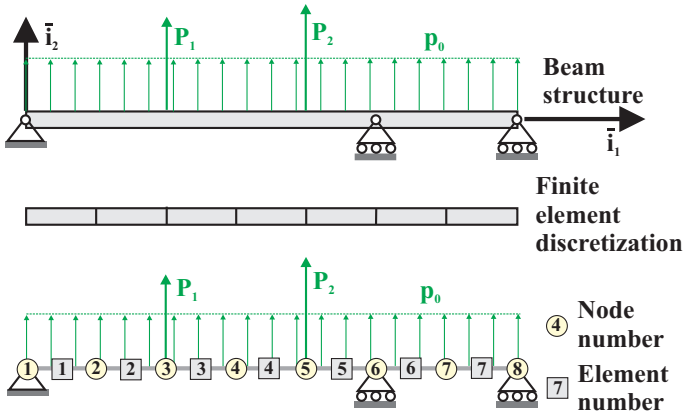


**Fig. 11.43.** Discretization of a beam into finite elements connected together at nodes.

The geometry of the beam is defined by the coordinates of its eight nodes. For instance, the components of the position vector of node 1 with respect to the origin of the coordinate system are denoted $x_1$ and $y_1$, along unit vectors $\bar{\imath}_1$ and $\bar{\imath}_2$, respectively, and stored in array $\underline{p}_1 = \{x_1,\ y_1\}^T$. Similar arrays[1] can be defined for all the nodes of the beam,

$$\underline{p}_1 = \begin{Bmatrix} x_1 \\ y_1 \end{Bmatrix}, \quad \underline{p}_2 = \begin{Bmatrix} x_2 \\ y_2 \end{Bmatrix}, \quad \ldots, \quad \underline{p}_8 = \begin{Bmatrix} x_8 \\ y_8 \end{Bmatrix}. \tag{11.81}$$

The subscript $(\cdot)_i$ will be used to indicate quantities pertaining to the i$^{\text{th}}$ node.

The generalized coordinates of the problem will be selected as the vertical displacement and rotation components of each of the 8 nodes, denoted $v_i$ and $\phi_i$, respectively. The following nodal displacement arrays will be used

$$\underline{q}_1 = \begin{Bmatrix} v_1 \\ \phi_1 \end{Bmatrix}, \quad \underline{q}_2 = \begin{Bmatrix} v_2 \\ \phi_2 \end{Bmatrix}, \quad \ldots, \quad \underline{q}_8 = \begin{Bmatrix} v_8 \\ \phi_8 \end{Bmatrix}. \tag{11.82}$$

Array $\underline{q}_1$ stores the two degrees of freedom at node 1, while array $\underline{q}_i$ stores those at node $i$. It will also be necessary to define a *global displacement array*, $\underline{q}$, that stores

[1] This notation uses symbols $x$, $y$, and $z$, to denote position components, instead of $x_1$, $x_2$, and $x_3$, which are used throughout this book. Notations with multiple subscripts, such as $x_{1i}$ to indicate the position component of node $i$ along axis $\bar{\imath}_1$ are thus avoided.

all the nodal displacement arrays in a single column as

$$\underline{q} = \left\{\underline{q}_1^T, \underline{q}_2^T, \underline{q}_3^T, \underline{q}_4^T, \underline{q}_5^T, \underline{q}_6^T, \underline{q}_7^T, \underline{q}_8^T\right\}^T . \tag{11.83}$$

As mentioned earlier, the finite element method first focuses on a generic finite element of the system, in this case, a generic element of the beam, to evaluate the strain energy stored in that specific element. Each element is connected to two nodes: a root node, denoted *Node 1*, and a tip node, denoted *Node 2*. These nodes are referred to as local nodes, and are used when focusing on a single element of the system.

On the other hand, when the complete beam is considered, global nodes must be used. For instance, referring to fig. 11.43, element 3 has two *local nodes*, denoted *Node 1* and *Node 2*, whereas its *global nodes* are nodes 3 and 4. Similarly, element 7 has two *local nodes*, denoted *Node 1* and *Node 2*, whereas its *global nodes* are nodes 7 and 8. Since the local nodes are denoted *Node 1* and *Node 2* for each and every element, they are not indicated on the figure as it would lead to confusion. This distinction between local and global nodes is important for the development of the method.

### 11.5.2 Kinematics of an element

The kinematics of a specific element of the beam will be studied first. Figure 11.44 depicts a single beam element of length $\hat{\ell}$ with local nodes at each end denoted as *Node 1* and *Node 2*. A *local coordinate system* is centered at the mid-point of the element and defined by unit vector $\bar{\jmath}_1$ aligned with the axis of the beam and $\bar{\jmath}_2$ normal to the beam. Only horizontal beams in two dimensions will be considered in this development, and therefore the local coordinate system, $\mathcal{J} = (\bar{\jmath}_1, \bar{\jmath}_2)$, is aligned with the global coordinate system, $\mathcal{I} = (\bar{\imath}_1, \bar{\imath}_2)$. If the beam is not aligned with the global axis system, the two systems will differ, requiring a coordinate transformation similar to that used for bar elements, see section 10.7.2.

The position vectors of the two local nodes of an element are denoted as

$$\underline{\hat{p}}_1 = \begin{Bmatrix} \hat{x}_1 \\ \hat{y}_1 \end{Bmatrix}, \text{ and } \underline{\hat{p}}_2 = \begin{Bmatrix} \hat{x}_2 \\ \hat{y}_2 \end{Bmatrix}, \tag{11.84}$$

where in this case $\hat{y}_1 = \hat{y}_2 = 0$. For clarity, the quantities pertaining to an element will be indicated with a caret $\hat{(\cdot)}$ to distinguish them from their global counterparts. For example, it is important to distinguish the position vector of node 1, denoted $\underline{p}_1$ as defined by eq. (11.81), from $\underline{\hat{p}}_1$, which indicates the position vector of *Node 1* of a generic bar element.

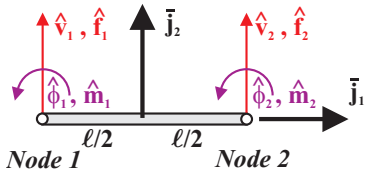


**Fig. 11.44.** Kinematic of a beam element.

Similarly, the displacements and rotations of the two nodes of an element can be expressed in global axis system, $(\bar{\imath}_1, \bar{\imath}_2)$ as

$$\underline{\hat{q}}_1 = \begin{Bmatrix} \hat{v}_1 \\ \hat{\phi}_1 \end{Bmatrix}, \quad \underline{\hat{q}}_2 = \begin{Bmatrix} \hat{v}_2 \\ \hat{\phi}_2 \end{Bmatrix}. \tag{11.85}$$

Because the global and local coordinate coincide, the displacements and rotations resolved in the two systems are identical. It will be convenient to combine the displacements and rotations of the element's two nodes into single array, called the *element displacement array*,

$$\hat{\underline{q}} = \begin{Bmatrix} \hat{\underline{q}}_1 \\ \hat{\underline{q}}_2 \end{Bmatrix}. \tag{11.86}$$

Finally, the length of the beam element, $\hat{\ell}$, can be computed from the position vectors of its end nodes as follows,

$$\hat{\ell} = \|\hat{\underline{p}}_2 - \hat{\underline{p}}_1\| = \sqrt{(\hat{x}_2 - \hat{x}_1)^2 + (\hat{y}_2 - \hat{y}_1)^2} = \sqrt{(\hat{x}_2 - \hat{x}_1)^2} = |\hat{x}_2 - \hat{x}_1|. \tag{11.87}$$

### 11.5.3 Element displacement field

The displacement and slope fields in the beam element must be continuous over the entire span of the element. At this point, however, displacements and rotations have been specified only at the nodes: eq. (11.85) defines the displacements and rotations at the element's two end points, but the displacement and rotation fields within the element remain unknown. If $-\hat{\ell}/2 \le \hat{x} \le \hat{\ell}/2$ is the variable that describes position along the axis of the beam element, the displacement field within the element, $\hat{v}(\hat{x})$, is as yet unknown. The displacement and rotation fields will be continuous over the entire span of the beam if the nodal displacement and rotation values for elements that share a common node match. Consequently, the displacement and rotation fields within the element must interpolate the values specified at its two nodes, as expressed by the following relationship

$$\hat{v}(\hat{\eta}) = \hat{v}_1 h_1(\hat{\eta}) + \frac{\hat{\ell}\hat{\phi}_1}{2} h_2(\hat{\eta}) + \hat{v}_2 h_3(\hat{\eta}) + \frac{\hat{\ell}\hat{\phi}_2}{2} h_4(\hat{\eta}), \tag{11.88}$$

where $\hat{\eta} = 2\hat{x}/\hat{\ell}$ is a non-dimensional variable along the span of the beam element, and $h_i(\hat{\eta})$ are *shape functions*. The four degrees of freedom are the two nodal displacements, $\hat{v}_1$ and $\hat{v}_2$, and the two nodal rotation, $\hat{\phi}_1$ and $\hat{\phi}_2$; the factor $\hat{\ell}/2$ is used to keep the shape functions non-dimensional. Variable $\hat{x}$ is dimensional: $-\hat{\ell}/2 \le \hat{x} \le \hat{\ell}/2$ between *Node 1* and *Node 2* of a typical beam element. Variable $\hat{\eta}$ is non-dimensional: $-1 \le \hat{\eta} \le +1$ between the same nodes. Note that $\mathrm{d}\hat{x}/\mathrm{d}\hat{\eta} = \hat{\ell}/2$.

Equation (11.88) defines the displacement field within the element based solely on the four degrees of freedom. For eq. (11.88) to be correct, the interpolated displacement field must yield the nodal displacements, $\hat{v}_1$ and $\hat{v}_2$, and rotations, $\hat{\phi}_1$ and $\hat{\phi}_2$, when evaluated at the nodes, $\hat{\eta} = \pm 1$. These requirements define 4 boundary conditions for the displacement field of the element

$$\begin{aligned} &\hat{v}(-1) = \hat{v}_1, \text{ and } \left.\frac{\mathrm{d}\hat{v}}{\mathrm{d}\hat{x}}\right|_{-\hat{\ell}/2} = \frac{2}{\hat{\ell}}\,\hat{v}'(-1) = \hat{\phi}_1 \text{ at } \textit{Node 1}, \text{ and} \\ &\hat{v}(+1) = \hat{v}_2, \text{ and } \left.\frac{\mathrm{d}\hat{v}}{\mathrm{d}\hat{x}}\right|_{+\hat{\ell}/2} = \frac{2}{\hat{\ell}}\,\hat{v}'(+1) = \hat{\phi}_2 \text{ at } \textit{Node 2}, \end{aligned} \tag{11.89}$$

where the notation $(\cdot)'$ indicates differentiation with respect to $\eta$.

At this point, the shape functions are not yet defined. All that is known, is that the displacement field, $\hat{v}(\hat{x})$, and rotation field, $\hat{\phi}(\hat{x}) = \mathrm{d}\hat{v}/\mathrm{d}\hat{x}$, must satisfy the four boundary conditions expressed by eqs. (11.89). These conditions alone do not uniquely define the shape functions. It is, however, convenient to select the displacement field, $\hat{v}(\hat{x})$, in the form of a cubic polynomials because a cubic polynomial presents four unknown coefficients which can be uniquely determined by the four boundary conditions expressed by eqs. (11.89).

The element displacement field is assumed to be a cubic polynomial

$$\hat{v}(\hat{x}) = c_1\hat{\eta}^3 + c_2\hat{\eta}^2 + c_3\hat{\eta} + c_4, \tag{11.90}$$

where $c_1$, $c_2$, $c_3$, and $c_4$ are four unknown coefficients. The boundary conditions expressed by eqs. (11.89) imply the following equations

$$\begin{aligned} \hat{v}(-1) &= -c_1 + c_2 - c_3 + c_4 = \hat{v}_1,\ \hat{v}'(-1) = 3c_1 - 2c_2 + c_3 = \frac{\hat{\ell}}{2}\hat{\phi}_1, \\ \hat{v}(+1) &= \ \ c_1 + c_2 + c_3 + c_4 = \hat{v}_2,\ \hat{v}'(+1) = 3c_1 + 2c_2 + c_3 = \frac{\hat{\ell}}{2}\hat{\phi}_2, \end{aligned} \tag{11.91}$$

which form a set of four linear equations for the four unknown coefficients. The solution of this system yields the coefficients $c_1$, $c_2$, $c_3$, and $c_4$, and eq. (11.90) then gives the displacement field in the element as

$$\begin{aligned} \hat{v}(\hat{x}) = &\ \frac{1}{4}(-1+\hat{\eta})^2(2+\hat{\eta})\hat{v}_1 + \frac{1}{4}(-1+\hat{\eta})^2(1+\hat{\eta})\frac{\hat{\ell}}{2}\hat{\phi}_1 \\ &+ \frac{1}{4}(1+\hat{\eta})^2(2-\hat{\eta})\hat{v}_2 + \frac{1}{4}(1+\hat{\eta})^2(-1+\hat{\eta})\frac{\hat{\ell}}{2}\hat{\phi}_2 \\ =&\ h_1(\hat{\eta})\hat{v}_1 + h_2(\hat{\eta})\frac{\hat{\ell}}{2}\hat{\phi}_1 + h_3(\hat{\eta})\hat{v}_2 + h_4(\hat{\eta})\frac{\hat{\ell}}{2}\hat{\phi}_2. \end{aligned} \tag{11.92}$$

The shape functions of an element, $h_i(\hat{\eta})$, are given as

$$\begin{aligned} h_1(\hat{\eta}) &= \frac{1}{4}(1-\hat{\eta})^2(2+\hat{\eta}), \quad h_2(\hat{\eta}) = \frac{1}{4}(1-\hat{\eta})^2(1+\hat{\eta}), \\ h_3(\hat{\eta}) &= \frac{1}{4}(1+\hat{\eta})^2(2-\hat{\eta}), \quad h_4(\hat{\eta}) = -\frac{1}{4}(1+\hat{\eta})^2(1-\hat{\eta}). \end{aligned} \tag{11.93}$$

The derivatives of the *shape functions* are

$$\begin{aligned} h_1'(\hat{\eta}) &= -\frac{3}{4}(1-\hat{\eta}^2), \quad h_2'(\hat{\eta}) = -\frac{1}{4}(1-\hat{\eta})(1+3\hat{\eta}), \\ h_3'(\hat{\eta}) &= \frac{3}{4}(1-\hat{\eta}^2), \quad h_4'(\hat{\eta}) = -\frac{1}{4}(1+\hat{\eta})(1-3\hat{\eta}). \end{aligned} \tag{11.94}$$

The polynomial shape functions and their derivatives are shown in figs. 11.45 and 11.46, respectively.

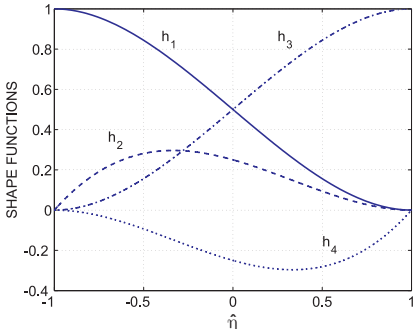


**Fig. 11.45.** Beam element shape functions. $h_1$: solid line; $h_2$: dashed line; $h_3$: dash-dotted line; $h_4$: dotted line.

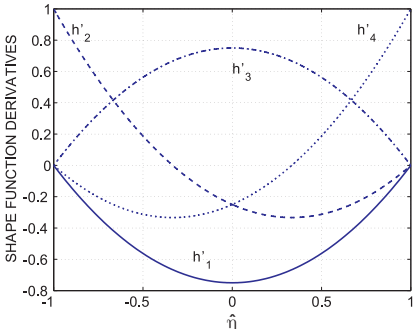


**Fig. 11.46.** Derivatives of the beam element shape functions. $h_1'$: solid line; $h_2'$: dashed line; $h_3'$: dash-dotted line; $h_4'$: dotted line.

### 11.5.4 Element curvature field

The distribution of curvature over the element is obtained from its definition, eq. (5.6), as

$$\hat{\kappa}_3(\hat{\eta}) = \frac{\mathrm{d}^2\hat{v}(\hat{\eta})}{\mathrm{d}\hat{x}^2} = \left(\frac{2}{\hat{\ell}}\right)^2 \hat{v}''(\hat{\eta})$$
$$= \left(\frac{2}{\hat{\ell}}\right)^2 \left[\hat{v}_1 h_1''(\hat{\eta}) + \frac{\hat{\ell}\hat{\phi}_1}{2} h_2''(\hat{\eta}) + \hat{v}_2 h_3''(\hat{\eta}) + \frac{\hat{\ell}\hat{\phi}_2}{2} h_4''(\hat{\eta})\right].$$

This expression can be recast in a compact format as

$$\hat{\kappa}_3(\hat{\eta}) = \underline{\hat{b}}^T(\hat{\eta})\underline{\hat{q}}, \tag{11.95}$$

where the curvature interpolation array, $\underline{\hat{b}}(\hat{\eta})$, is defined as

$$\underline{\hat{b}}(\hat{\eta}) = \left(\frac{2}{\hat{\ell}}\right)^2 \left\{h_1''(\hat{\eta}), \frac{\hat{\ell}}{2} h_2''(\hat{\eta}), h_3''(\hat{\eta}), \frac{\hat{\ell}}{2} h_4''(\hat{\eta})\right\}^T. \tag{11.96}$$

### 11.5.5 Element strain energy and stiffness matrix

The strain energy stored in a beam subjected to bending is given by eq. (10.39). For the beam element under consideration, the strain energy is obtained by integration over the span of the element to find

$$\hat{A} = \frac{1}{2}\int_0^{\hat{\ell}} H_{33}^c \hat{\kappa}_3^2(\hat{\eta})\, \mathrm{d}\hat{x} = \frac{1}{2}\int_{-1}^{+1} H_{33}^c \left[\underline{\hat{q}}^T \underline{\hat{b}}(\hat{\eta})\right]\left[\underline{\hat{b}}^T(\hat{\eta})\underline{\hat{q}}\right] \frac{\hat{\ell}}{2}\mathrm{d}\hat{\eta},$$

where the curvature field is expressed using eq. (11.95) to find $\hat{\kappa}_3^2 = [\underline{\hat{b}}^T\,\underline{\hat{q}}]^T[\underline{\hat{b}}^T\,\underline{\hat{q}}] = [\underline{\hat{q}}^T\,\underline{\hat{b}}][\underline{\hat{b}}^T\,\underline{\hat{q}}]$. The nodal degrees of freedom stored in array $\underline{\hat{q}}$ are independent of $\hat{\eta}$, and therefore, they can be placed outside the integral to find

$$\hat{A} = \frac{1}{2}\,\underline{\hat{q}}^T \left[ \frac{\hat{\ell}}{2} \int_{-1}^{+1} \underline{\hat{b}}(\hat{\eta}) H_{33}^c(\hat{\eta}) \underline{\hat{b}}^T(\hat{\eta})\, \mathrm{d}\hat{\eta} \right] \underline{\hat{q}} = \frac{1}{2}\,\underline{\hat{q}}^T \underline{\underline{\hat{k}}}\, \underline{\hat{q}}, \tag{11.97}$$

where $\underline{\underline{\hat{k}}}$ is the *element stiffness matrix*.

If the bending stiffness is constant over the span of the element, the stiffness matrix can be evaluated to find

$$\underline{\underline{\hat{k}}} = \frac{\hat{\ell}}{2} \int_{-1}^{+1} \underline{\hat{b}}(\hat{\eta}) H_{33}^c \underline{\hat{b}}^T(\hat{\eta})\, \mathrm{d}\hat{\eta} = \frac{H_{33}^c}{\hat{\ell}^3} \left[\begin{array}{cc|cc} 12 & 6\hat{\ell} & -12 & 6\hat{\ell} \\ & 4\hat{\ell}^2 & -6\hat{\ell} & 2\hat{\ell}^2 \\ \hline & & 12 & -6\hat{\ell} \\ sym & & & 4\hat{\ell}^2 \end{array}\right]. \tag{11.98}$$

This $4 \times 4$ element stiffness matrix describes the stiffness of the beam element between *Node 1* and *Node 2*. In particular, the first and third rows and columns represent the stiffness associated with the displacement degrees of freedom, $\hat{v}_1$ and $\hat{v}_2$, respectively. The second and fourth rows and columns represent the stiffness associated with the rotational degrees of freedom, $\hat{\phi}_1$ and $\hat{\phi}_2$, respectively. Because, the displacement and rotation degrees of freedom are of different units, the entries of the stiffness matrix are also of different units.

### 11.5.6 Element external potential and load array

As illustrated in fig. 11.43, the externally applied loading consists of concentrated and distributed loads. For a typical element, concentrated loads, $\hat{f}_1$ and $\hat{f}_2$, are applied at *Node 1* and *Node 2*, respectively. Concentrated moments, $\hat{m}_1$ and $\hat{m}_2$, are applied at the same nodes, respectively. Finally, a distributed transverse load, $p_2(\hat{x})$, is applied over the span of the element. The potential of these externally applied loads then follows from eq. (10.59) as

$$\hat{\Phi} = -\hat{f}_1 \hat{v}_1 - \hat{m}_1 \hat{\phi}_1 - \hat{f}_2 \hat{v}_2 - \hat{m}_2 \hat{\phi}_2 - \int_0^{\hat{\ell}} \hat{p}_2(\hat{x}) \hat{v}(\hat{x})\, \mathrm{d}\hat{x}.$$

Introducing the interpolated displacement field, eq. (11.88), in the last term yields the following expression

$$\hat{\Phi} = -\underline{\hat{q}}^T \underline{\hat{f}}, \tag{11.99}$$

where the element load array is

$$\underline{\hat{f}} = \left\{ \begin{array}{l} \hat{f}_1 + \dfrac{\hat{\ell}}{2} \displaystyle\int_{-1}^{+1} p_2(\hat{\eta}) h_1(\hat{\eta})\, \mathrm{d}\hat{\eta} \\ \hat{m}_1 + \dfrac{\hat{\ell}^2}{4} \displaystyle\int_{-1}^{+1} p_2(\hat{\eta}) h_2(\hat{\eta})\, \mathrm{d}\hat{\eta} \\ \hat{f}_2 + \dfrac{\hat{\ell}}{2} \displaystyle\int_{-1}^{+1} p_2(\hat{\eta}) h_3(\hat{\eta})\, \mathrm{d}\hat{\eta} \\ \hat{m}_2 + \dfrac{\hat{\ell}^2}{4} \displaystyle\int_{-1}^{+1} p_2(\hat{\eta}) h_4(\hat{\eta})\, \mathrm{d}\hat{\eta} \end{array} \right\}. \tag{11.100}$$

For a given applied distributed load, the integral can be evaluated to find the element load array, $\hat{\underline{f}}$. For instance, if the element is subjected to a uniform distributed load of magnitude $\hat{p}_0$, the element load array becomes

$$\hat{\underline{f}} = \left\{ \frac{\hat{p}_0 \hat{\ell}}{2}, \frac{\hat{p}_0 \hat{\ell}^2}{12}, \frac{\hat{p}_0 \hat{\ell}}{2}, -\frac{\hat{p}_0 \hat{\ell}^2}{12} \right\}^T .$$

The first and third terms represent the nodal loads equivalent to the applied distributed load. The total load applied to the element is $p_0 \hat{\ell}$, and half of this load is applied to each of the two end nodes. The second and fourth terms represent the nodal moments equivalent to the applied distributed load. Equal and opposite moments of magnitude $\hat{p}_0 \hat{\ell}^2/12$ are applied to each of the two end nodes.

The work done by these nodal forces and moments is identical to that done by the distributed loading, within the approximation of the interpolated displacement field given by eq. (11.88). For this reason, these nodal forces and moments are sometimes referred to as "work-equivalent" nodal forces.

### 11.5.7 Assembly procedure

In the previous sections, attention is focused on a single, generic beam element to determine its *element* stiffness matrix, eq. (11.98), and *element* load array, eq. (11.100). These two quantities are obtained from the element strain energy and external potential, respectively. In this section, attention shifts to the overall beam problem to determine the *global stiffness matrix* and *global load array*. These two quantities will be obtained from the system's total strain energy and total external potential, respectively. Because both strain energy and external potential are scalar quantities, their combined total will be evaluated simply by summing up the contributions from the individual elements.

The total strain energy stored in the beam is the sum of the contributions of all elements. In eq. (11.97), the strain energy of a single, generic beam element is denoted $\hat{A}$, and this notation is not ambiguous because only a single element is considered. It now becomes necessary, however, to add the element identification using the subscript $(.)_{(i)}$ introduced earlier. Summing over all elements yields

$$A = \sum_{i=1}^{N_e} \hat{A}_{(i)} = \frac{1}{2} \sum_{i=1}^{N_e} \hat{\underline{q}}_{(i)}^T \hat{\underline{\underline{k}}}_{(i)} \hat{\underline{q}}_{(i)}, \tag{11.101}$$

where $N_e$ is the number of elements in the beam ($N_e = 7$ for the beam illustrated in fig. 11.43). In this case, it is also necessary to add the element identification subscript to both the element stiffness matrix, $\hat{k}_{(i)}$, and the nodal displacement array, $\hat{\underline{q}}_{(i)}$.

Equation (11.101) gives the total strain energy in the structure, but it is not easy to manipulate because each term in the sum is expressed in terms of a different set of degrees of freedom. For example, with reference to fig. 11.43, element 3 is connected to global nodes 3 and 4 which are local *Node 1* and *Node 2* for the element, respectively. The element stiffness, $\hat{\underline{\underline{k}}}_{(3)}$, is defined in terms of these global nodes, see

eq. (11.98), and the corresponding element displacement array is $\hat{\underline{q}}^T_{(3)} = \left\{\hat{\underline{q}}^T_1, \hat{\underline{q}}^T_2\right\} = \left\{\underline{q}^T_3, \underline{q}^T_4\right\}^T = \left\{v_3, \phi_4, v_4, \phi_4\right\}^T$.

To remedy this situation, a *connectivity matrix*, $\underline{\underline{C}}_{(i)}$, for the $i^{\text{th}}$ element is introduced following the same approach used for a truss in section 10.7.6. This matrix is designed to extract the specific terms of the element displacement array from the global displacement array defined by eq. (11.83). This operation can be written as

$$\hat{\underline{q}}_{(i)} = \underline{\underline{C}}_{(i)} \underline{q}. \tag{11.102}$$

To best understand this abstract relationship, consider a specific element of the beam, say element 3, as shown in fig. 11.43. Its local nodes, *Node 1* and *Node 2*, are associated with the global node numbers 3 and 4, respectively, so that $\hat{\underline{q}}_1 = \underline{q}_3$ and $\hat{\underline{q}}_2 = \underline{q}_4$. The element displacement array, $\hat{\underline{q}}_{(3)}$, can thus be written as

$$\hat{\underline{q}}_{(3)} = \begin{Bmatrix} \hat{\underline{q}}_1 \\ \hat{\underline{q}}_2 \end{Bmatrix}_{(3)} = \begin{Bmatrix} \underline{q}_3 \\ \underline{q}_4 \end{Bmatrix} = \begin{bmatrix} \underline{\underline{0}} & \underline{\underline{0}} & \underline{\underline{I}} & \underline{\underline{0}} & \underline{\underline{0}} & \underline{\underline{0}} & \underline{\underline{0}} & \underline{\underline{0}} \\ \underline{\underline{0}} & \underline{\underline{0}} & \underline{\underline{0}} & \underline{\underline{I}} & \underline{\underline{0}} & \underline{\underline{0}} & \underline{\underline{0}} & \underline{\underline{0}} \end{bmatrix} \begin{Bmatrix} \underline{q}_1 \\ \underline{q}_2 \\ \underline{q}_3 \\ \underline{q}_4 \\ \underline{q}_5 \\ \underline{q}_6 \\ \underline{q}_7 \\ \underline{q}_8 \end{Bmatrix} = \underline{\underline{C}}_{(3)} \underline{q},$$

where $\underline{\underline{0}}$ and $\underline{\underline{I}}$ represent the $2 \times 2$ null and identity matrices, respectively. The connectivity matrix, $\underline{\underline{C}}_{(3)}$, is called a *Boolean matrix* because its entries consist solely of 0's and 1's. Matrix $\underline{\underline{C}}_{(3)}$ establishes the connections of beam element 3 within the entire beam by indicating the nodes to which this beam is connected, and this explains its name of "connectivity matrix."

Expressing the element nodal displacement arrays, $\hat{\underline{q}}_{(i)}$, in terms of the global displacement array, $\underline{q}$, with the help of eq. (11.102), the total strain energy of the truss given by eq. (11.101) now becomes

$$A = \frac{1}{2} \sum_{i=1}^{N_e} \left(\underline{q}^T \underline{\underline{C}}^T_{(i)}\right) \hat{\underline{\underline{k}}}_{(i)} \left(\underline{\underline{C}}_{(i)} \underline{q}\right) = \frac{1}{2}\, \underline{q}^T \left[\sum_{i=1}^{N_e} \underline{\underline{C}}^T_{(i)} \hat{\underline{\underline{k}}}_{(i)} \underline{\underline{C}}_{(i)}\right] \underline{q}.$$

This expression can be simplified to

$$A = \frac{1}{2}\, \underline{q}^T \underline{\underline{K}}\, \underline{q}, \tag{11.103}$$

where the *global stiffness matrix*, $\underline{\underline{K}}$, is defined as

$$\underline{\underline{K}} = \sum_{i=1}^{N_e} \underline{\underline{C}}^T_{(i)} \hat{k}_{(i)} \underline{\underline{C}}_{(i)}. \tag{11.104}$$

The potential of the externally applied loads, $\Phi$, is found by adding the contributions of all beam elements

$$\Phi = \sum_{i=1}^{N_e} \hat{\Phi}_{(i)} = -\sum_{i=1}^{N_e} \underline{\hat{q}}_{(i)}^T \underline{\hat{f}}_{(i)}, \tag{11.105}$$

where $\underline{\hat{f}}_{(i)}$ is the load array for the $i^{\text{th}}$ element, as defined by eq. (10.79) for a generic beam element. Here again, it is convenient to use the connectivity matrix defined in eq. (10.81) to evaluate the potential,

$$\Phi = -\sum_{i=1}^{N_e} \left( \underline{\underline{C}}_{(i)} \underline{q} \right)^T \underline{\hat{f}}_{(i)} = -\underline{q}^T \left\{ \sum_{i=1}^{N_e} \underline{\underline{C}}_{(i)}^T \underline{\hat{f}}_{(i)} \right\}.$$

This expression can be simplified to

$$\Phi = -\underline{q}^T \underline{Q}, \tag{11.106}$$

by defining the *global load array*, $\underline{Q}$, as

$$\underline{Q} = \sum_{i=1}^{N_e} \underline{\underline{C}}_{(i)}^T \underline{\hat{f}}_{(i)}. \tag{11.107}$$

Finally, the total potential energy, $\Pi$, of the complete beam is obtained by adding the potential of the external loads, eq. (11.106), to the total strain energy, eq. (11.103), to find

$$\Pi = A + \Phi = \frac{1}{2} \underline{q}^T \underline{\underline{K}} \underline{q} - \underline{q}^T \underline{Q}. \tag{11.108}$$

This compact expression for the total potential energy of the complete system is only possible because the matrix notation encapsulates the nodal and element quantities in arrays and matrices. The total strain energy is a quadratic form of the generalized coordinates, whereas the potential of the externally applied loads is a linear form of the same variables. It should also be noted that the total strain energy is a positive-definite quantity because it is the sum of positive-definite strain energies for each beam element.

### 11.5.8 Alternative description of the assembly procedure

The assembly procedure described in terms of the connectivity matrix defined in eq. (11.102) is formally correct, but it is not easy to understand nor is it computationally efficient for realistic beams with many nodes. The connectivity matrix, $\underline{\underline{C}}_{(i)}$, has four lines and $2N$ columns, where $N$ is the total number of nodes. For beam modeled with many nodes, this matrix becomes very large with a total of $8N$ entries, and yet, only four entries have a unit value while all $(8N - 4)$ others are zero. Furthermore, the evaluation of the global stiffness matrix involves a triple matrix

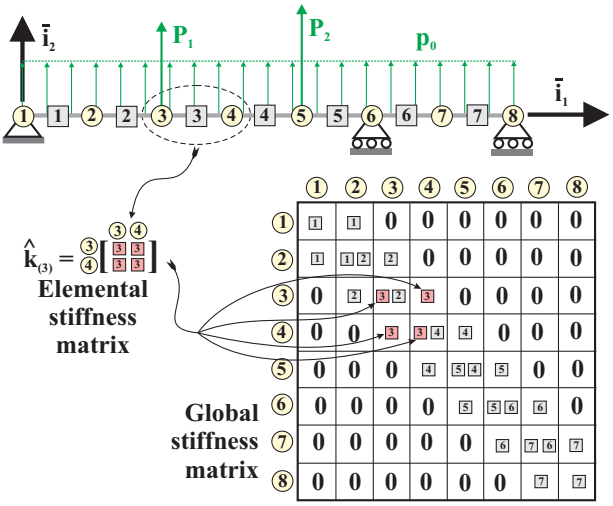


**Fig. 11.47.** Illustration of the assembly procedure.

product for each element, see eq. (11.104). These become increasingly expensive to perform as the problem size increases, and they also are very wasteful because most operations actually are multiplications by zero.

It is possible to give a more graphical visualization of the assembly process. Figure 11.47 depicts the seven element, eight node beam problem under consideration, together with a pictorial representation of the global stiffness matrix. The 8 rows and columns in the matrix are labeled with their corresponding node numbers. Each node has two degrees of freedom (the vertical displacement and rotation component at that node), so each of the entries is actually a $2 \times 2$ matrix and the size of the global stiffness matrix itself is $16 \times 16$.

Consider now a typical element of the beam, say element 3. Its local nodes, *Node 1* and *Node 2*, are associated with the global node numbers 3 and 4, respectively. The stiffness matrix for this beam element, $\underline{\underline{\hat{k}}}_{(3)}$, can be partitioned into four $2 \times 2$ matrices, as shown in eq. (11.98). Beam element 3 is connected to global nodes 3 and 4, and therefore, the four sub-matrices of the local stiffness matrix can simply be added to entries $\underline{\underline{K}}(3,3)$, $\underline{\underline{K}}(4,4)$, $\underline{\underline{K}}(3,4)$, and $\underline{\underline{K}}(4,3)$ in the global stiffness matrix, as indicated by the arrows in fig. 11.47. Note that the indices used with $\underline{\underline{K}}$ in this discussion refer to the nodes shown in fig. 11.47 and not to the individual degrees of freedon actually used to index $\underline{\underline{K}}$.

This procedure is repeated for each beam element to give the final result shown in fig. 11.47. The final figure requires careful interpretation. Each of the 64 squares represents a $2 \times 2$ matrix and may contain 0 or more element numbers. Each of the element numbers shown in square boxes defines a $2 \times 2$ matrix extracted from the corresponding element stiffness matrix. These $2 \times 2$ matrices are added together to produce the final result in the global stiffness matrix.

Another way to look at the same process is to consider the fully assembled global stiffness matrix in fig. 11.47. Diagonal entry $\underline{\underline{K}}(2,2)$ collects contributions from elements 1 and 2, because these two beam elements are all physically connected to node 2. Similarly, diagonal entry $\underline{\underline{K}}(5,5)$ collects contributions from elements 4, and 5, because these two beam elements connect to node 5.

At completion of the assembly process, many entries of the global stiffness matrix remain empty or null. For instance, entries $\underline{\underline{K}}(2,6) = \underline{\underline{K}}(6,2) = 0$, because no beam element directly connects nodes 2 and 6. Similarly, $\underline{\underline{K}}(1,4) = \underline{\underline{K}}(4,1) = 0$ because nodes 1 and 4 are not directly connected by a beam element.

The procedure described here is identical to that presented in sections 10.7.7 and 10.7.6 for truss structures. Although the stiffness matrices for bar and beam elements are different, their assembly process is identical.

### 11.5.9 Derivation of the governing equations

The total potential energy of the beam is given by eq. (11.108), and application of the principle of minimum total potential energy, eq. (10.17), now implies

$$\frac{\partial \Pi}{\partial \underline{q}} = \frac{\partial}{\partial \underline{q}} \left( \frac{1}{2}\, \underline{q}^T \underline{\underline{K}}\, \underline{q} - \underline{q}^T \underline{Q} \right) = \underline{\underline{K}}\, \underline{q} - \underline{Q} = 0. \tag{11.109}$$

To compute the derivative of the total potential energy, eqs. (A.29) and (A.27) are used to evaluate the derivatives of the strain energy and potential of the externally applied loads, respectively. The particular form of this result is due to the fact that the stiffness matrix is symmetric, as described in section A.2.9.

The governing equation of the system take the form of a linear system of equations,

$$\underline{\underline{K}}\, \underline{q} = \underline{Q}. \tag{11.110}$$

The process used to establish the governing equations for beam problems is identical to that used for trusses. The linear algebra formalism hides the fact that the entries of the stiffness matrix and load arrays are different for beam and truss problems. Once the total potential energy is evaluated in terms of a finite number of degrees of freedom, the derivation of the governing equations is formally identical for both types of structures.

### 11.5.10 Solution procedure

The linear system given in eq. (11.110) cannot be solved because the global stiffness matrix is singular.

This situation arises because the element stiffness matrices that make up the global stiffness matrix are each singular. Calculation of the eigenvectors and eigenvalues of the element stiffness matrix, $\hat{\underline{\underline{k}}}$, given by eq. (11.98), reveals more information about this rank deficiency. Two of the four unit eigenvectors of this matrix are

$$\underline{n}_1 = \frac{1}{\sqrt{2}} \begin{Bmatrix} 1 \\ 0 \\ 1 \\ 0 \end{Bmatrix}, \; \underline{n}_2 = \frac{\ell}{\sqrt{8+2\ell^2}} \begin{Bmatrix} -1 \\ 2/\ell \\ 1 \\ 2/\ell \end{Bmatrix},$$

and the corresponding eigenvalues are $\lambda_1 = \lambda_2 = 0$. The last two eigenvalues of the stiffness matrix do not vanish. Consequently, each element stiffness matrix is two times singular. These two eigenvectors represent the two rigid body motion of the beam element: its vertical translation and rotation, corresponding to $\underline{n}_1$ and $\underline{n}_2$, respectively. By definition, rigid body motions create no deformation or straining of the element, and hence, no strain energy is associated with rigid body modes. Clearly, the presence of two rigid body modes for the structure implies the rank deficiency of 2 for the element stiffness matrix. The entire beam also presents two rigid body modes, and hence, the global stiffness matrix also features a rank deficiency of 2.

The physical interpretation of this situation is that boundary conditions have not yet been applied to the beam, which is still free to translate vertically and rotate in plane $(\bar{\imath}_1, \bar{\imath}_2)$. Figure 11.47 shows that nodes 1, 6 and 8 are pinned to the ground, preventing any rigid body motion of the beam. These conditions, however, are not reflected in the global stiffness matrix given by eq. (11.104).

The boundary conditions can be imposed through the following process: *(1)* eliminate the rows and columns of the stiffness matrix corresponding to constrained degrees of freedom to create its reduced counterpart, $\underline{\underline{\bar{K}}}$; *(2)* eliminate the corresponding entries of the global displacement array, $\underline{q}$, to create its reduced counterpart, $\underline{\bar{q}}$; and finally, *(3)* eliminate the corresponding entries of the global load array, $\underline{Q}$, to create its reduced counterpart, $\underline{\bar{Q}}$. The system of equations for the truss then reduces to

$$\underline{\underline{\bar{K}}}\,\underline{\bar{q}} = \underline{\bar{Q}}. \tag{11.111}$$

The reduced stiffness matrix will now be non-singular, and the solution of the problem is found by solving the linear system to find the remaining nodal displacements as $\underline{\bar{q}} = \underline{\underline{\bar{K}}}^{-1}\underline{\bar{Q}}$. A more detailed justification of the procedure is described in section 10.7.9.

Although the stiffness matrices for truss and beam elements are quite different, see sections 10.7.4 and 11.5.5, respectively, many aspects of the formulation of the finite element method for the two types of structures are very similar, and often identical. In fact, once cast within the formalism of linear algebra, the governing equations for both problems are identical, see eqs. (10.89) and (11.110), for trusses and beams, respectively. The treatment of the boundary conditions, discussed in sections 10.7.9 and 11.5.10 for truss and beam structures, respectively, is also identical. A formal treatment of the boundary conditions based on partitioning is described in details for truss structures in section 10.7.10 and applies to beam structures as well.

The above discussion underlines one of the important advantages of the finite element method. Different types of structural components generate stiffness matrices and load arrays that reflect the specific nature of each structural component. For instance, the strain energy of a bar is based on the extensional strain of the component, whereas that of a beam is based on its curvature. Once the stiffness matrices and load

arrays of all components have been generated, the remainder of the process does not distinguish between the various types of structural components. Consequently, the assembly procedure, the generation of the governing equations, and the various details of the solution procedure are identical for all types of structural elements because they correspond to generic, linear algebra operations. This very systematic approach to the solution of general structural problems is one of the key reasons for the immense success of the finite element method.

***Example 11.16. Cantilevered beam with a mid-span support***

Consider the uniform cantilevered beam with a mid-span support shown in fig. 11.48. For this simple problem, two finite elements will be used: the first extends from the left clamp to the mid-span support, the second from the mid-span support to the beam's tip. The two element are delimited by three nodes, for a total of 6 degrees of freedom.

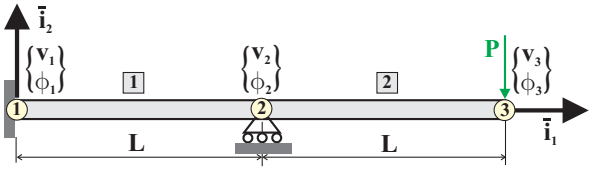


**Fig. 11.48.** Two-element model of cantilever with mid-span support.

Because the two elements are of equal length, $\hat{\ell} = L$, and bending stiffness, the stiffness matrix for each element is given by eq. (11.98). The $6 \times 6$ global stiffness matrix then consists of the assembly of the two $4 \times 4$ element stiffness matrices. Proceeding as described in section 11.5.8, the global stiffness matrix is found as

$$\underline{\underline{K}} = \frac{H^c_{33}}{L^3} \left[\begin{array}{cc|cc|cc} 12 & 6L & -12 & 6L & 0 & 0 \\ & 4L^2 & -6L & 2L^2 & 0 & 0 \\ \hline & & (12+12) & (-6L+6L) & -12 & 6L \\ & & & (4L^2+4L^2) & -6L & 2L^2 \\ \hline & & & & 12 & -6L \\ sym & & & & & 4L^2 \end{array}\right] .$$

The partitioning indicated in the above equation corresponds to the contributions of the degrees of freedom associated with the three nodes: the first two rows and columns correspond to the degrees of freedom of node 1, the next two rows and columns to those of node 2, and the last two rows and columns to those of node 3. The $4 \times 4$ stiffness matrix of the first element is assembled in the first four rows and columns of the global stiffness matrix, while the $4 \times 4$ stiffness matrix of the second element is assembled in the last four rows and columns of the global stiffness matrix. The two elements are connected at a common node, node 2. It follows that the middle two rows and columns of the global stiffness matrix store the sum of contributions from both elements.

The governing equations of the problem are in the form of eq. (11.110). In this case, the nodal load array is given as $\underline{Q} = \left\{R_1, M_1, R_2,\ 0, -P,\ 0\right\}^T$ where $R_1$ and $R_2$ are the reaction forces at nodes 1 and 2, respectively, and $M_1$ is the root clamping moment.

The solution phase of the problem will follow the partitioning approach developed in section 10.7.10. The first three degrees of freedom, $v_1$, $\phi_1$, and $v_2$, are the prescribed degrees of freedom, *i.e.*, $\underline{q}_p = \left\{v_1, \phi_1, v_2\right\}^T = 0$. The corresponding load array stores the reaction forces, $\underline{Q}_p = \left\{R_1, M_1, R_2\right\}^T$. The last three degrees of freedom, $\phi_2$, $v_3$, and $\phi_3$, are the unconstrained degrees of freedom, $\underline{q}_u = \left\{\phi_2, v_3, \phi_3\right\}^T$. The corresponding load array stores the externally applied loads, $\underline{Q}_u = \left\{\ 0, -P,\ 0\right\}^T$.

The global stiffness matrix is partitioned accordingly to find

$$\underline{\underline{K}}_{uu} = \frac{H_{33}^c}{L^3}\begin{bmatrix} 8L^2 & -6L & 2L^2 \\ -6L & 12 & -6L \\ 2L^2 & -6L & 4L^2 \end{bmatrix}, \quad \underline{\underline{K}}_{pu} = \frac{H_{33}^c}{L^3}\begin{bmatrix} 6L & 0 & 0 \\ 2L^2 & 0 & 0 \\ 0 & -12 & 6L \end{bmatrix}.$$

Matrix $\underline{\underline{K}}_{uu}$ corresponds to the lower right $3 \times 3$ partition of the global stiffness matrix, whereas matrix $\underline{\underline{K}}_{pu}$ corresponds to the upper right $3 \times 3$ partition of the same matrix.

Since $\underline{q}_p = 0$, eq. (10.96) reduces to $\underline{\underline{K}}_{uu}\,\underline{q}_u = \underline{Q}_u$ and the unknown degrees of freedom are $\underline{q}_u = \underline{\underline{K}}_{uu}^{-1}\underline{Q}_u$, whose components are

$$\phi_2 = -\frac{PL^2}{4H_{33}^c}, \quad v_3 = -\frac{7PL^3}{12H_{33}^c}, \quad \text{and} \quad \phi_3 = -\frac{3PL^2}{4H_{33}^c}.$$

The reaction forces are now computed with the help of eq. (10.97), which reduces to $\underline{Q}_p = \underline{\underline{K}}_{up}^T\underline{q}_u$, with components given by

$$R_1 = -\frac{3P}{2}, \quad M_1 = -\frac{PL}{2}, \quad \text{and} \quad R_2 = \frac{5P}{2}.$$

Next, the displacement field within each element can be computed with the help of eq. (11.88). For the first element, $v_1 = \phi_1 = v_2 = 0$, and the displacement field reduces to $\hat{v}(\hat{\eta}) = \hat{\ell}\hat{\phi}_2 h_4(\hat{\eta})/2$. Introducing the shape functions defined in eq. (11.93) then yields

$$\hat{v}(\hat{\eta}) = \frac{PL^3}{32H_{33}^c}(1+\hat{\eta})^2(1-\hat{\eta}).$$

Note that $\hat{\eta} = -1$ at node 1 and $\hat{\eta} = +1$ at node 2. For the second element, the displacement field reduces to $\hat{v}(\hat{\eta}) = L\phi_2 h_2/2 + v_3 h_3 + L\phi_3 h_4/2$, and introducing the shape function defined in eq. (11.93) then yields

$$\hat{v}(\hat{\eta}) = -\frac{PL^3}{96H_{33}^c}(1+\hat{\eta})\left[3(1-\hat{\eta})^2 + 14(1+\hat{\eta})(2-\hat{\eta}) - 9(1+\hat{\eta})(1-\hat{\eta})\right].$$

Note that $\hat{\eta} = -1$ at node 2 and $\hat{\eta} = +1$ at node 3, because $\hat{\eta}$ is a local variable defined within each element. The non-dimensional displacement field over the entire span of the beam is shown in fig. 11.49 as a function of a global non-dimensional variable, $\eta = x_1/(2L)$.

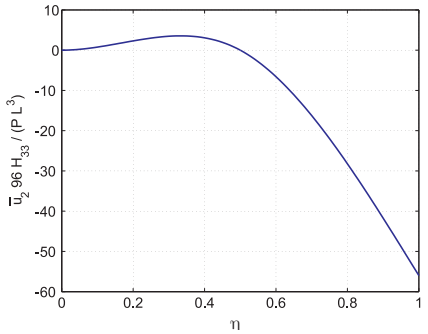


**Fig. 11.49.** Deflection of beam elements 1 and 2.

This deflected shape looks quite reasonable with zero displacement and slope at the root end and zero deflection at the mid-span support. It is, in fact, the exact solution to this problem. This is because in the element formulation, a cubic polynomial is assumed for the deflected shape and this is the exact form of the solution for a beam segment with only concentrated forces and/or moments applied at the ends.

### 11.5.11 Summary

The finite element approach presented in this section addresses the challenging problem of selecting good shape functions for complex beam problems. Instead of considering the entire beam, an approximate solution is created for a finite number of beam elements. Within each beam element, it is a easy to choose shape functions that easily satisfy the constraints imposed at the end nodes.

The solution to the full problem is then constructed by assembling the governing equations for each of the small elements into a formulation for the entire beam. This assembly process is systematic and lends itself to computer implementation. A set of linear algebraic equations results that can be solved easily. For this reason, the finite element method for developing approximate solutions is preferred over approaches that attempt to select approximations over the entire span of the beam.

The development of the finite element analysis method is a rich area to explore, and a considerable amount of research has been performed over the past decades. The finite element method has been incorporated into a number of large commercial software packages, which can be applied to solve a wide range of structural engineering and "multi-physics" problems. This chapter provide only the most basic introduction to this fascinating field.

### 11.5.12 Problems

**Problem 11.20. Cantilever with mid-span load and tip support**
Consider the cantilever beam of length $2L$ shown in fig. 11.50. A concentrated load is applied at mid-span and the tip is pinned. Construct a finite element solution to this problem using two elements of length $L$. *(1)* Determine the nodal displacements and rotations and compare to the exact results obtained using the unit load method. *(2)* Determine the nodal reactions for the constrained degrees of freedom. *(3)* Construct a plot of the deflected shape for the beam.

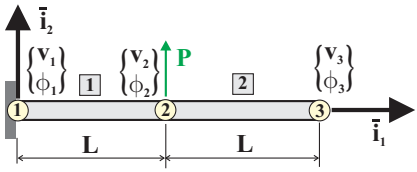


**Fig. 11.50.** Cantilever with tip support and concentrated load applied at mid-span.

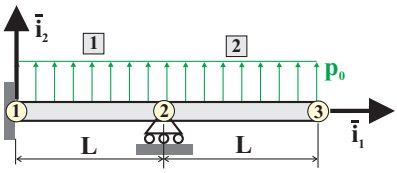


**Fig. 11.51.** Cantilever with mid-span support and a uniform load.

**Problem 11.21. Cantilever with mid-span support and uniform load**
A cantilever beam is supported at mid-span and carries a uniform load $p_0$ as shown in fig. 11.51. (Note that this is very similar to example above.) Construct a finite element solution to this problem using two elements of length $L$. *(1)* determine the nodal displacements and rotations and compare to the exact results obtained using the unit load method. *(2)* Determine the nodal reactions for the constrained degrees of freedom. *(3)* Construct a plot of the deflected shape for the beam.

**Problem 11.22. Simply supported beam with nonuniform bending stiffness**
In this problem you are to reconsider the simply supported beam with nonuniform bending stiffness treated in problem 11.12. The present solution is to be developed using the finite element approach. Construct a 2-element solution using elements for the left and right halves of the beam. *(1)* Compute the nodal displacements and rotations at each node. *(2)* Compare the solution for the mid-span deflection with the exact solution computed using the unit load method. *(3)* Compare the solution for the mid-span deflection with the solution from problem 11.12.